2005

Constraining temporal relationships among the draining of Glacial Lake Missoula the retreat of the Flathead ice lobe and the development of the lower Flathead River Valley

Garrett K. Timmerman
The University of Montana

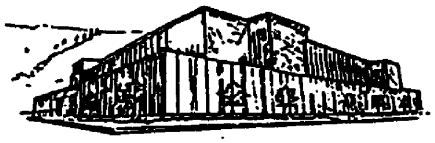

Maureen and Mike
MANSFIELD LIBRARY

The University of
Montana

CONSTRAINING TEMPORAL RELATIONSHIPS AMONG THE DRAINING OF GLACIAL LAKE MISSOULA, THE RETREAT OF THE FLATHEAD ICE LOBE, AND THE DEVELOPMENT OF THE LOWER FLATHEAD RIVER VALLEY

by

Garrett K. Timmerman

B.Sc. Michigan Technological University, 2003

presented in partial fulfillment of the requirements

for the degree of

Master of Science

The University of Montana

December 2005

Approved by:

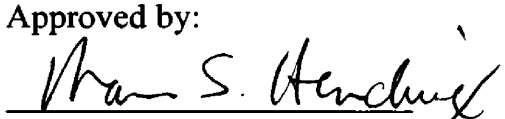

Chair

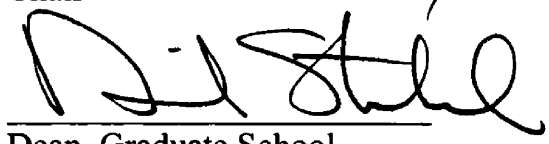

Dean, Graduate School

12-30-05

Date

ProQuest LLC.
789 East Eisenhower Parkway
P.O. Box 1346
Ann Arbor, MI 48106 - 1346

Timmerman, Garrett K. M.S., December. 2005 Geology

Constraining temporal relationships among the draining of glacial Lake Missoula, the retreat of the Flathead Ice Lobe, and the development of the lower Flathead River

Chair: Marc S. Hendrix MSH

Quaternary sediments in the Mission Valley, northwestern Montana, contain a suite of latest Pleistocene glacial and glacio-lacustrine deposits that are overlain by younger, mostly Holocene post-glacial deposits. Mapping of these sediments and their associated geomorphic features has revealed the presence of four Quaternary units; massive diamict glacial lake deposits; thinly-bedded, locally varved glacial lake deposits; older alluvium of stream channels; and modern alluvium of stream channels. I interpret the massive diamict and glacial lake sediments to have been deposited in glacial Lake Missoula. The spatial distribution of these units was influenced by the geometry of the Mission Valley. The older alluvium contains a series of fluvial terraces that are related to deglaciation in the area and record the drainage of ancestral Lake Flathead and the development of the lower Flathead River valley.

Correlation of the onshore sedimentary record with sediment cores and seismic reflection data recovered from the Flathead Lake sub-bottom suggests that between 14,150 and 13,180 cal yr BP the bedrock spillway impounding ancestral Lake Flathead was down-cut 35-50m during multiple periods of rapid incision. Incision was initiated by meltwater outbursts associated with deglaciation in the region that also resulted in substantial turbidite deposition in the sediments of Flathead Lake. Subsequently, the lowering of the spill-point through incision changed the stability of the lower Flathead River and initiated terrace development along the river valley. After deposition of the Glacier Peak tephra (13,180 cal yr BP) the bedrock spill-point was incised an additional 10 to 20m, lowering the spillway to near its present level and stabilizing the lower Flathead River at near its present position.

Correlation of the measured paleomagnetic secular variation (PSV) records in the Flathead Lake sediments with the well-dated PSV records from Fish Lake, Oregon, improved sediment core chronostratigrapy within the study area. PSV correlation was used to construct age-depth and sedimentation rate curves for several sediment cores, and also quantified the amount of time missing from over-penetration of the coring apparatus during core recovery. Analysis of the PSV data also constrained the duration of non-deposition and/or erosion associated with an angular unconformity observed in the seismic data as occurring between 4,300 and 7,600 cal yr BP.

Contents

Tables

Figures

I – Introduction

Quaternary sediments and associated landforms in northwestern Montana preserve a detailed record of the terminal history of glacial Lake Missoula and deglaciation of the region. Perhaps the best-preserved sedimentary record of deglaciation in northwestern Montana is the suite of Quaternary glacial, glacio-lacustrine, and post-glacial deposits preserved in and around Flathead Lake. Over 135m of glacial and post-glacial sediments are preserved in the Flathead Lake basin itself (Hofmann et al., 2003). South of Flathead Lake in the lower Flathead River valley, a well-exposed 150m thick section of glacio-lacustrine sediments is preserved in natural cliffside exposures (Levish, 1997). Fluvial terraces preserved along the river valley record the dissection of these sediments by the lower Flathead River after the terminal draining of glacial Lake Missoula and likely relate to large discharge flows resulting from rapid deglaciation in the region.

Despite the potential value of Quaternary sediments and landforms in the Flathead Lake area as a record of deglaciation, the chronology of these sediments and landforms is yet poorly documented. In order to improve this chronology and provide an overview of the geometric relations among Quaternary features, I employed a three-pronged approach. First, I mapped Quaternary deposits and erosional surfaces of the lower Flathead River valley at 1:24,000 to document their depositional character and overall architecture. Second, I refined the chronology of a series of piston cores from Flathead Lake by acquiring and correlating paleomagnetic secular variation (PSV) records among the cores and indexing these PSV records to a well-dated reference record from Fish

Lake, Oregon. Third, I correlated the mapped deposits to the lacustrine record of Flathead Lake, using event stratigraphy and a volcanic tephra present in the region.

II – Geologic Setting

Regional Geology and Physiography

The Mission and Flathead Valleys are located in northwestern Montana in the northern Rocky Mountains, a region dominated by glaciated mountain ranges and intermontane valleys. These valleys are located at the southern end of the Rocky Mountain trench, a northwest-southeast topographic depression produced by a linear system of half- and full-grabens that stretches from east-central British Columbia southward into northwest Montana. The Flathead and Mission Valleys are structurally bound on the east by the Mission Fault, a seismically active westward dipping normal fault (Ostenaa et al., 1995). To the west, the valleys are bound by the Salish Mountain Range (Figure 1).

With a surface area of 496km^2, Flathead Lake is located at the southern end of the Flathead Valley (Figure 1). Flathead Lake is the largest naturally-occurring fresh water lake west of the Mississippi River. The modern bathymetry of Flathead Lake is dominated by a north-south trending trough up to 100m deep on its eastern side. A broad bathymetric bench with an average depth of about 60m occurs in the western half of the lake. Shallow embayments (15-25m depth) occur in the westernmost and southernmost parts of the lake (Figure 2).

The bedrock in the region consists of metasedimentary rocks of the Mesoproterozoic Belt Supergroup (Johns, 1970). These rocks are prevalent

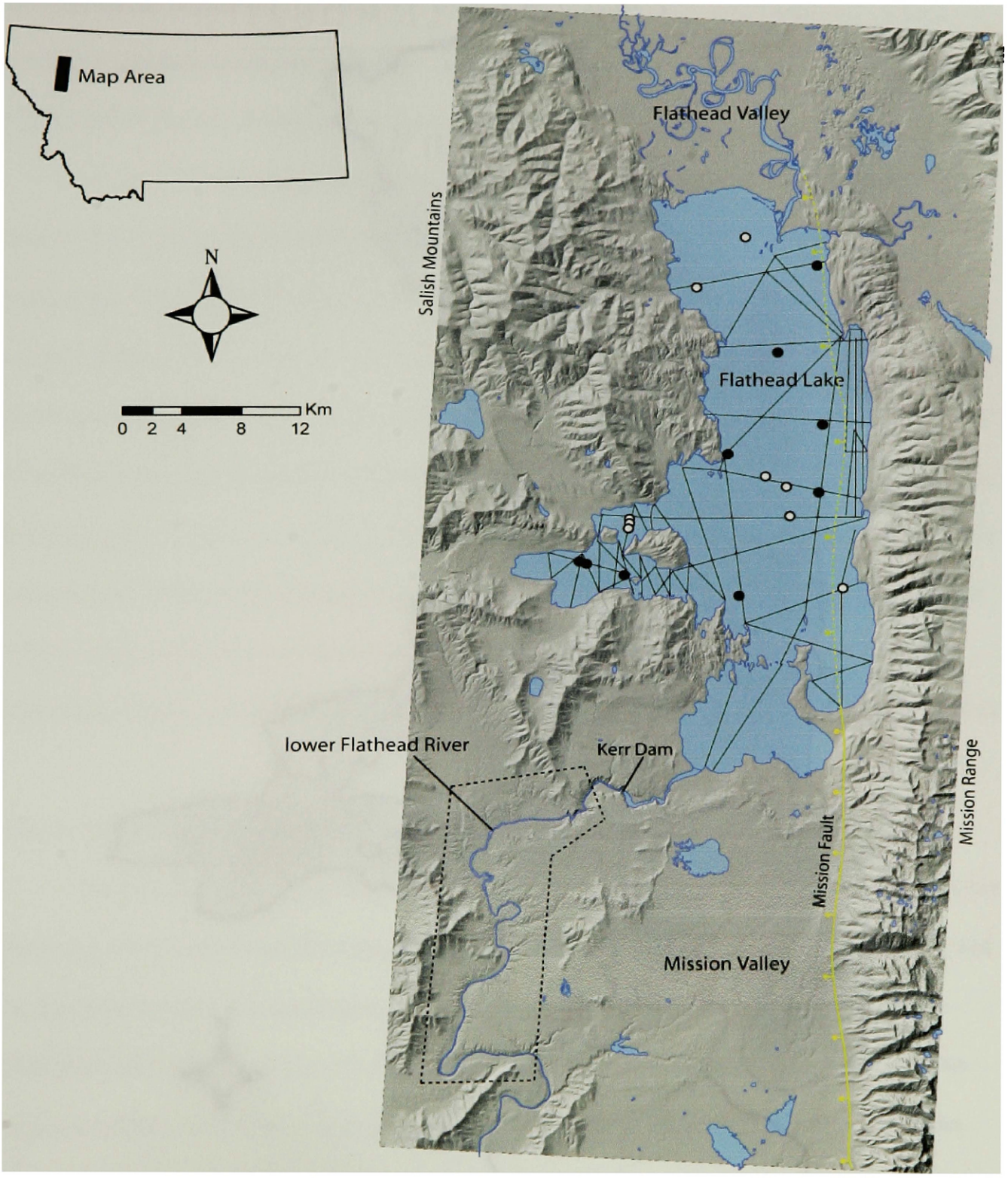

Figure 1. Hill-shaded digital elevation model of the study area. Dots show location of piston cores collected from the lake, open dots being cores used for paleomagnetic analysis. Seismic reflection profiles are indicated by the solid lines (Kogan, 1980). The Mission Fault system is shown in yellow and is dashed where the main fault is inferred. The map area is indicated by the dashed polygon.

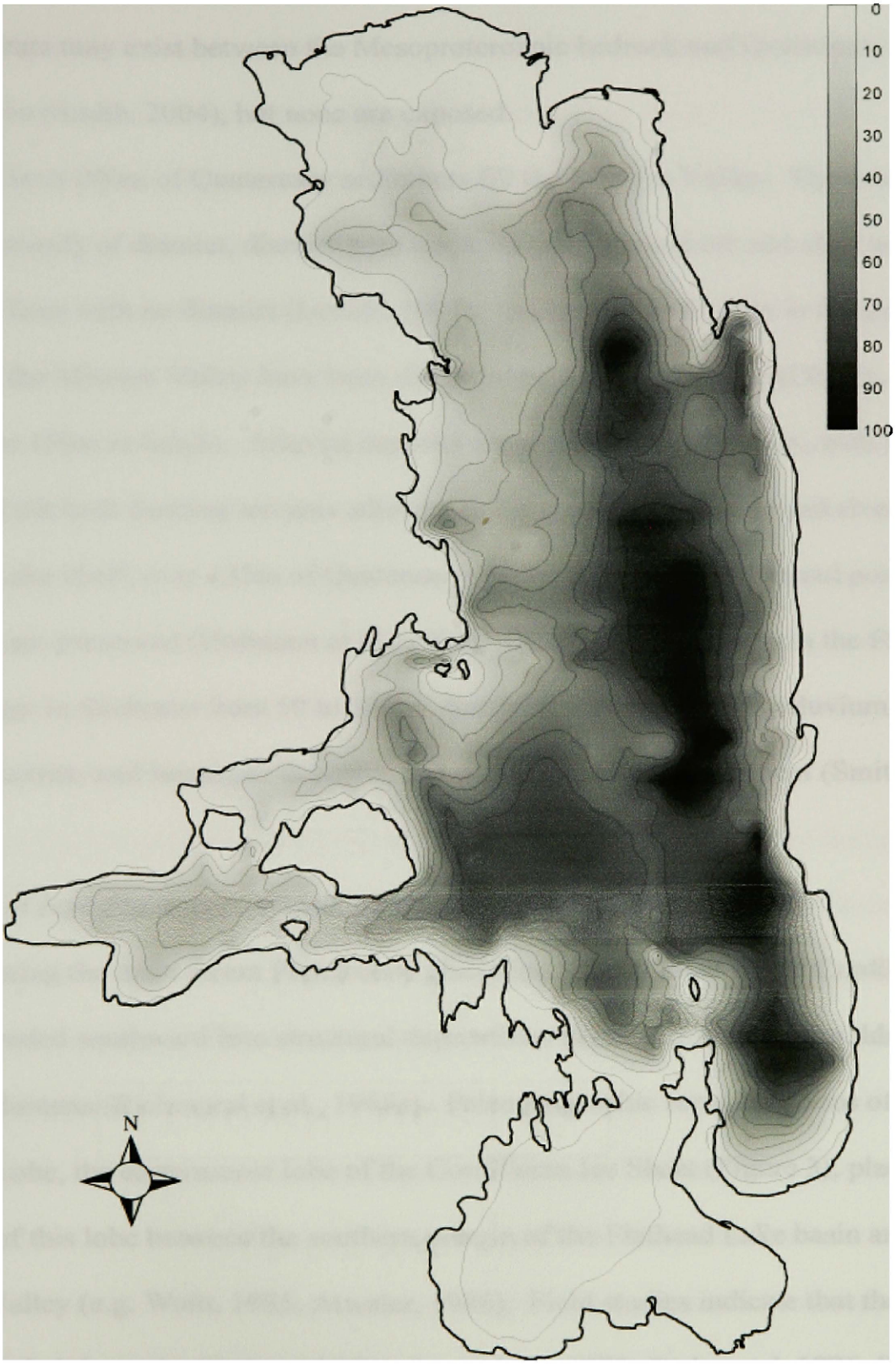

Figure 2. Modern bathymetry of Flathead Lake. Bathymetric contours are in meters. After Hofmann et al. (in press).

throughout the region and account for the majority of clasts in Quaternary deposits. Tertiary strata may exist between the Mesoproterozoic bedrock and Quaternary sediments in the region (Smith, 2004), but none are exposed.

At least 200m of Quaternary sediments fill the Mission Valley. These sediments consist primarily of diamict, diamict with intercalated laminated silt and clay, and laminated fines with no diamict (Levish, 1997). Quaternary sediments in the western portion of the Mission Valley have been dissected by the lower Flathead River, exposing bluffs up to 150m in height. Alluvial deposits are present along the river, with a series of gravel and silt beds forming terraces adjacent to the modern floodplain and riverbed. In Flathead Lake itself, over 135m of Quaternary glacial, glacio-lacustrine and post-glacial sediments are preserved (Hofmann et al., 2003). Quaternary sediments in the Flathead Valley range in thickness from 50 to 300m. Surficial deposits include alluvium, till, glacio-lacustrine and lacustrine deposits, and eolian and alluvial sediment (Smith, 2004).

Overview of Late Pleistocene Glacial & Glacial Lake History

During the most recent Pleistocene glaciation, glacial lobes of the Cordilleran Ice Sheet extended southward into structural depressions in eastern Washington, Idaho, and western Montana (Richmond et al., 1965a). Paleogeographic reconstructions of the Flathead Lobe, the easternmost lobe of the Cordilleran Ice Sheet (Figure 3), place the terminus of this lobe between the southern margin of the Flathead Lake basin and the Mission Valley (e.g. Waitt, 1985; Atwater, 1986). Field studies indicate that the Flathead Lobe extended down the Flathead Valley (e.g. Alden, 1953; Richmond, 1986; Smith, 2004) to a stable position at Polson, Montana (Levish, 1997; Hofmann & Hendrix, 2004).

This interpretation is supported by the presence of a terminal moraine, named the Polson moraine (Elrod, 1903; Davis, 1920; Alden, 1953) that represents a period of ice sheet stability. Although the moraine has yet to be directly dated, an age between 15,000 and 20,000 cal yr BP has been suggested by Hofmann and Hendrix (2004) based on morphostratigraphic correlations and age control from other moraines in the region (Smith, 1966; Elison, 1981). Sedimentary investigations of the Polson moraine show an abundance of sub-aqueous climbing ripples and a lack of ice contact structures associated with sub-aerial moraines, suggesting that the moraine was deposited in a sub-aqueous environment (Hofmann and Hendrix, 2004). This interpretation is supported circumstantially by the broad low-amplitude geomorphic expression of the landform and evidence of a contemporaneous glacial lake occupying the Mission Valley to the south indicated by wave-cut features on the south side of the moraine (Alden, 1953; Levish, 1997; Hofmann et al., 2003).

Late Quaternary sediments of the Mission Valley were previously interpreted as a series of till sheets representing multiple advances and retreats of the Cordilleran Ice Sheet with glacio-lacustrine deposition occurring during ice sheet advance and retreat (Nobles, 1952; Alden, 1953; Richmond et al., 1965a; 1965b; Richmond, 1986; Curry et al., 1977; Stoffel, 1980; Ostenna et al., 1990). Upon detailed sedimentary and stratigraphic investigation of these Quaternary sediments, Levish (1997) reinterpreted them to be glacio-lacustrine deposits. The adjacent Flathead Lobe and over a dozen alpine glaciers in the Mission Range terminated into a large glacial lake occupying the valley, introducing large volumes of sediment into the glacio-lacustrine environment. Suspension, ice rafting, and sub-aqueous density flows were the primary means of

sediment transport, with the geometry of the lake floor influencing the patterns of flow and deposition in the Mission Valley (Levish, 1997).

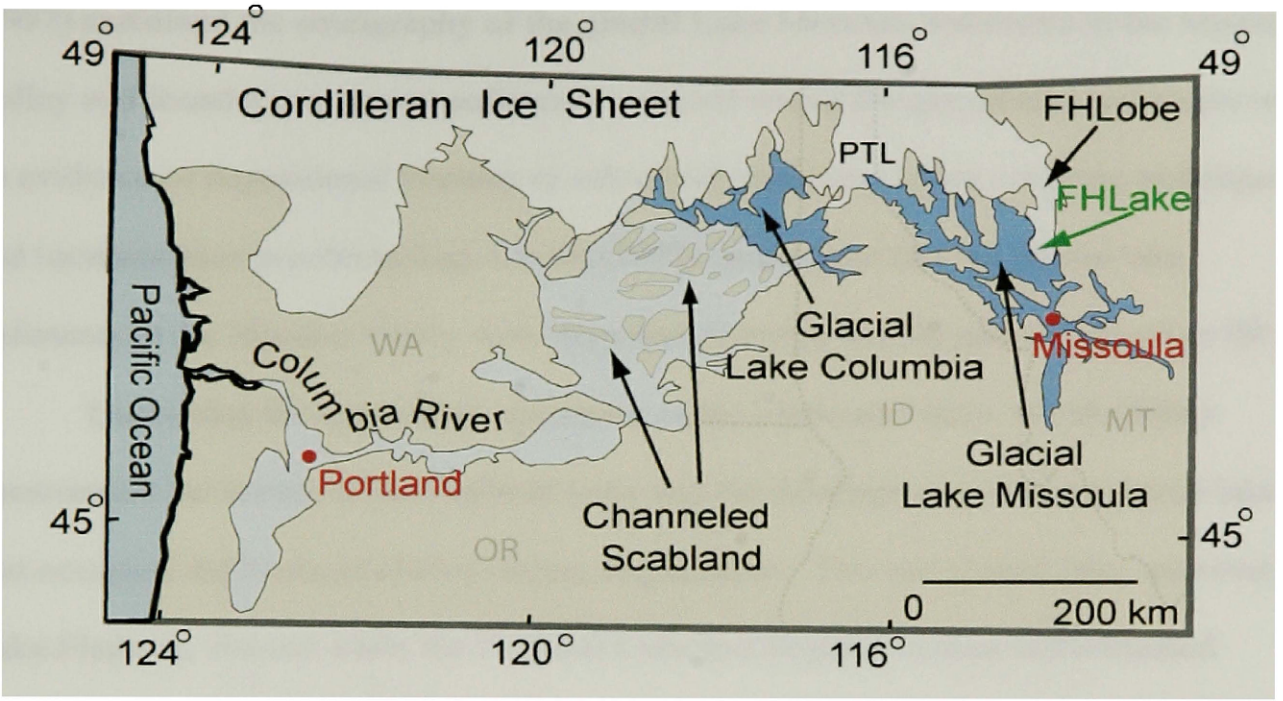

Figure 3. Schematic reconstruction of the last glacial maxima showing the position of the Flathead Lobe (FHLobe) and glacial Lake Missoula, which was impounded behind the Purcell Trench Lobe (PTL). After Waitt, 1985.

The glacial lake that occupied the Mission Valley is part of glacial Lake Missoula (Pardee, 1910 and 1942), a glacial lake that occupied several intermontane valleys in northwestern Montana (Figure 3). Glacial Lake Missoula was formed by damming of the Clark Fork River drainage near the present site of Lake Pend Oreille by a lobe of glacial ice that advanced down the Purcell trench in northern Idaho (Figure 3). The glacial lake surface reached a level of at least 1265m in elevation (Waitt and Atwater, 1989) with a maximum water depth of 670m, and a volume greater than 2500km^3 (Craig, 1987). The Mission Valley has the largest surface area and volume in the glacial Lake Missoula basin, is one of the deepest basins, and contains the thickest section of sediment recording the history of the lake (Levish, 1997). There are several theories as to the drainage

history of glacial Lake Missoula, pertaining mainly to the number and scale of lake drainages (e.g. Waitt, 1985; Atwater, 1986; Levish, 1997; Shaw et al., 1999). Levish (1997) examined the stratigraphy of the glacial Lake Missoula sediments in the Mission Valley and found a continuous sedimentary record within the glacial lake sediments with no evidence of depositional hiatuses or sub-aerial exposure. Using counting techniques and luminescence geochronology Levish (1997) determined that the glacial lake sediments in the Mission Valley were deposited between 19,200 and 16,000 cal yr BP.

Examining the Quaternary sediments of the Flathead Valley, Smith (2004) documented the retreat of the Flathead Lobe and the development of a pro-glacial lake that occupied the Flathead Valley during deglaciation. This pro-glacial lake, ancestral Lake Flathead, formed while the Flathead Lobe had begun to retreat and remained separated from glacial Lake Missoula by the Polson moraine. After the drainage of glacial Lake Missoula, ancestral Lake Flathead remained impounded by the Polson moraine and a bedrock spill-point near the current position of Kerr Dam (Figure 4; Smith, 2004). Using the presence of the Glacier Peak tephra (13,180 cal yr BP, Foit et al., 1993) in eolian deposits in the northern Flathead Valley as a minimum age constraint, Smith (2004) calculated recession rates of 26-150m $year^{-1}$ for the Flathead Lobe from the Polson moraine to the north 87km.

Over 270km of single channel, high-resolution seismic data has been shot across Flathead Lake (Kogan, 1980; Wold 1982). These seismic data have been used to define bathymetry and seismic facies within the lake basin and identify sedimentary regimes preserved in the sediments (Hofmann et al., in press). Hofmann et al. (in press) identified six seismic facies in the data resulting from variations in sedimentation and lake level due

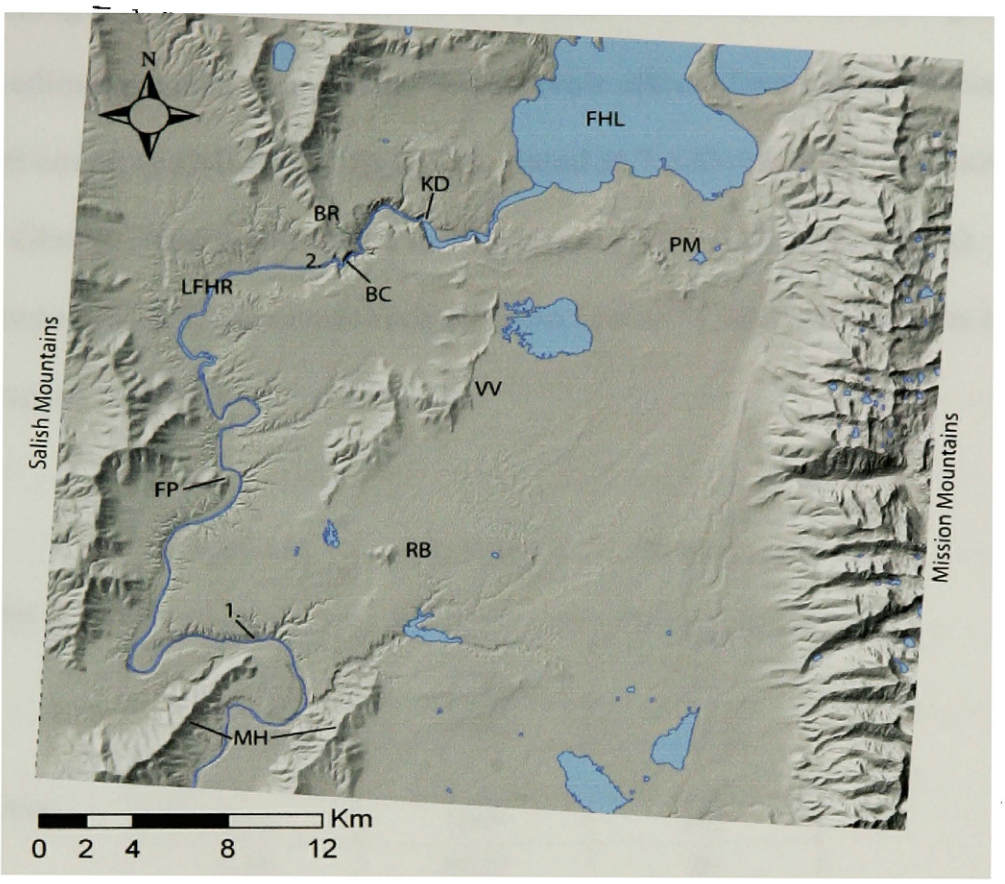

Figure 4. Hillshade of the Mission Valley identifying physiographic features in the valley. FHL – Flathead Lake; PM – Polson moraine; KD – Kerr Dam; BR – Buffalo ridge; BC – Buffalo canyon; LFHR – lower Flathead River; VV – Valley View Hills; FP – Finley Point; RB – Round Butte; MH – Moiese Hills. 1. Location of fluvial terrace containing the Glacier Peak tephra (Figure 12). 2. Outlet of Buffalo canyon, location of Figures 13 and 14.

to deglaciation and Holocene climate changes. They also identified a prominent erosional unconformity that was on-lapped by overlying sediments shown by a change in seismic facies. These architectural relations record erosion resulting during significant lake level lowering (volume loss) and subsequent refilling and lake level rise.

To supplement the seismic data, a set of 19 piston cores ranging between 5 and 11.5m in length were recovered from the lake at locations along the seismic lines (Figure 1). A multitude of analyses have been completed on the cores including multi-sensor logging, grain-size analysis, and chemical analysis (Hofmann, in prep; Sperazza, in prep).

Bulk carbon dating of the sediment cores is not possible because of the fine-grained nature of the sediments and a significant ^{14}C reservoir effect. Two tephras occur in many of the sediment cores; the Mt. Mazama tephra, dated at 7,630 cal yr BP (Zdanowicz et al., 1999) and the Glacier Peak tephra dated at 13,180 cal yr BP (Foit et al., 1993). Additional chronostratigraphic control comes from seven ^{14}C dates from three cores (Table 1; Sperazza, in prep.).

Core	Depth (m)	cal yr BP	Error (±yrs.)
FL-03-15K			
	0.44	2980	145
	0.95	7700	65
	2.22	9760	125
FL-03-16K			
	0.44	5040	205
	3.39	8650	80
	4.54	10210	40
	5.99	12220	95
FL-03-19K			
	4.96	14150	145

Volcanic Tephras

Tephra	Cal. Yrs. B.P.	Error (yrs.)
Mt. Mazama	7630	80
Glacier Peak	13180	120

Table 1. Radiometric ^{14}C dates recovered from detritus in the sediment cores (Sperazza, in prep.) and volcanic tephras (Zdanowicz et al., 1999; Foit et al., 1993) prevalent through the core suite.

Despite these age control points, the overall chronology of the core suite remains poorly constrained. In order to improve this chronology, I measured the natural

remanent magnetization (NRM) of nine cores in order to document the paleomagnetic secular variation (PSV) trends preserved in the cored sediments. Records of the PSV trends allowed for the establishment of time-series data sets that could be correlated among cores within the Flathead Lake basin as well as with regional reference records from outside the Flathead Lake basin. With few chronstratigraphic constraints, construction of age-depth models and accurate correlation of data among the sediment cores is severely limited. Age control from paleomagnetic dating provides improvements on age-depth models for the cores, allowing for tighter age control on sedimentary events and calculations of sedimentation rates. Additionally, more accurate temporal constraints on observations of basin scale changes related to deglaciation and regional climate shifts are possible with the improved chronostratigraphy.

III – Field Mapping of the Lower Flathead River

Methods

I mapped sedimentary facies and geomorphic landforms in the northwestern Mission Valley at 1:24,000 scale. Most exposures of Quaternary sediments are along the bluffs of the lower Flathead River; other natural exposures exist along confluent drainage valleys. Very few human-made outcrops exist in the map area. Most outcrops required cleaning with a shovel and brush to expose sedimentary features. Map units have been distinguished primarily on the basis of sedimentology, secondarily on the basis of geomorphology. The sedimentary section containing the Glacier Peak tephra was measured with cm scale resolution to accurately document and interpret its depositional environment and compare that with similar deposits throughout the map area (Figure 12). Aerial photographs and 10m Digital Elevation Models (DEMs) were used to aid mapping, investigation, and interpretation. Once field maps were completed they were digitized utilizing ArcGIS software. Contacts between map units were input via a graphical user interface utilizing basic topology rules and spatial analysis tools (e.g. slope and hillshade analysis). The digitized geologic map was then draped over a shaded relief map of the region (Figure 5a).

Results and Interpretations

I differentiated five units in the mapping area: bedrock of the Belt Supergroup, massive diamict glacial lake deposits, laminated glacial lake deposits, alluvium of older stream channels, and alluvium of modern stream channels. The map is shown in Figure 5a and the map units are summarized in Figure 5b.

Bedrock – description

The bedrock in this region is part of the Mesoproterozoic Belt Supergroup, a group of greenschist facies metasedimentary rocks and minor igneous rocks which are prevalent in northwestern Montana (Johns, 1970). Lithologies in the map area include purple and green argillite, fine-grained quartzite, carbonaceous argillite and siltite of the Mesoproterozoic Ravalli Group, Empire Formation, and Helena Formation.

Massive Diamict – description

This unit is characterized by massive diamict consisting of a light brown to grayish silt and clay matrix with pebble to boulder-sized clasts (Figure 6). The unit also contains a sub-facies consisting of 2-10cm thick of intercalated beds of laminated light brown to grayish silt with pebble to boulder size dropstones, and clast supported gravel beds consisting of cobble to pebble sized clasts 30 to 50cm in thickness (Figure 7).

The diamict generally contains ~10-20% clasts that are unbedded and disorganized and range in size from pebbles to boulders. Clasts are sub-rounded to sub-

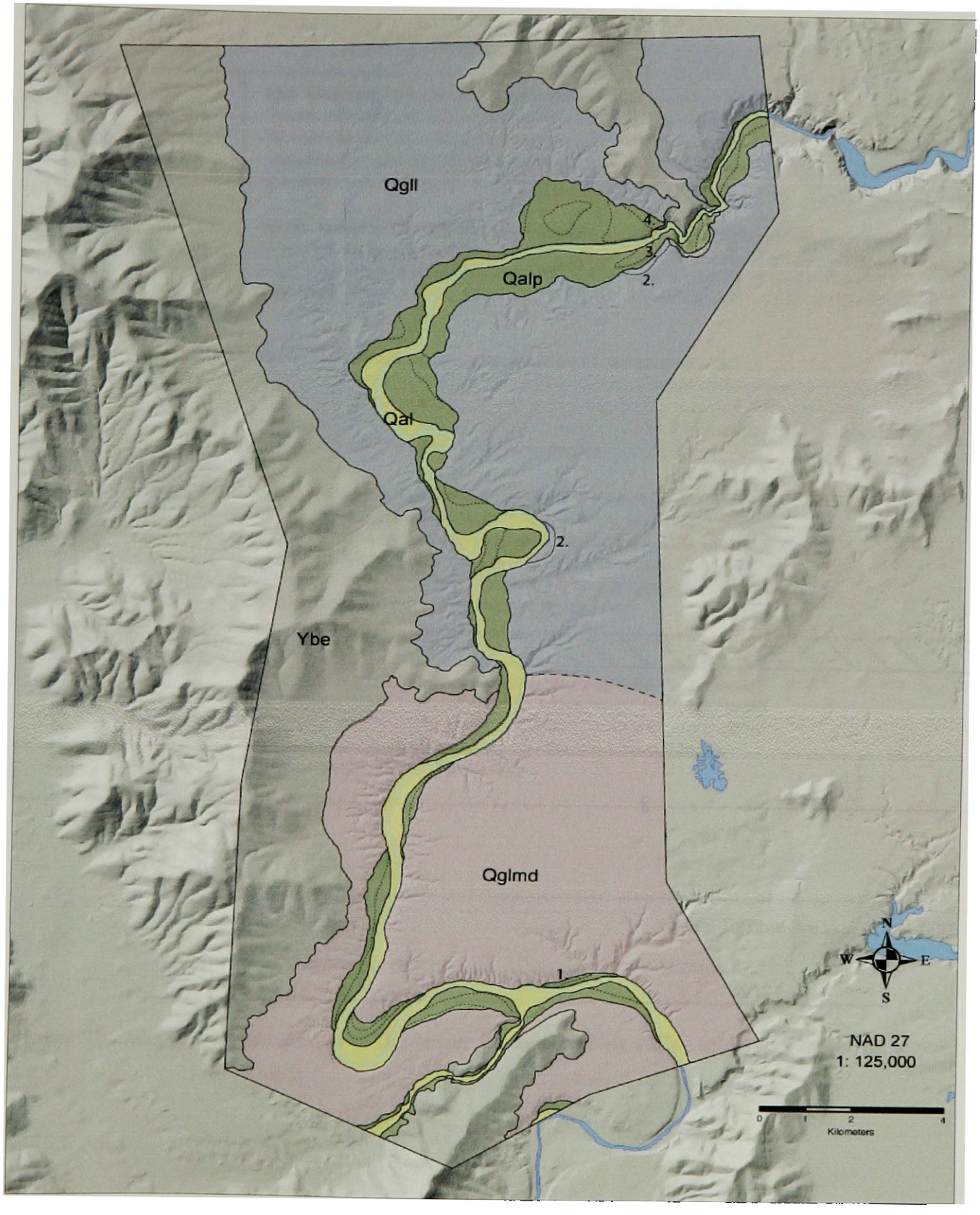

Figure 5a. Surficial geologic map of the lower Flathead River valley. 1. Location of Sloan fluvial terrace shown in figure 12. 2. Locations of slumps shown in figure 10. 3. Location of large boulder deposits shown in figure 13. 4. Location of fluvial terraces shown in figure 14. See figure 5b for unit descriptions and map legend.

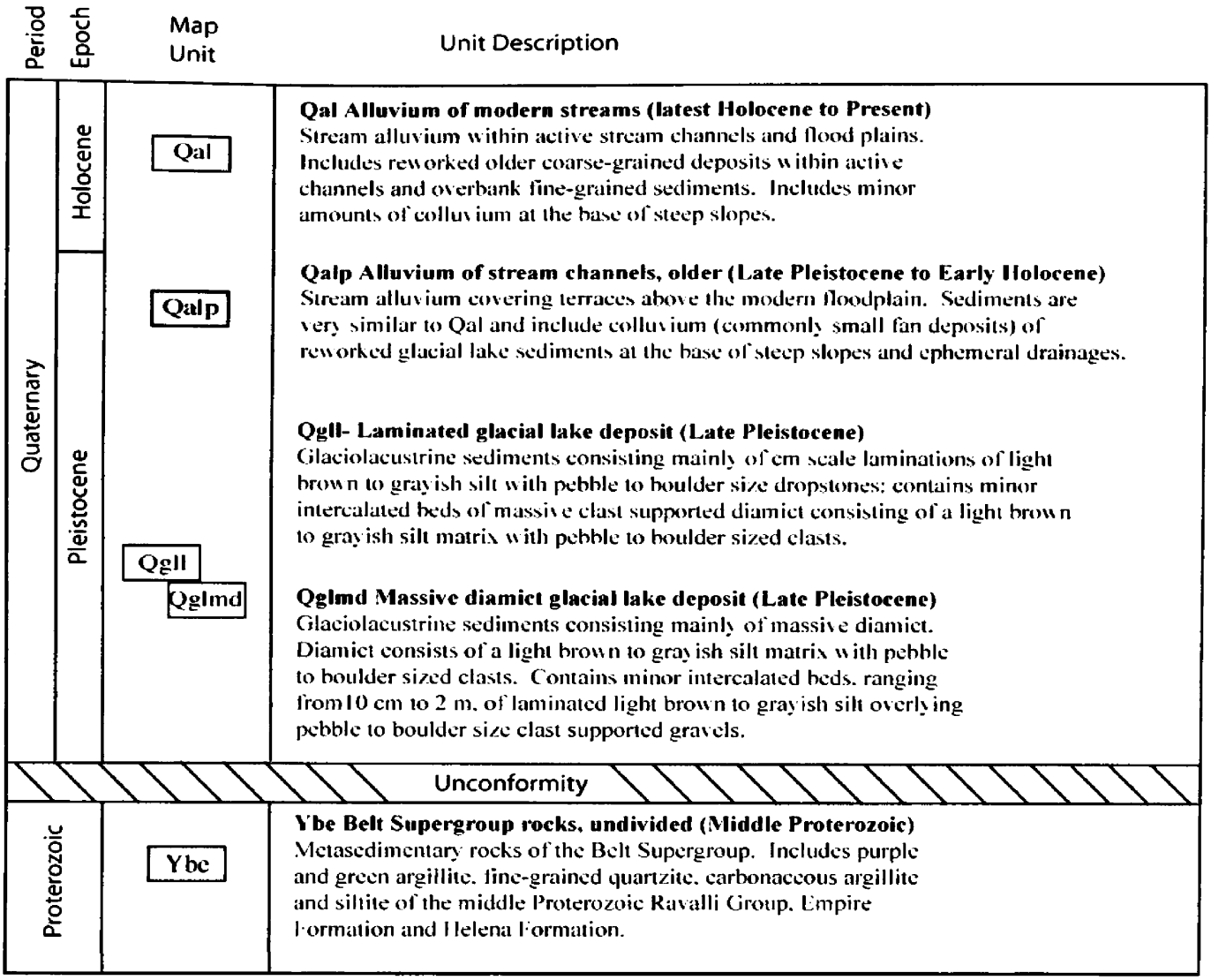

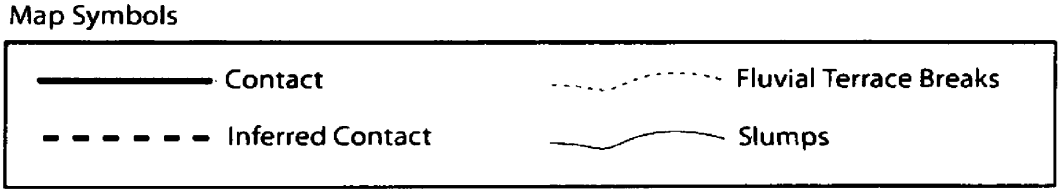

Figure 5b. Map unit descriptions of the lower Flathead River valley and accompanying legend.

Figure 6. Picture of massive diamict. Also present in the photograph is an intercalated layer of gravels and fines at the bottom of the outcrop.

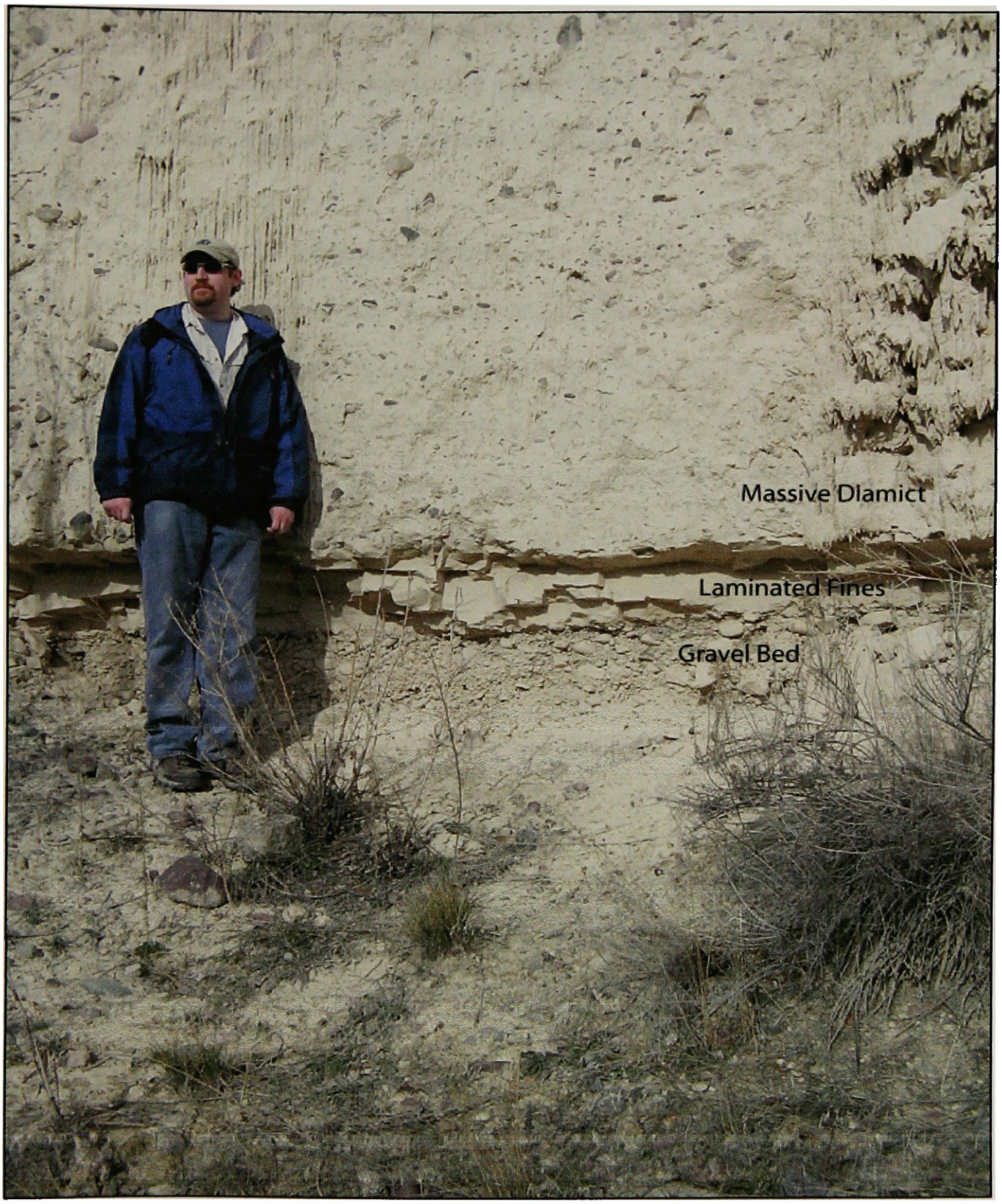

Figure 7. Picture of intercalated gravel bed with overlying laminated fines grading into massive diamict. The layer of gravel with overlying laminated silt is the same as that shown in figure 6.

angular in shape. The majority consists of argillite, siltite and quartzite of the Belt Supergroup. The matrix of the diamict is a massive light brown to grayish silt and clay. Clast supported gravel lenses within this unit (1-10m in size) are massive and show no bedding (Figure 8).

The sub-facies of intercalated beds is below the resolution of the map scale and has been included within this unit. Beds of clast supported gravels within the sub-facies lie on a gradually undulating scoured surface with less than a meter of relief. Gravel beds are generally less than a meter thick and pinch out locally. Gravel clasts range in size from pebbles to cobbles, are sub-rounded to sub-angular and similar in lithology to clasts within the diamict. Gravels are unorganized, commonly display slight upward fining, and are associated with a matrix of medium to coarse grained sand. These gravel beds are conformably overlain by beds of laminated and massive silt and clay. Silt beds are brown to grayish in color, range from 2-10cm in thickness, and contain local dropstones. The fines in these beds are generally lighter colored than the diamict matrix. Silt beds conformably grade into overlying massive diamict.

The diamict unit is well exposed along the lower Flathead River, forming steep, flat-faced, unstable cliff exposures. Other exposures exist in minor tributary drainages to the Flathead River, forming steep slot canyons with unstable badland topography.

Massive Diamict – interpretation

I interpret that the massive diamict was deposited in a glacio-lacustrine environment. The massive matrix can be attributed to high suspension settle-out rates,

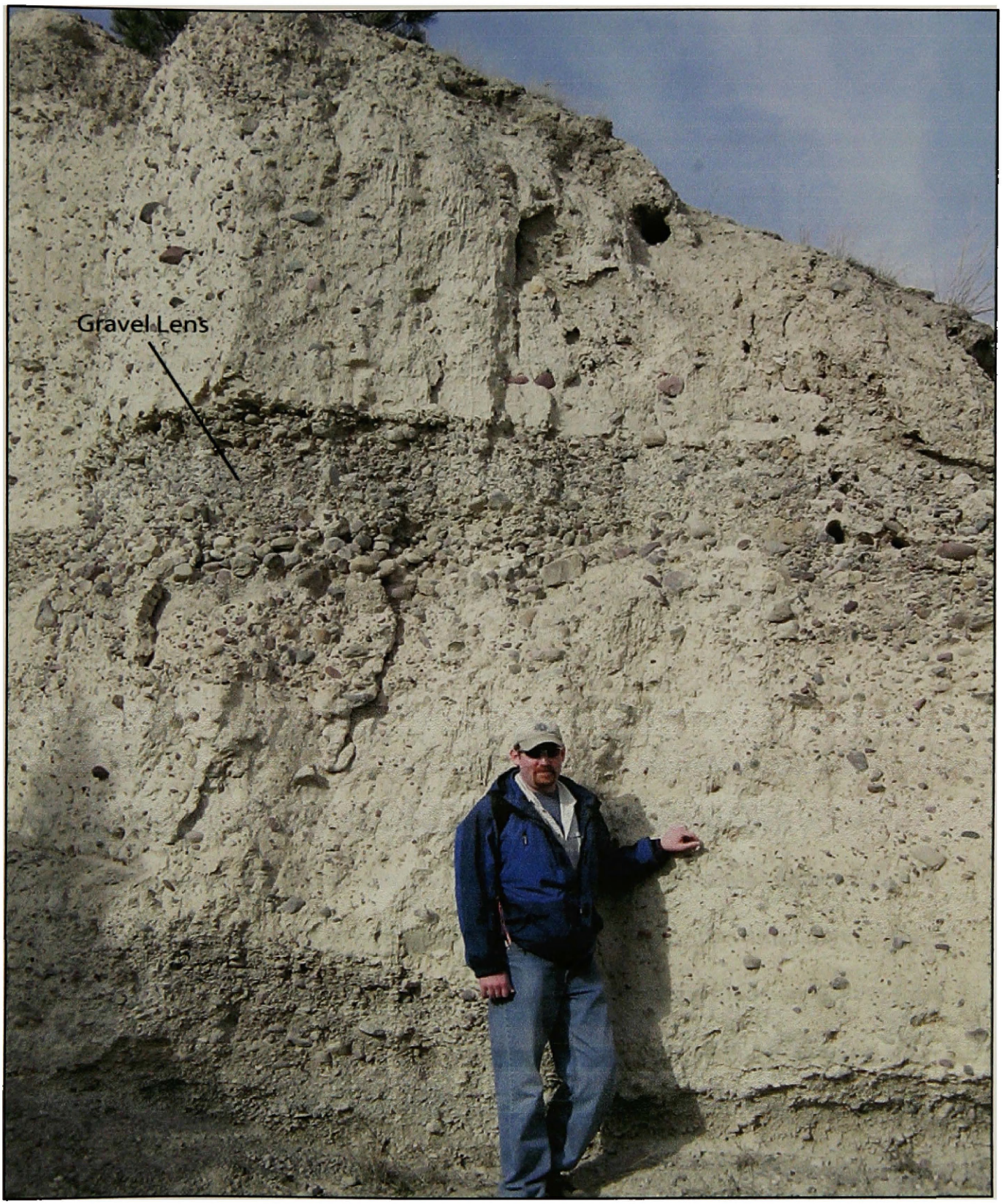

Figure 8. Picture of a gravel lens within the massive diamict. Lens is about 0.5m in height and 2-3m in width.

with the sediment-water interface being constantly disturbed by clast rainout from icebergs. This unit is analogous to facies described in models of pro-glacial lacustrine environments associated with very high sedimentation rates (Eyles and Eyles, 1983; Eyles and Miall, 1984). The gravel lenses within the diamict appear to be iceberg dump structures (Thomas and Connel, 1984). The intercalated beds of gravel and fines are interpreted to represent partial Bouma sequences deposited by sub-aqueous density flows (Bouma, 1962; Lowe, 1982; Eyles and Clark, 1987).

The glacio-lacustrine interpretation is further supported by the lack of structures indicative of ice contact (Eyles and Miall, 1984). The intercalated beds of gravel and silt can be traced for several kilometers in the area of Sloan Bridge (Levish, 1997), something that would not be expected of tills or pro-glacial fluvial outwash.

Laminated silts and clays – description

This unit consists of cm scale laminated silt and clay with pebble to boulder sized dropstones (Figure 9). Locally the unit contains thin intercalated layers of massive diamict up to 4m thick. The silt and clay has a similar light brown to gray color and composition to that of the matrix of the massive diamict unit. The unit features distinct bedding ranging in thickness from <1cm up to 1m. Most laminations are 1-6cm thick. The majority of these laminations form rhythmites of grayish white silt grading into brown clay. Dropstones are mostly cobble size sub-rounded to sub-angular argillite, siltite and quartzite that tend to deform underlying laminations and are, in turn, draped by overlying laminations. Local gravel lenses (1-6m in length 0.5-2m in height) exist within

Figure 9. Laminated silt and clays within the map area; (a) Exposure along the lower Flathead River, white bar is about a meter in height; (b) Close up of an exposure with dropstones highlighted by arrows.

this unit and severely disrupt surrounding laminations. Diamict beds varying in thickness between 0.5 and 2m and are mostly present in the southern end of the unit near the contact with the massive diamict.

This unit is interfingered with the massive diamict unit. The contact between the two units has been mapped along a zone where the majority of outcrop (60-70%) is laminated silts and clays. The two units interfinger for about 1/2km north and south of the mapped contact, and diminish with distance from the mapped contact.

This unit is well exposed along the banks (mainly cut-banks) of the Flathead River and along actively eroding confluent drainages. This unit erodes very quickly, progressing from badland topography to steep hill slopes with dendritic erosional patterns. Where this unit has formed slopes it commonly is slumped, indicating high instability even with a vegetative cover (Figure 10).

Laminated silts and clays – interpretation

I interpret this unit as a varved glacio-lacustrine deposit (Agterberg and Banerjee, 1969; Ashley, 1975; Ashley, 1995). Local clasts are dropstones from iceberg rainout, and gravel lenses are likely iceberg dump structures (Thomas and Connel, 1984). The intercalated layers of diamict were deposited by periods of increased sediment input into the glacio-lacustrine environment.

This unit exhibits significantly fewer pebble to boulder sized clasts than the massive diamict unit and mostly occurs in the northern part of the map area (Figure 5a). Bedrock highs associated with Buffalo ridge and the Valley View hills apparently

Figure 10. Pictures of slumps within the laminated silts and clays; (a) Slump in sediments with vegetative cover; (b) Slump blocks along the lower Flathead River.

dammed icebergs and diverted sub-aqueous sediment flows from glacial input to the north and east (Figure 11). The interfingering between this unit and the massive diamict in interpreted to reflect variances in sediment input into the glacio-lacustrine system. This unit is interpreted to be temporally concurrent with the massive diamict unit.

Alluvium of stream channels, older – description

This unit is characterized by 3-6m of open framework gravel beds overlain by 0.5-1m of faintly laminated silts and clays (Figure 12). These deposits are located in

terraces with 6 to 12m risers and flat treads that range in width from 10 to several hundred meters dependent on location and surrounding morphology. Small alluvial fan deposits exist along the treads, originating from erosion of adjacent terrace risers or the adjacent glacio-lacustrine deposits. The terraces are cut by the modern flood plain and channel and are dissected by ephemeral drainages.

Gravel beds in this facies are clast supported. Clasts are sub-rounded to sub-angular, range in size from cobbles to pebbles, and display a slight upward fining. Clasts are composed mostly of argillite, siltite and quartzite of the Belt Supergroup. Overlying silt and clay is brown to light gray in color and has faint horizontal laminations at a millimeter scale. Thin horizontal layers (1-4mm) of medium to fine grained sand and small pebbles are commonly interbedded with these overlying fines.

One terrace deposit has a volcanic tephra within the silt and clay series (Figure 12). The tephra layer is 1 to 2cm thick, fine grained, and white in color and has been determined to be the Glacier Peak tephra (Sperazza, in prep; Foit et al., 1993) dated at 13,180 cal yr BP.

At the outlet of Buffalo Canyon, a large bedrock canyon that confines the lower Flathead River (Figure 4) is a terrace series containing large boulders (2-6m) that are angular and imbricated. These boulders gradually decrease in size downstream over the distance of ~1/2km to 1 meter and less, but remain angular and imbricated (Figure 13).

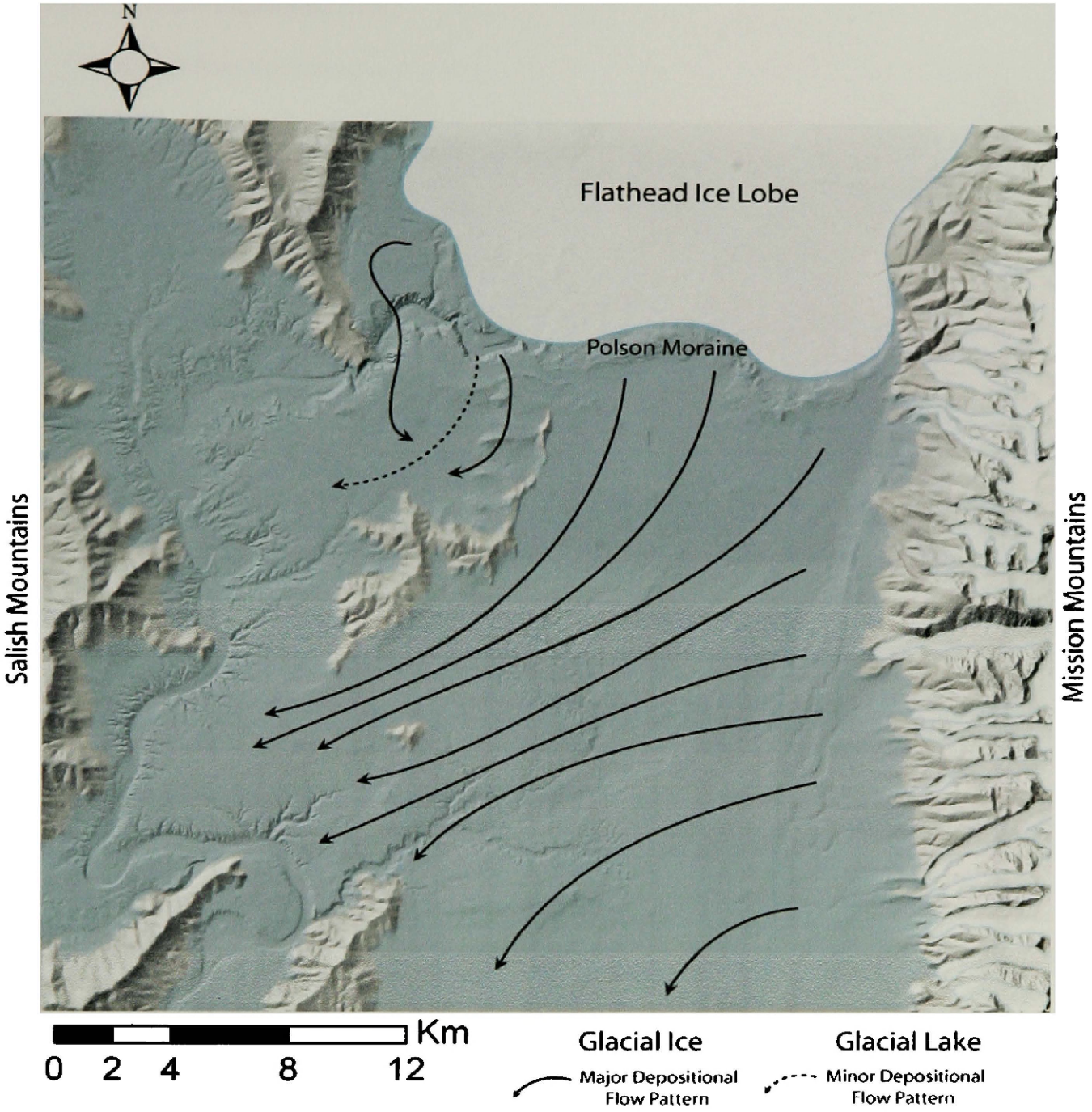

Figure 11. Schematic reconstruction of the Mission Valley during the last glacial maxima. The Flathead Ice Lobe and several glaciers from the Mission Mountain Range (shown in white) provide sediment input into glacial Lake Missoula (shown in blue). Depositional flow patterns within the Mission Valley are heavily influenced by the topographic expressions of Buffalo Ridge and the Valley View Hills, which limit sediment input to the north-eastern portion of the Mission Valley.

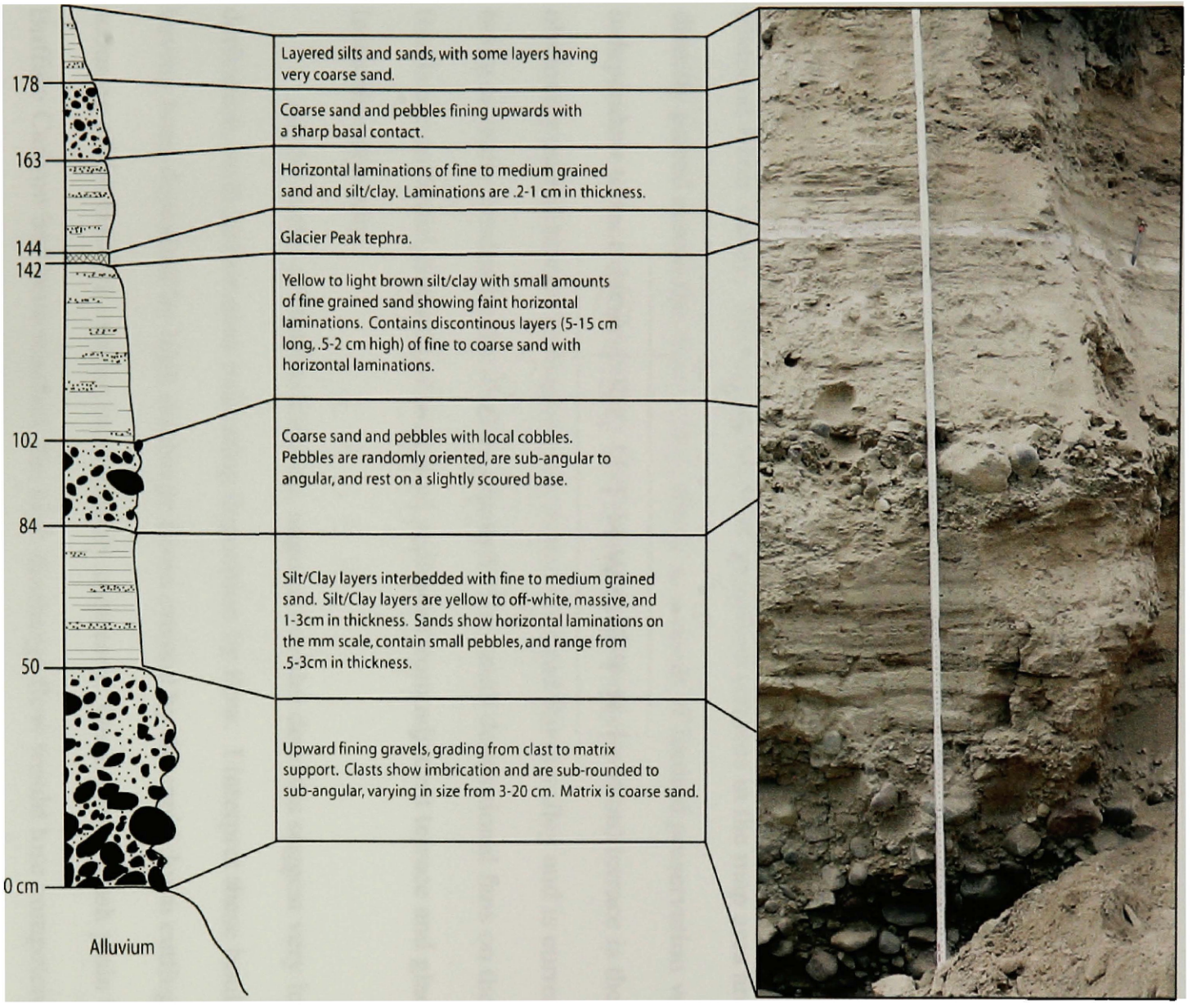

Figure 12. Stratigraphic section of the Sloan fluvial terrace deposit containing the Glacier Peak tephra. Pencil for scale in upper right of photograph.

Alluvium of stream channels, older – interpretation

I interpret that the terraces making up this unit are fluvial depositional terraces. The gravel layers represent fluvial channel deposits and the overlying fines represent over-bank deposits (Miall, 1996; Wegmann and Pazzaglia, 2002). The terraces record changes in the flow regime of the lower Flathead River with individual terraces representing periods of stability and aggradation of the lower Flathead River. Multiple changes in flow regime are indicated by terrace series along the lower Flathead River (Figure 14). Terrace preservation is limited due to frequent changes in flow regimes of the Flathead River related to deglaciation and due to the narrow character of the lower Flathead River valley. The majority of the preserved terraces in the map area are not directly paired across the river valley, likely as a result of limited preservation versus independent terrace development. The youngest (lowest elevation) terrace is the only obviously paired terrace throughout the lower Flathead River valley and is currently being laterally eroded by the modern channel. The small depositional fans on the terrace treads are colluvial deposits of reworked sediment from adjacent terrace and glacio-lacustrine deposits.

At the outlet of Buffalo Canyon, angular boulder deposits suggest very local derivation, with imbrication indicating deposition by flow. I interpret these boulders as having been deposited by high discharge flows created by the rapid down cutting and scouring of the bedrock canyon immediately upstream. Once the outwash plain below Buffalo Canyon had been reached, the high discharge flow would lose competence, causing rapid deposition of the boulders. This interpretation is supported by the downstream decrease in mean boulder size (Figure 13).

Figure 13. Characteristics of the fluvial terrace at the outlet of Buffalo canyon. In the top photograph the camera is looking west, southwest. (a) Large, imbricated, and angular boulders at the mouth of the canyon. Camera is looking north, northwest. Distribution marked by the solid white line in the top photo. (b) Smaller boulders further downstream occurring within the dashed white line in the top photo.

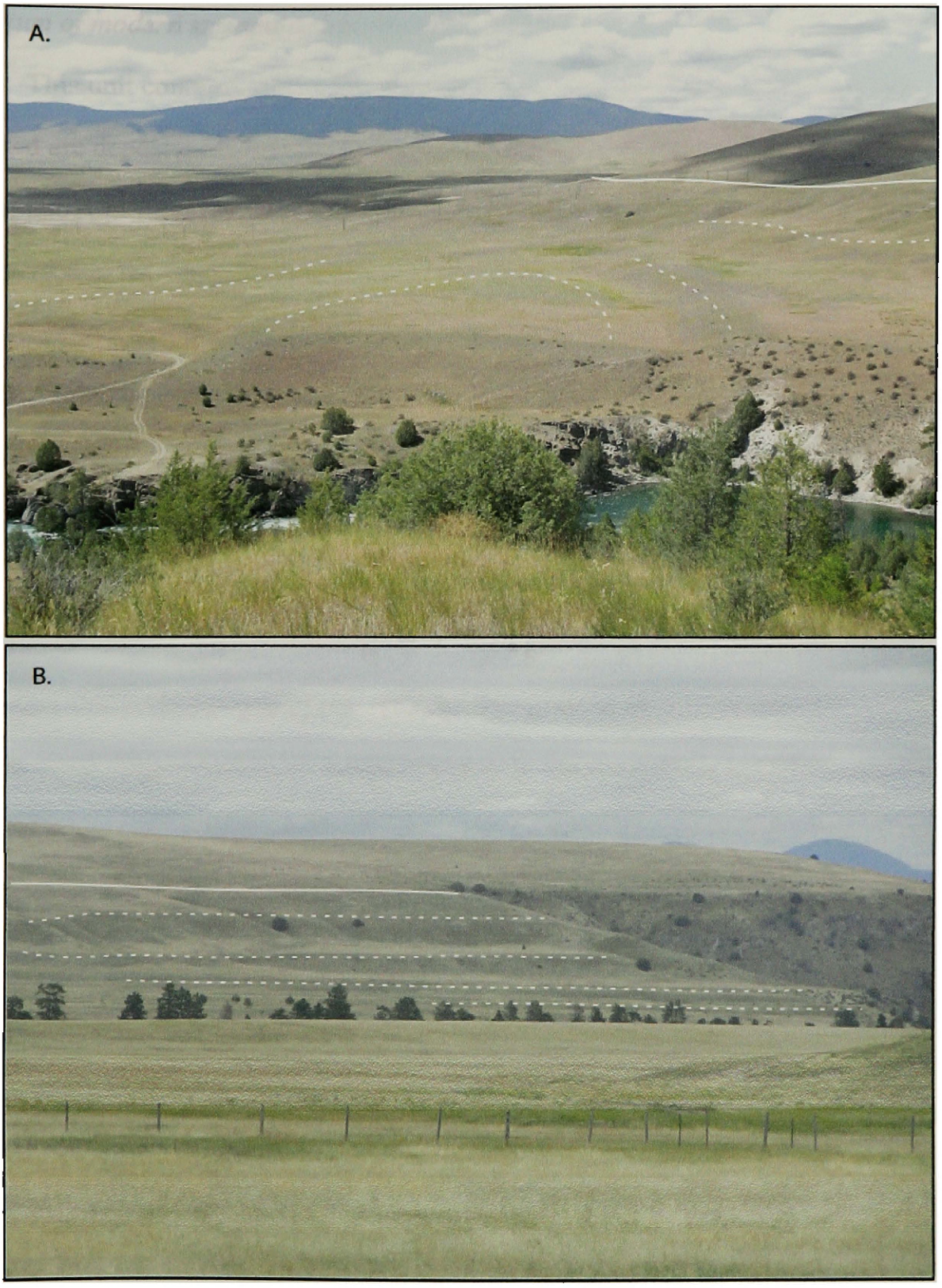

Figure 14. Fluvial terraces along the lower Flathead River. The solid line shows the uppermost surface of glacio-lacustrine sediments cut by the river. The dashed lines highlight the slope breaks between consecutive terraces. A. View looking north-northwest from across the river. B. View looking northeast towards the outlet of Buffalo Canyon.

Alluvium of modern streams – description

This unit contains alluvium within active stream channels and flood plains. Included are deposits of clast supported sub-angular to sub-rounded cobbles and pebbles, with a matrix of fines ranging from coarse sand to silt. A few sub-rounded boulders are interspersed in the streambeds across the map area. Overbank deposits consist of fine-grained, yellow to light brown silt. Depositional fans consisting of colluvium are common at the base of steep slopes.

Alluvium of modern streams – interpretation

This unit represents the modern deposits of the lower Flathead River and confluent drainages. The cobble to pebble-sized gravels in stream beds are reworked from older coarse-grained deposits, with the fine-grained over bank deposits representing modern flood-stage deposition. Large boulders in the streambeds have been eroded out of the adjacent glacio-lacustrine sediment. The modern channel is degrading its bed with significant lateral erosion as the lower Flathead River increases its sinuousity.

Discussion

I interpret the massive diamict and laminated silts and clays to have been deposited in glacial Lake Missoula. The distribution of these units within the map area conforms well to previous interpretations that bedrock highs in the Mission Valley influenced deposition in the glacio-lacustrine environment, with the laminated silts and clays accumulating in protected areas downstream of these bedrock highs, and the

massive diamict being deposited where these highs did not provide a barrier to flow (Figure 11; Levish, 1997).

After the final draining of glacial Lake Missoula, the development of the lower Flathead River valley began. This process was largely controlled by the drainage of ancestral Lake Flathead. Ancestral Lake Flathead was impounded by ~45m of unconsolidated sediment from the Polson moraine and a bedrock ridge that the lower Flathead River has since incised 60-78m (Smith, 2004). Down-cutting of unconsolidated sediments of the Polson moraine was likely rapid, as was erosion and down-cutting of unconsolidated glacio-lacustrine sediments along the lower Flathead River. Once the bedrock spill-point at the outlet of ancestral Lake Flathead was reached, rates of down-cutting would have been greatly reduced, and discharge along the lower Flathead River would have stabilized. Smith (2004) made conservative calculations of bedrock incision rates of 0.9-1.3m 100 year $^{-1}$ for the uppermost 35-50m of the bedrock dam.

The majority of down-cutting of this bedrock spill-point resulted from high discharge flow events scouring the spillway. A series of anomalously coarse "event beds" immediately overlie terminal glacio-lacustrine varved sediments in cores from Flathead Lake and may be attributed to meltwater surges from the retreating Flathead Lobe (Figure 15; Hoffman, in prep.). These beds are located beneath the Glacier Peak tephra (13,180 cal yr BP) and overlie glacial varves that yielded a radiocarbon date of 14,150 cal yr BP in core FL-03-19K.

Evidence of rapid down-cutting of the Polson moraine and the bedrock spill-point is present in the angular boulder deposits at the mouth of Buffalo Canyon. Although there is only one series of terraces containing large boulders, evidence of multiple phases

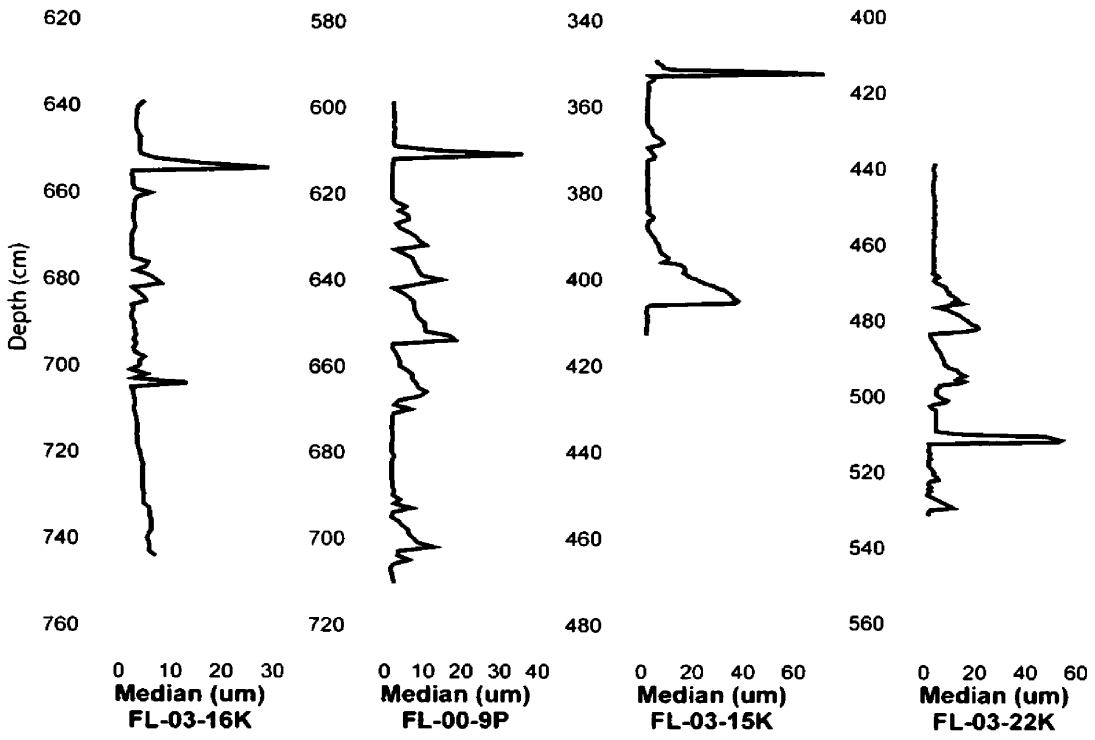

Figure 15. Median grain size (μm) versus depth from four cores showing abrupt increases in grain size interpreted to be turbidite deposits or 'event beds.'

of rapid down-cutting is suggested by the series of well-defined terraces along the hill-slopes below the canyon outlet (Figure 14). Outburst flooding associated with rapid down-cutting likely initiated terrace formation (Ritter, 1982; Harden, 2004). Four distinct terraces exist at the mouth of the canyon, with the lowest elevation terrace containing the large boulder deposits. After the series of rapid down-cutting events I infer there to have been a significant period of channel stability, during which time the Glacier Peak tephra was deposited and preserved in the Sloan terrace deposit (Figure 12). This period of channel stability is supported by the presence of a well-developed terrace pair that is preserved along the lower Flathead River at elevations above the modern channel (5-8m) similar to that of the Sloan terrace.

Seismic and recovered core data suggest a shift in early Holocene climate that greatly lowered the level of Flathead Lake (Hoffman et al., in press), significantly reducing flow to the lower Flathead River to the point where it became an ephemeral or dry stream. Following this low-stand, the Flathead Lake level surface began to gradually rise to its present level (Hoffman et al., in press). During this time the lower Flathead River had stable input flows and began to meander across its valley, as it does today. Bedrock control points along the channel, one near the location of Kerr dam and another at Finley Point, contributed to this channel stability. Although the bedrock spill-point at the location of Kerr dam was very influential on the development of the lower Flathead River, the bedrock at Finley Point is incised by only 2-3m and is below the elevation of the youngest terraces in the region, suggesting that this erosion occurred in the late Holocene.

IV – Paleomagnetic age correlation of Flathead Lake sediments

Methods

Nine cores rangin in length from 6.9 to 10.3m were selected for magnetic analysis based upon proximity to available seismic lines, spatial distribution throughout the lake basin, and core quality (Figure 1). Core collection was completed in 2000 and 2003 using a Kullenberg piston-coring device. Cores were cut into 1.5m sections and transported to the Limnology Research Center at the University of Minnesota for splitting, multi-sensor logging, digital imaging, and initial sampling. The core sections were then returned to the University of Montana for further study and refrigeration.

Split cores were sub-sampled for magnetic analysis at the University of Montana, using plastic U-channels that have a square 2cm cross-section and lengths matching the sampled core sections, generally 1.5m. Split core surfaces were cleaned, and U-channels were pressed upside down into the center of the section's flat face. The U-channels were then extracted by stretching monofilament-fishing line across the U-channel bridge, then running the line down the length of the U-channel such that it cut the mud across the bridge of the U-channel. The mud within the U-channel was then lifted out of the main core section, using the fishing line to aid in lifting of the U-channel. Upon complete separation from the main core, U-channels were capped and cleaned of extraneous sediment. The ends of each U-channel were sealed with plastic sheeting to prevent desiccation.

U-channels were measured at UC Davis' Paleomagnetism Laboratory using a 2-G Enterprises Model 755 Cryogenic Magnetometer (Verosub, 1998) featuring three

orthogonal DC SQUIDs (Superconducting Quantum Interface Device) optimized for the study of U-channels (Nagy & Vallet, 1993, Verosub et al., 2001). The system automatically corrects for offset and drift of the SQUIDs as well as for magnetization of the sample tray (Verosub et al., 2001). The instrument contains an in-line three-axis alternating field demagnetizer, which was used for automated step-wise demagnetization of the samples. The samples of seven cores (FL-00-7P, FL-00-8P, FL-00-9P, FL-03-15K, FL-03-16K, FL-03-19K, and FL-03-22K) were subjected to peak alternating fields of 0, 5, 10, 15, 20, 25, 30, 40, 50, and 60 mT. Once the samples were determined to have only one significant component of magnetization, demagnetization steps were reduced to 0, 10, 20, 30, 40, 50, and 60 mT for the remaining two cores (FL-03-14K and FL-03-26K) to reduce measurement time. Measurements were made after each demagnetization step at a measurement interval of 1cm, with measurements extending 10cm beyond the U-channel in both directions.

Although measurements were taken every cm, individual measurements cannot be considered independent due to the response curves of the SQUID detectors (Nagy and Valet, 1993). Response curves for the SQUIDs are measures of the intensity of a dipole point source passing through the instrument. The spatial resolution of the SQUIDs is determined by the half-power width of the response curve, in this case 4.5 cm (Weeks et al., 1993, Verosub et al., 2001). Although there is a lack of independence between the measurements, the SQUIDs still provide enough spatial resolution for the detection of short-length stratigraphic features on the order of 3 to 5cm (Nagy and Valet, 1993).

Initial data processing was completed using an Excel macro to convert the measured orthogonal components into the corresponding inclination, declination and

intensity vector components. Data from the first and last 5cm of each U-channel were deleted before the sections were combined to construct full-core curves with 10cm gaps in the data between sections, as measurements off of the end of the U-channels are affected by the aforementioned response curves.

Vector component diagrams, or Zijderveld diagrams, were used for initial analysis of the measured data (Figure 16). From these diagrams I concluded that the sampled sediments have only one component of magnetization that is generally isolated by the second demagnetization step. The majority of the slight magnetic overprint present is attributed to effects from the coring procedure, but may also be in part due to chemical remagnetization from the initial stages of diagenesis. Due to the directional variances of the magnetic vectors down the cores (20-40° in inclination, 30-100° in declination) it is concluded that the measured vectors represent the preserved paleomagnetic secular variation, and do not represent viscous remanent magnetization incurred after deposition of the sediments.

I performed principal component analysis (Kirschvink, 1980) on each core. Principal component analysis is a statistical method that combines the measured directional vectors across the demagnetization steps using a best least-squares fit. The principal component analysis was compared to the directional vectors of the 30mT step for each core with high correspondence between the two records and few minor differences across the core suite (Figure 17). Based upon the vector and principal component analyses I concluded that the 30mT demagnetization step accurately reflects the characteristic remanent magnetization (ChRM) and therefore used it for correlation.

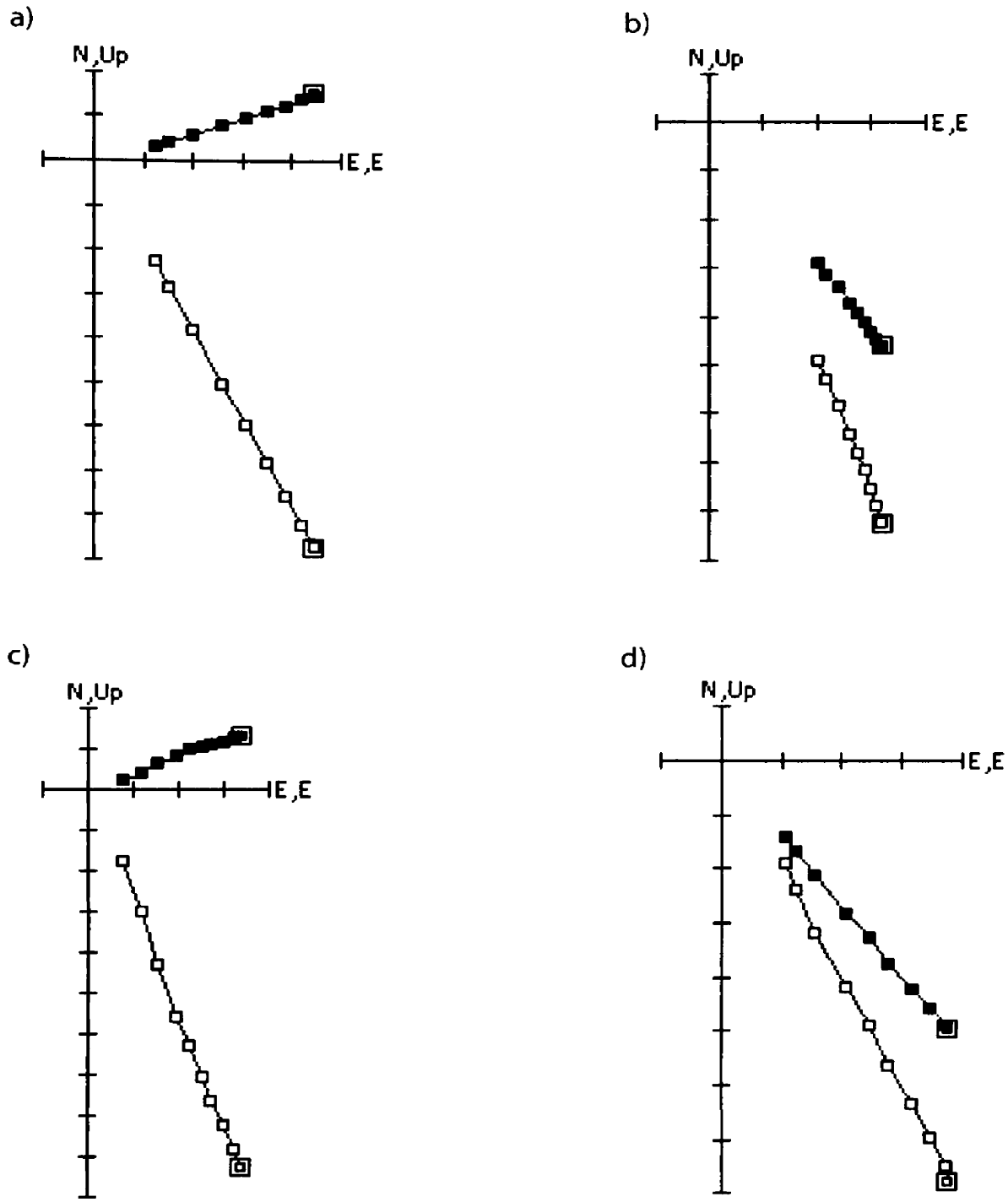

Figure 16. Vector component diagrams of four typical samples: (a) Core FL-00-9P at 2.8m; (b) Core FL-03-15K at 5.9m; (c) FL-03-16K at 2.1m; (d) Core FL-00-22K at 4.6m. Closed squares are north and east components; open squares are vertical and east components.

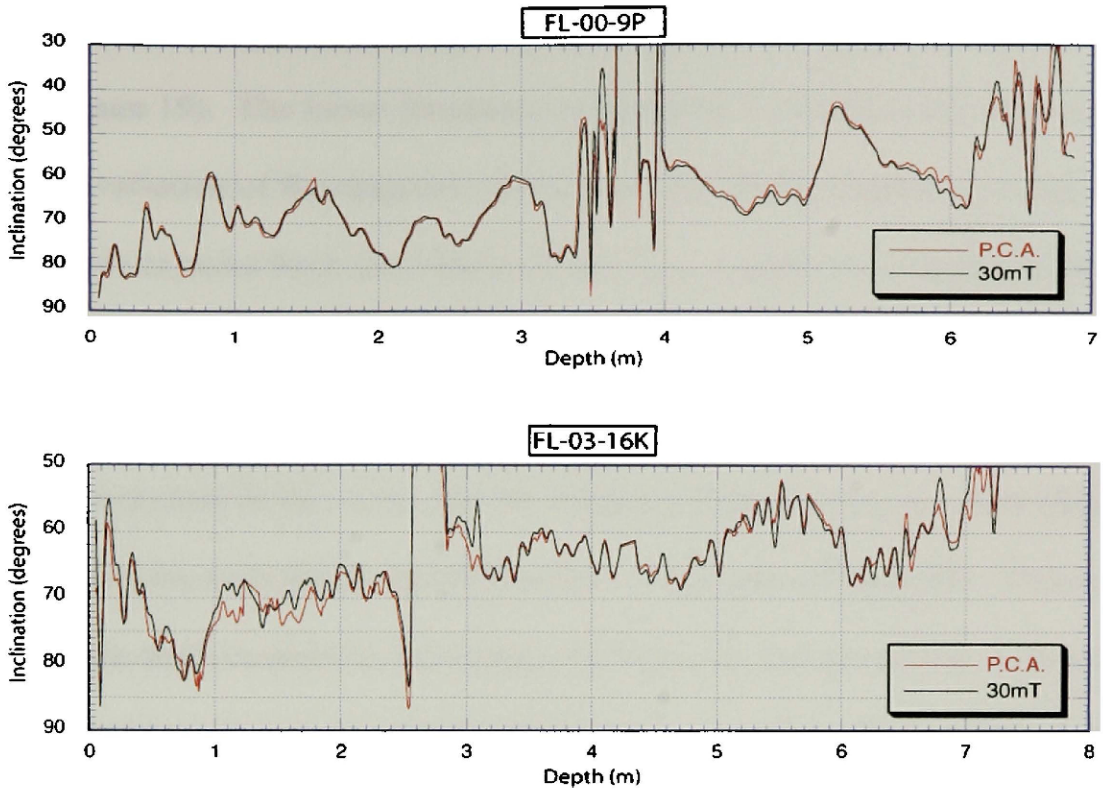

Figure 17. The principle components analysis and 30mT demagnetization step of the inclination records for cores FL-00-9P and FL-03-16K.

Data and Analysis

From the initial data processing, depth series data sets for inclination, declination, and intensity were produced (Figure 18). The declination records required directional adjustments between sections, because the core sections were not split on a common plane. For data correlation only the declination and inclination components of the measured magnetic vectors were used. The intensity component was not used in this study because that component is not only dependent upon the strength of the Earth's magnetic field at the time of deposition, but also on the quantity of detrital magnetic sediment and its mineralogy.

Upon initial examination of the curves, high and low frequency signals are apparent (Figure 19). The lower frequency component is inferred to be the recorded paleosecular variation of the magnetic field, while the higher frequency component may be related more to noise from inter-basin effects (e.g., variations in sedimentation). Based on these interpretations, the lower frequency signal was used as the primary guide for signal correlation.

Where present in the cores, the Mt. Mazama tephra produces a very large anomaly in both the inclination and declination components (Figure18). This is attributed to the high contrast in mineralogy between the tephra and the surrounding sediment. The large change in intensity produced by the mineralogy contrast erroneously influences the measurements due to the shape of the response curves for the SQUIDs (Nagy and Valet, 1993; Weeks et al., 1993). This drastic change in intensity can produce spurious measurements for both the inclination and declination components (Nagy and Valet, 1993; Weeks et al., 1993). Although the magnetic measurements of the Mt. Mazama tephra are spurious, the location of the tephra in the sediment cores and the date are known, which provides a common point of correlation across the core suite (Figure 20). The Glacier Peak tephra did not produce an anomaly in the magnetic record of the cores, but was still used as a common point of correlation (Figure 20).

The paleomagnetic secular variation (PSV) data acquired from Flathead Lake cores were correlated primarily with the well-dated record from Fish Lake, OR (Figure 20, Appendix A; Verosub et al., 1986). This record extends from 11,300 cal yr BP to the present and has been used as a regional reference record in similar studies (e.g. Hanna and Verosub, 1988; Verosub et al., 2001). A secondary reference record from Lake St.

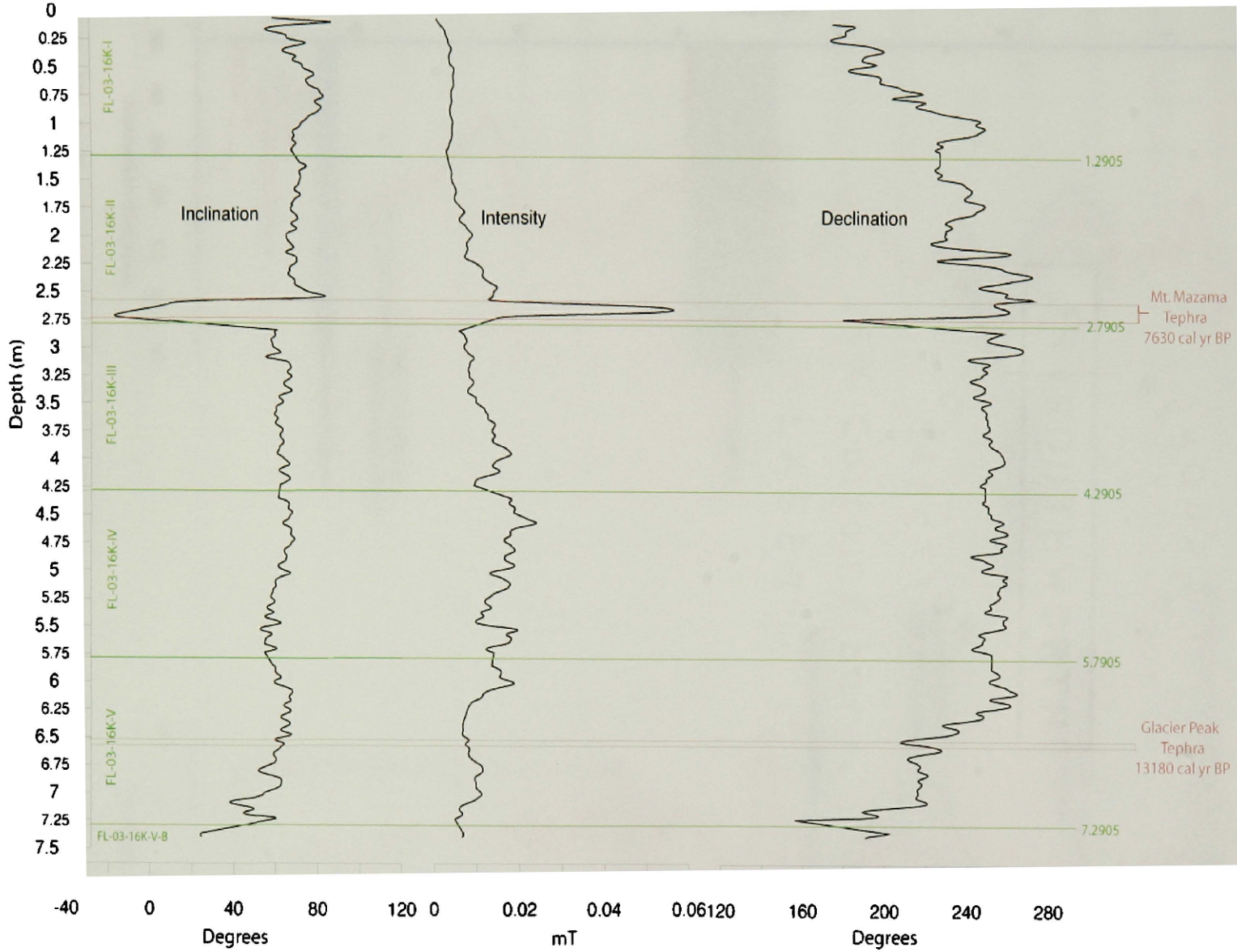

Figure 18. The compiled inclination, intensity, and declination records for core FL-03-16K showing section breaks (green lines) and volcanic tephras (red lines). Note the large anomalies in the records produced by the Mt. Mazama tephra.

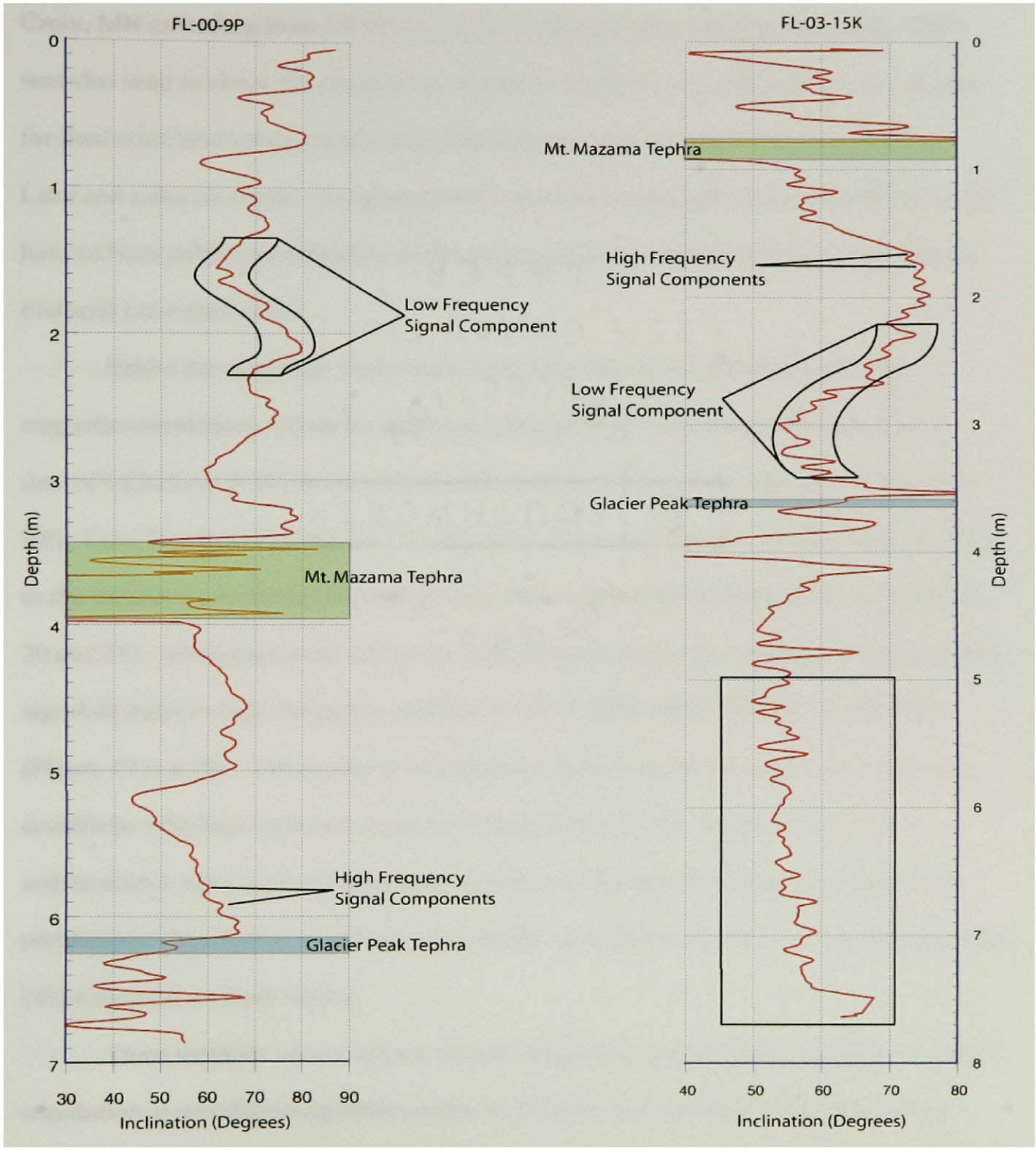

Figure 19. Inclination records for FL-00-9P and FL-03-15K at 30mT highlighting the low frequency signal components and high frequency signal components observed in the magnetic records. In FL-03-15K the signal character changes below 5m (highlighted by the black box) and features only the high frequency component.

Croix, MN extending from 10,900 cal yr BP to the present (Lund and Banerjee, 1985) was also used to check for consistency within the correlations, although it was not used for final correlation because of the significant geographic distance between Flathead Lake and Lake St. Croix. A regional PSV record extending earlier than 11,300 cal yr BP has not been published, therefore correlation beyond this date was limited to within the Flathead Lake core suite.

Below the upper age limit of the Fish Lake record (11,300 cal yr BP), the magnetic correlations within the Flathead Lake basin are constrained by only one ^{14}C date of 12,220 cal yr BP in core FL-03-16K and the Glacier Peak tephra (13,180 cal yr BP). Core FL-03-19K yielded a ^{14}C date of 14,150 cal yr BP, but this date was not used in the magnetic correlation because it came from a disturbed section of the core (Figure 20 and 25). Stratigraphically below the Glacier Peak tephra the character of the magnetic signal changes to high frequency variations with a stable low frequency component (Figure 19 and 20). This signal is interpreted to reflect glacio-lacustrine depositional conditions with high sediment input from deglaciation in the region. With high sedimentation rates such as these, determination of the secular variation component is problematic (Verosub et al., 2001). As a result, no effort was made to correlate the cores below the Glacier Peak tephra.

Three methods of correlating the paleomagnetic records were considered: visual correlation, a correlation algorithm using MATLAB, and software-aided time-series analysis (Paillard et al., 1996). The latter was chosen for the final correlations. Visual correlation is limited by the subjectivity of the person correlating the records. While certain features in the magnetic signals can be correlated with confidence, others can be

very equivocal, significantly lowering the confidence of the correlations across the records. Correlation of the records using the correlation function 'xcorr' from MATLAB's signal processing toolbox was also applied to the records in order to find an objective result that does not rely on visual correlation. Although the use of this function removes the subjectivity that limits the visual correlation, it is difficult to apply to the magnetic record of sediment cores. Variances between the cores such as differences in sedimentation rates and places where the magnetic signal may differ from local effects are not accounted for in the use of the correlation function. Software-aided time-series analysis (Paillard et al., 1996) was used to correlate the records because it combines both visual and mathematical methods in the correlation. The software, Analyseries, allows the user to visually pick tie points between the compared records while giving a quantitative measure of the correlation coefficient (Figure 21). Correlations between the records were chosen in order to maximize the coefficient corresponding to the best fit between the age record (Fish Lake) and the depth records (Flathead Lake).

For the final age-depth curves, points of correlation, tephras, and ^{14}C dates (where available) were fit using polynomial regressions (Appendix B). The order of the regressions used depended upon the number of correlation points, but ranged from 1st to 5th order, with all r-values being above 0.98. Sedimentation rates were calculated using the inverse of the slope from the fitted age-depth curves (Figure 22). A limitation to this method of correlating the paleomagnetic secular variation is the lack of statistically quantifiable error due to the dependence on visual correlation between the records. Although the correlated age record from Fish Lake, OR was constructed using ^{14}C dates, direct transfer of the ^{14}C uncertainty is not possible, because the points of correlation

A.

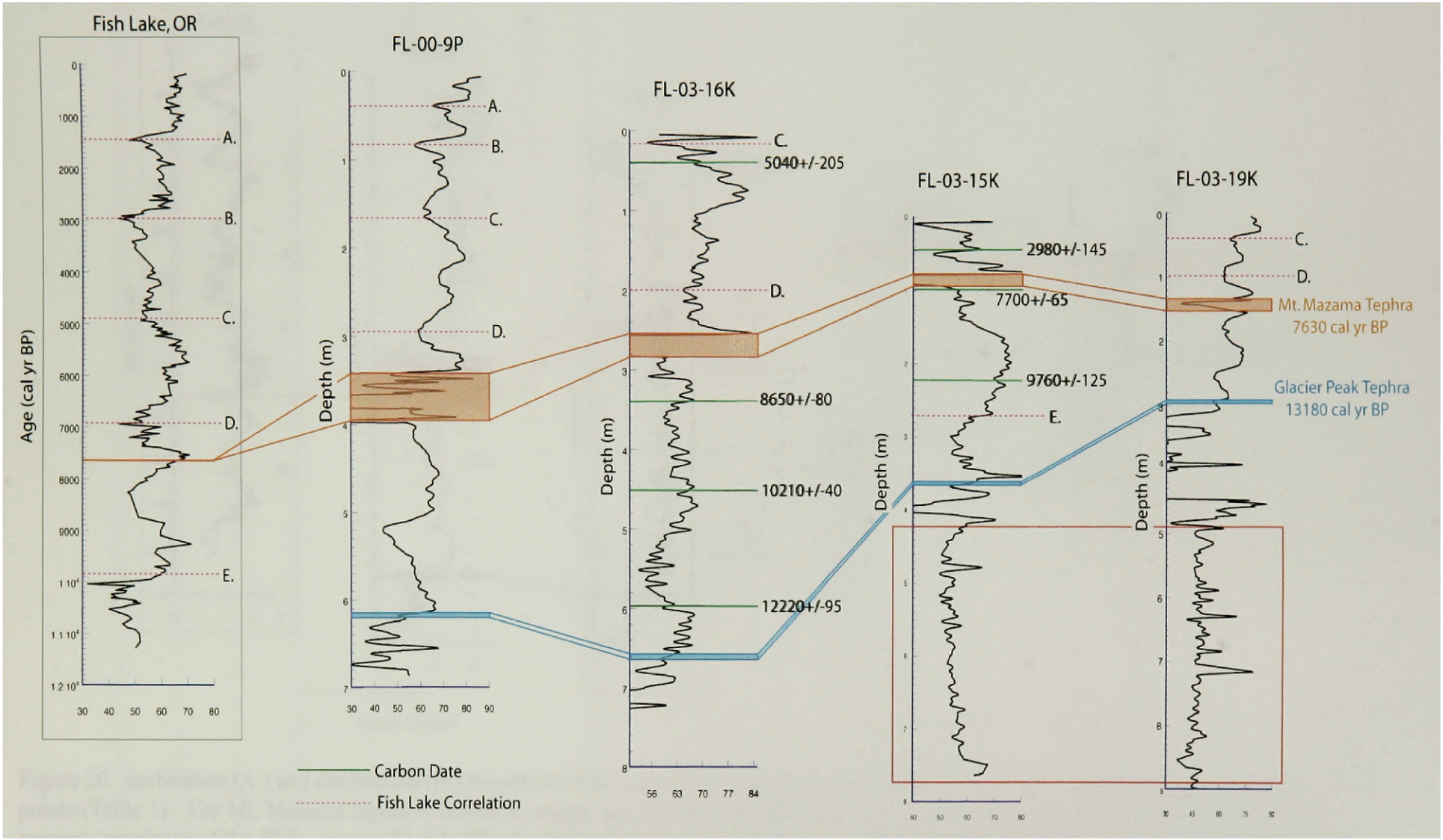

Figure 20-A. Inclination records for four cores from Flathead Lake and Fish Lake, OR. See page 45 for full description.

B.

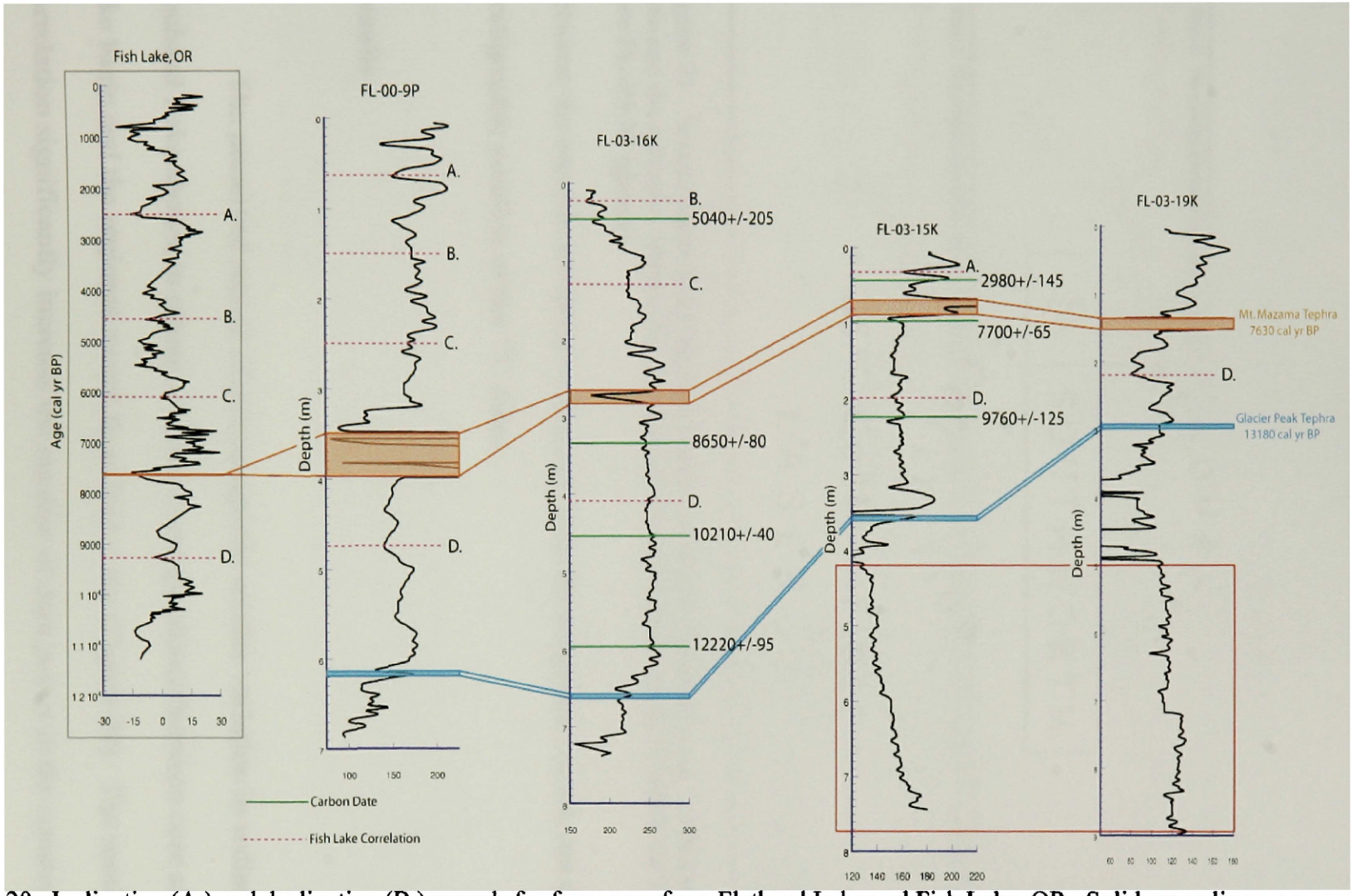

Figure 20. Inclination (A.) and declination (B.) records for four cores from Flathead Lake and Fish Lake, OR. Solid green lines represent ^{14}C date points (Table 1). The Mt. Mazama tephra is shown in orange, and the Glacier Peak tephra is shown in blue. The dashed pink lines represent general correlation of the PSV. In core FL-03-19K, the high amplitude signal from 3.5 to 5m represents a highly disturbed section of core likely incurred during core collection. In cores FL-03-15K and FL-03-19K the red box highlights a change in the signal character to a stable high frequency signal. This change in signal is interpreted to result from a significant increase in sedimentation characteristic of a glacio-lacustrine environment.

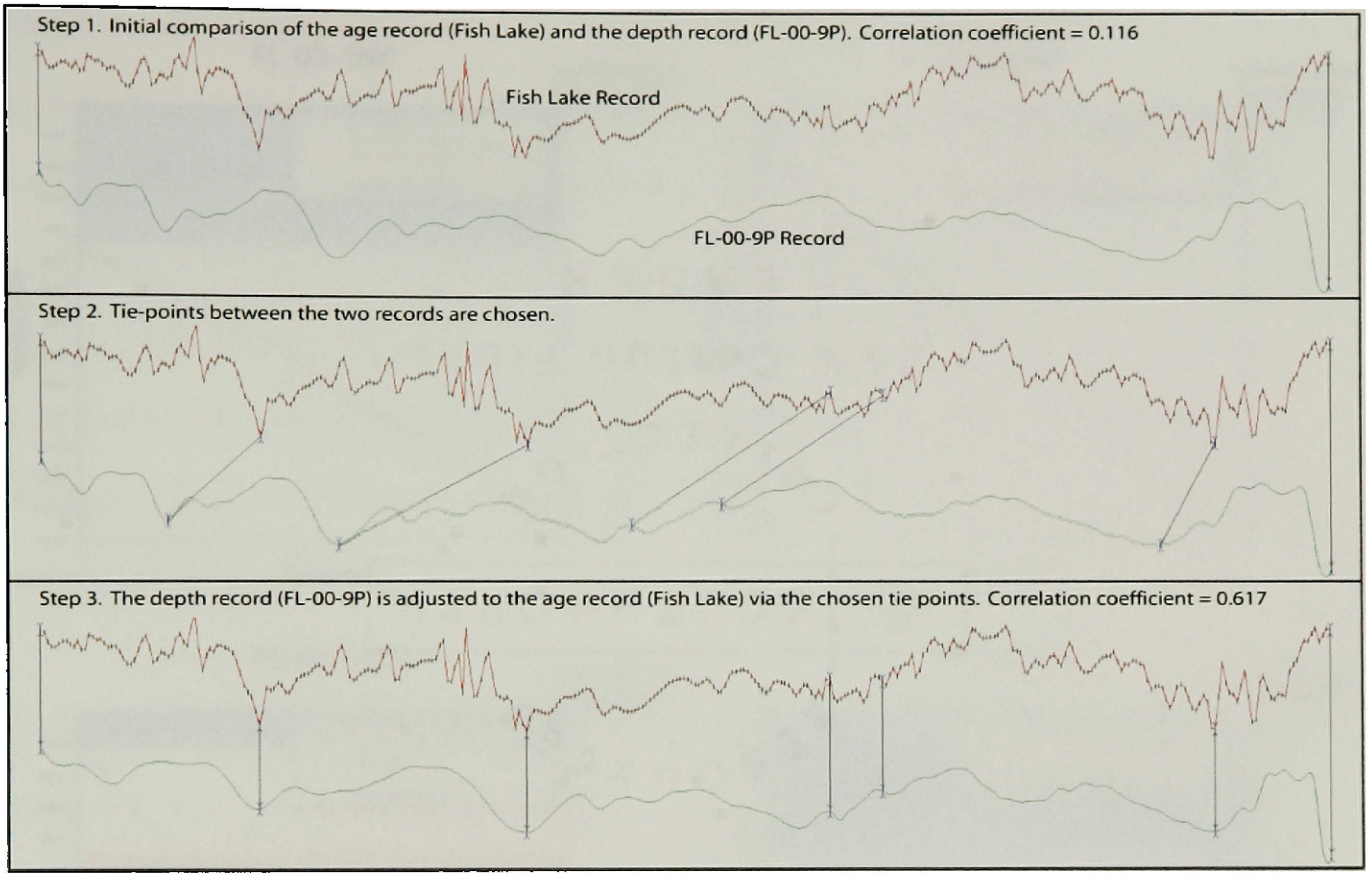

Figure 21. Screen shots from the Analyseries Software (Paillard et al., 1996) used for correlation between the records. Shown are sections of the inclination records from Fish Lake, OR (red) and core FL-00-9P (green).

between the records are made to features from the magnetic record, not the direct stratigraphic position of the ^{14}C dates.

Results

The preserved record of paleomagnetic secular variation in sediment cores of Flathead Lake shows, in places, a strong correspondence between core sites within the lake basin and the regional record from Fish Lake (Figure 20). The results of this correlation significantly increase the number of data points in the construction of age-

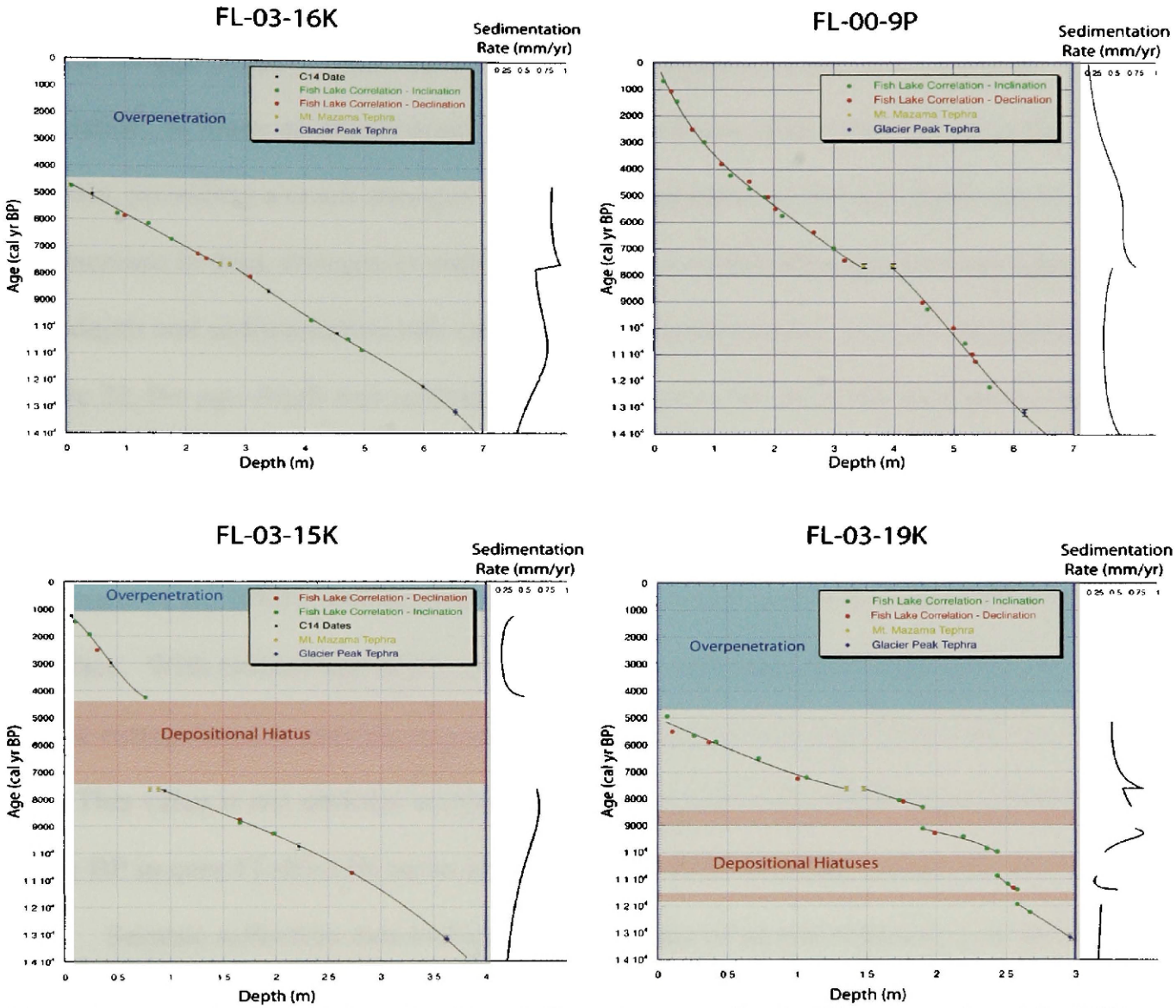

Figure 22. Age-depth models and sedimentation rate curves for 4 of 9 cores analyzed for PSV. The solid lines show age models calculated by polynomial regressions. Sedimentation rate is in mm/yr with the same age scale as the age-depth models. Improvements on the age-depth models show subtle changes in sedimentation rates, temporally constrain unconformities (FL-03-15K and FL-03-19K), and the degree of overpenetration during the core recovery process (FL-03-16K, FL-03-15K, and FL-03-19K).

depth curves for the sediment cores. Many of the sediment cores analyzed had only two tephras for age-depth control. However, with the addition of the paleomagnetic correlation, as many as twenty-four additional age-depth points were added to the analysis, providing a much stronger basis for construction of the age-depth curves. With this increase in data, changes in sedimentation rates within the cores become apparent. Age-depth and sedimentation rate curves from four representative cores are shown in Figure 22, the age-depth and sedimentation rate curves for all of the measured cores are presented in Appendix B.

During recovery, many of the sediment cores apparently over penetrated (Hofmann et al., 2003), so that the top of the core is not equivalent to the water-sediment interface. With revised age-depth curves based on paleomagnetic correlation, the data can be extrapolated to provide an estimate of the depositional age of the core top (Figure 22). This value is not uniform across the core suite, and varies from approximately 1100 cal yr BP in core FL-03-15K up to approximately 4600 cal yr BP in core FL-03-19K.

Seismic reflection data indicates the presence of an unconformity just above the Mt. Mazama tephra in shallow parts of the Big Arm Bay region (Figure 23; Hofmann et al., 2005). Core FL-03-15K was positioned to penetrate this unconformity. The presence of the unconformity in core FL-03-15K is confirmed and constrained by the paleomagnetic data (Figure 22). A maximum temporal window of 4,300 to 7,600 cal yr BP has been determined for the depositional hiatus based on the paleomagnetic data.

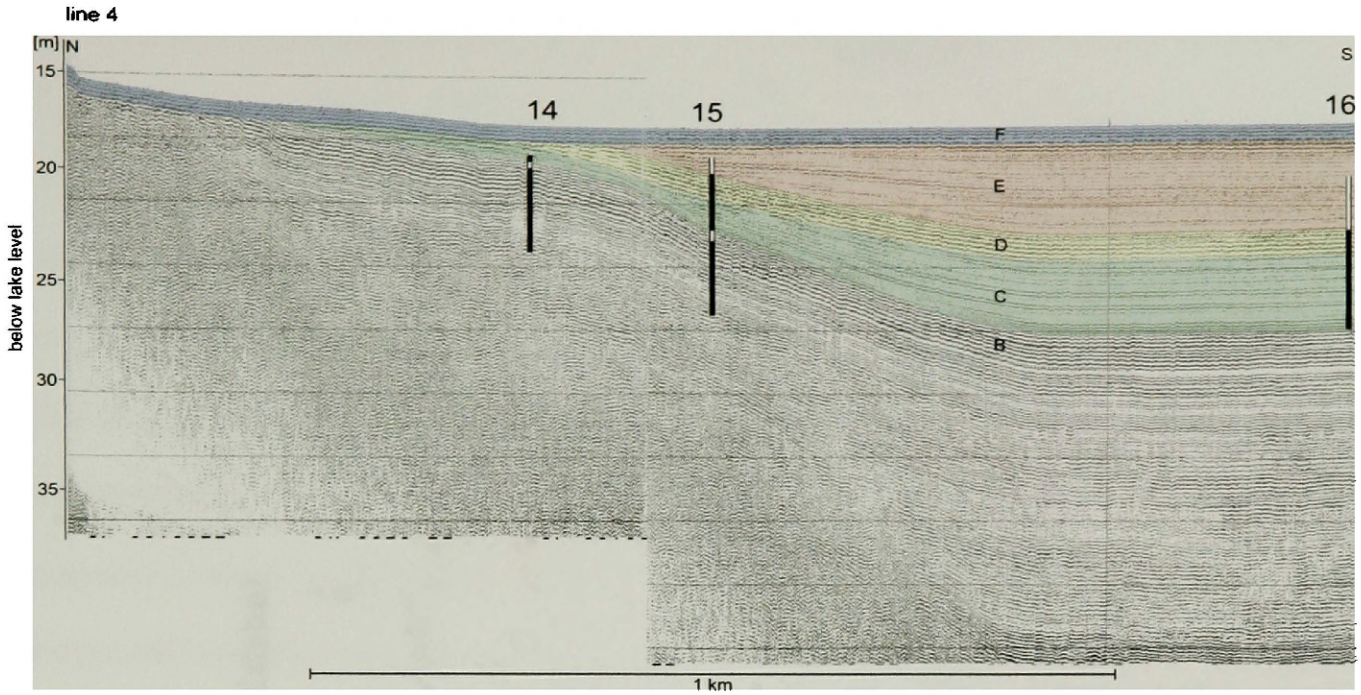

Figure 23. Interpreted seismic reflection profile with the locations of cores FL-03-14K, FL-03-15K, and FL-03-16K shown. At the base of seismic facies E (orange) is an onlap sequence indicating the presence of a depositional hiatus between seismic facies D and E. After Hofmann et al. (in press).

Correlation of the paleomagnetic data has also been used to confirm observations in other data sets collected from the core suite. Analysis of grain size data from the cores suggests three small depositional hiatuses in core FL-03-19K (Figure 22 and 24; Hofmann, in prep.). When these hiatuses are applied to the paleomagnetic data the correlation coefficients between the records improves significantly, indicating a convergence between the grain size data and paleomagnetic data (Figure 24).

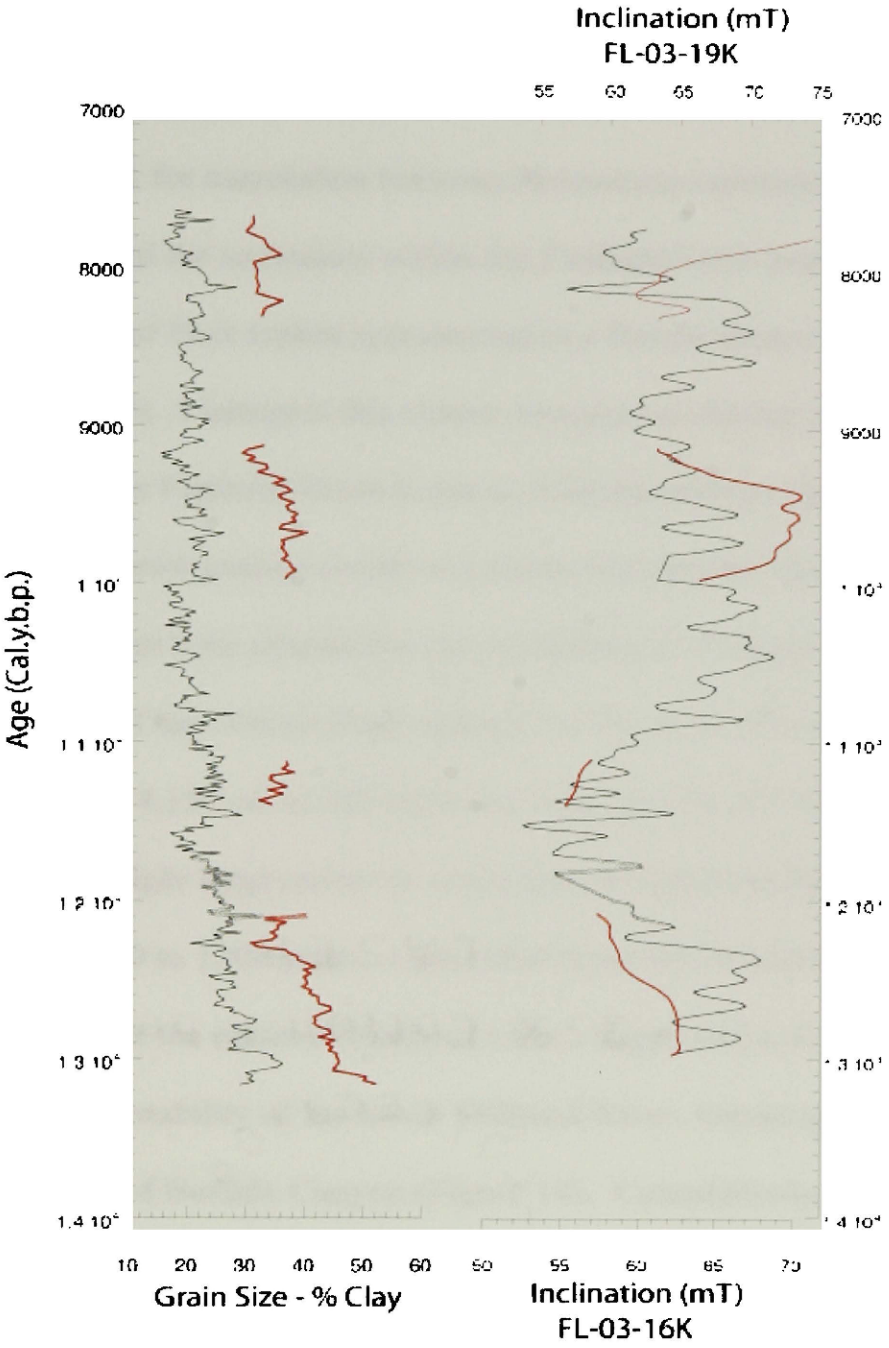

Figure 24. Grain size and inclination data for cores FL-03-16K (black curves) and FL-03-19K (red curves) between the Mt. Mazama (7,630 cal yr BP) and the Glacier Peak (13,180 cal yr BP) tephras. When the breaks in core FL-03-19K identified by grain size analysis are applied to the magnetic data, the correspondence between the records increases.

V – Correlation of mapped onshore facies with offshore lacustrine core sediments

The primary link for correlation between Pleistocene sediments exposed along the lower Flathead River and the sediments within the Flathead Lake basin is the Glacier Peak tephra. The Glacier Peak tephra is preserved in a fluvial terrace just north of the Sloan Bridge (Figure 12). I interpret this terrace to represent the last period of channel stability before the lower Flathead River began to form its modern channel. I have interpreted a series of down-cutting events and preserved terraces along the lower Flathead River with event beds observed in the sediments of Flathead Lake, all of which predate the deposition of the Glacier Peak tephra (13,180 cal yr BP) and all of which post-date a ^{14}C date of 14,150 cal yr BP collected from core FL-03-19K (Figure 25). The event beds suggest multiple large pulses of water into the ancestral Flathead Lake basin within a period from 600 to 1300 years. I infer that these floods caused rapid erosion of the bedrock spill-point at the outlet of Flathead Lake. Rapid incision of the spill-point would alter the channel stability of the lower Flathead River, initiating the development of terraces at the outlet of Buffalo Canyon (Figure 14). Cumulatively, these episodes of incision would have lowered the bedrock spill-point 35 to 50 meters, based upon the presence of the Glacier Peak tephra in eolian sediments of the northern Flathead Valley that limits the elevation of the ancestral Flathead Lake surface (Smith, 2004). A period of stability existed between these initial episodes of incision and the final episode of incision that has taken place since the deposition of the Glacier Peak tephra. This final episode of incision has exposed a large, well-preserved terrace series that locally contains the tephra. I interpret the final episode of spill-point incision to have been caused by

steady fluvial erosion that lowered the dam 10 to 20m, to near its present elevation (Figure 26). This interpretation is supported by the seismic reflection data that indicates a period of steady lake lowering and stability near the Pleistocene-Holocene transition (Hofmann et al., in press). The events related to the development of the lower Flathead River valley are all near the lower limit of accuracy for the paleomagnetic age correlation. The paleomagnetic age correlation builds a strong chronostratigraphy for the lacustrine sediments in the Holocene and latest Pleistocene, but sedimentologic and geomorphic expression of this period along the lower Flathead River is limited by the degradational nature of the channel during this period.

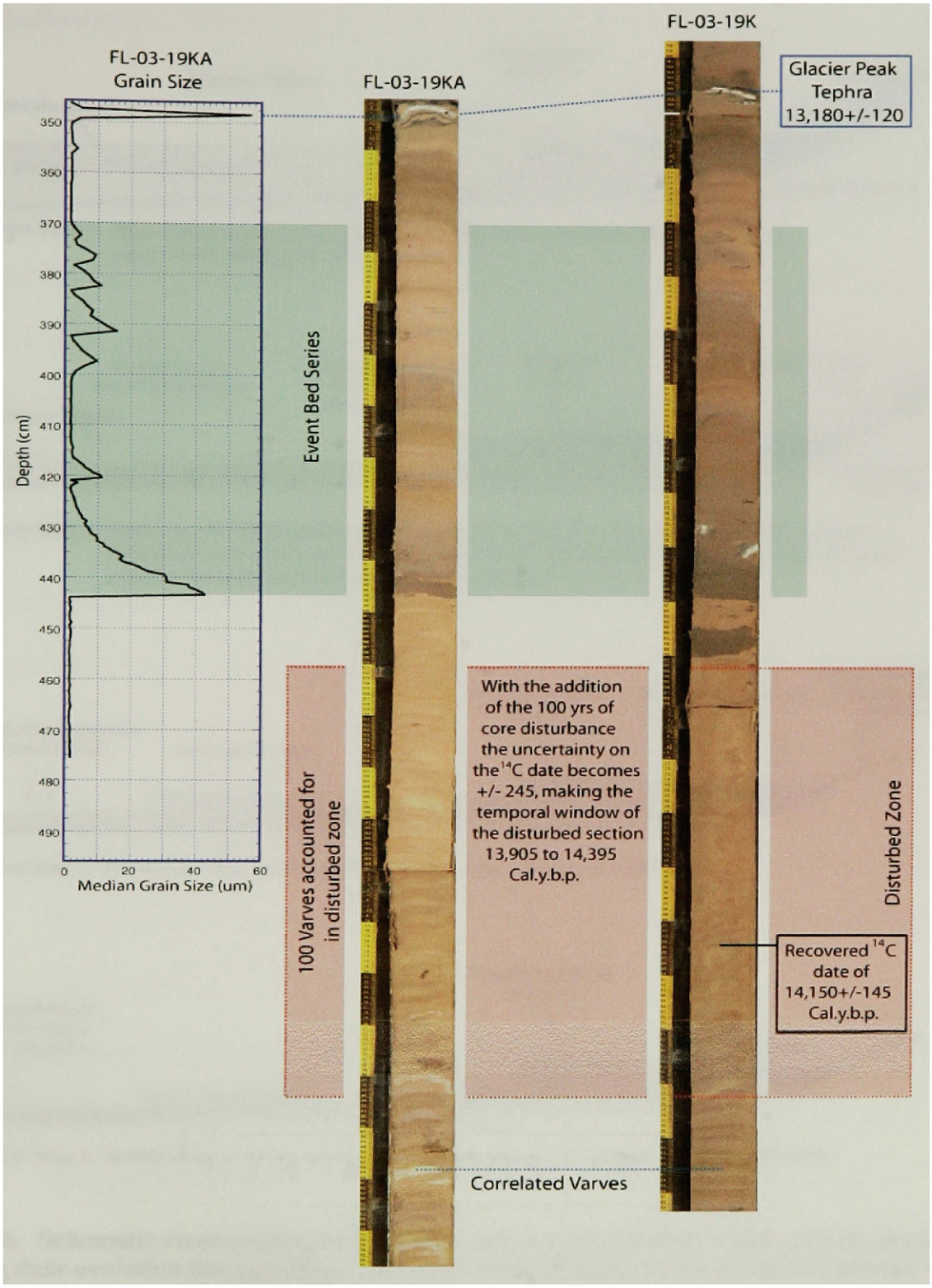

Figure 25. Core photos of two proximal cores (FL-03-19K and FL-03-19KA) showing age control on the event beds (represented by sudden increases in grain size and highlighted in green). The Glacier Peak tephra and a ^{14}C date temporally constrain the event beds. The ^{14}C date was recovered in a 0.79m disturbed section representing 100 correlated varves. This 100 years of uncertainty decreases precision of the ^{14}C date. The disturbed zone is confined below by correlated varve sequences and above by the event beds, confining it to a temporal window of 13,905 to 14,395 cal yr BP.

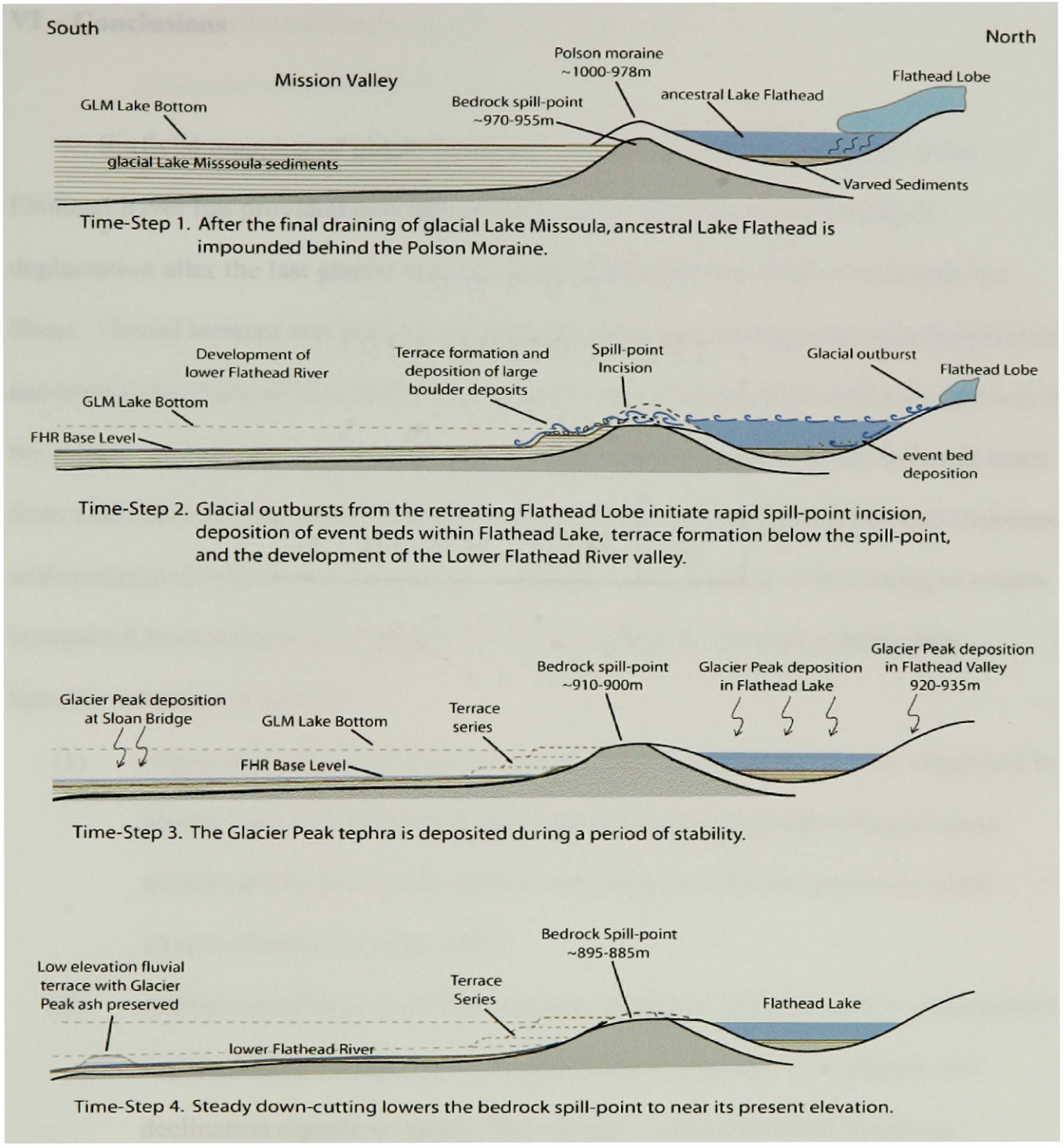

Figure 26. Schematic cross-section of Flathead Lake and the Mission Valley and the processes affecting their evolution through time. The cross-section begins in the northern Flathead Valley and runs south through Flathead Lake to the spill-point near Kerr Dam where it follows the lower Flathead River to Sloan.

VI – Conclusions

Surficial mapping of glacio-lacustrine and fluvial deposits along the lower Flathead River has provided new information on and the history and timing of deglaciation after the last glacial maxima of the Flathead Lobe of the Cordilleran Ice Sheet. Fluvial terraces and lacustrine sediments show that drainage and impoundment of ancestral Lake Flathead was influenced by meltwater outbursts from retreating glaciers in the region. Correlation of paleomagnetic secular variation trends among sediment cores from Flathead Lake has provided improved age control for late Pleistocene and Holocene sedimentation events and, by extension, improved understanding of the timing of events interpreted from seismic stratigraphic analysis of 3.5 kHz reflection seismic data. Specific conclusions include:

(1) Glacio-lacustrine sediments along the lower Flathead River were deposited in glacial Lake Missoula, with their spatial distribution supporting previous interpretations that sedimentation was influenced by the geometry of the Mission Valley (Levish, 1997).

(2) Around 14,000 cal yr BP the magnetic character of the lacustrine sediments in Flathead Lake changed from high frequency dominated inclination and declination signals to signals that include a substantial low frequency component, interpreted to represent paleomagnetic secular magnetic variation. This change in magnetic character coincides with a shift in depositional character within the Flathead Lake basin brought about by the transition from

a glacio-lacustrine environment to oligotrophic lacustrine conditions more characteristic of the Holocene.

(3) Between 14,150+/-245 and 13,180+/-180 cal yr BP the bedrock spill-point impounding ancestral Lake Flathead was down cut by 35-50m during multiple periods of rapid incision. The significant increases in incision were likely initiated by meltwater outbursts associated with deglaciation in the region that also produced turbidite deposition in the sediments of Flathead Lake. Subsequently the lowering of the spill-point changed the stability of the lower Flathead River and initiated terrace development along the river valley with large outburst floods depositing large boulders on the terrace treads.

(4) A final period of incision of the bedrock spill-point lowered it an additional 10 to 20m to near its present level, and the lower Flathead River stabilized at near its present position.

(5) Correlating the measured paleomagnetic secular variation in the Flathead Lake sediments with the well-dated record from Fish Lake, Oregon made age-depth and sedimentation rate curves for Flathead Lake sediment cores. This improved the chronostratigraphic accuracy for sediment cores and seismic reflection data.

(6) Paleomagnetic correlation of sediment cores recovered from Flathead Lake helps quantify the amount of time missing due to over-penetration incurred during core collection. The value is not uniform across the core suite, and varies from approximately 1100 cal yr BP in core FL-03-15K up to approximately 4600 cal yr BP in core FL-03-19K.

(7) A depositional hiatus recognized in the seismic reflection data has been temporally constrained by paleomagnetic data as between 4,300 and 7,600 cal yr BP in core FL-03-15K. This depositional hiatus has been interpreted to be caused by a regional shift in climate that lowered the lake level.

(8) The paleomagnetic correlations have been successfully used to confirm three depositional hiatuses in core FL-03-19K identified by grain size analysis.

References Cited

Agterberg, F.P., and Banerjee, I., 1969. Stochastic model for the deposition of varves in glacial Lake Barlow – Ojibway, Ontario, Canada: Canadian Journal of Earth Sciences, v. 6, p.625-652.

Alden, W.C., 1953. Physiography and Glacial Geology of western Montana and adjacent areas: United States Geological Survey Professional Paper 231, 200pp.

Ashley, G.M., 1975. Rhythmic sedimentation in Glacial Lake Hitchcock, Massachusetts – Connecticut. *In* A.V. Jopling and B.C. McDonald, *eds.*, Glaciofluvial and Glaciolacustrine Sedimentation, Society of Economic Paleontologists and Mineralogists Special Publication No. 23, p.304-320.

Ashley, G.M., 1995. Glaciolacustrine environments, *in* Menzies, J., *ed.,* Modern glacial environments: Boston, Butterworth Heinemann, p.417-444.

Atwater, B.F., 1986. Pleistocene glacial-lake deposits of the Sanpoil River valley, northeastern Washington: United States Geological Survey Bulletin 1661, 39p.

Bouma, A.H., 1962. Sedimentology of some flysch deposits: Amsterdam, Elsevier, 168pp.

Craig, R.G., 1987. Dynamics of a Missoula flood, *in* Mayes, L., and Nash, D. eds., Catastrophic Flooding: Allen and Unwin, Boston, p. 305-332.

Creer, K.M., Tucholka, P., 1982. Construction of type curves of geomagnetic secular variation for dating lake sediments from east central North America: Can. J. Earth Sci. v.19 p.1106-1115.

Curry, R.R., Lister, J.C., and Stoffel, K., 1977. Glacial history of Flathead Valley and Lake Missoula Floods, *in* Glacial Geology of Flathead Valley and Catastrophic

Drainage of Glacial Lake Missoula: Geological Society of America, Rocky Mountain Section 30th Annual Meeting, Field Guide No. 4, p.14-38.

Davis, W.M., 1920, Features of glacial origin in Montana and Idaho: Annals of the Association of American Geographers, v.10, p.75-148.

Elison, M.W., 1981. Relative dating of major moraines of the Southeast Jocko Valley: Northwest Geology, vol.10, p.20-31.

Elrod, M.J., 1903. The physiography of the Flathead Lake region, University of Montana, B, vol.16, p.197-203.

Eyles, C.H., and Eyles, N., 1983. Sedimentation in a large lake: a reinterpretation of the late Pleistocene stratigraphy at Scarborough Bluffs, Ontario, Cananda: Geology, v.11, p.146-152.

Eyles, N., and Miall, A.D., 1984. Glacial Facies *in* Walker, R.G., ed., Facies Models, Second Edition: Geoscience Canada Reprint Series 1, p.15-38.

Eyles, N., and Clark, B.M., 1987. Coarse-grained sediment gravity flow facies in a large supraglacial lake: Sedimentology, v.34, p.193-216.

Foit, F.F., Mehringer, P.J., Sheppard, J.C., 1993. Age, distribution, and stratigraphy of Glacier Peak tephra in eastern Washington and western Montana, United States: Canadian Journal of Earth Sciences, vol.30, no.3, p.535-552.

Hanna, R.L. and Verosub, K.L., 1988. A 3500 year paleomagnetic record of late Holocene secular variation from Blue Lake, Idaho: Geophysical Research Letters, v.15, no.7, p.685-688.

Harden, C., 2004. Terrace, River *in* Goudie, A.S. ed., Encyclopedia of geomorphology: International Association of Geomorphologists, 1156pp.

Hendrix, M.S., Sperazza, M., Gerber, T., and Moore, J.N., 2001. Sedimentary record of Late Pleistocene-Holocene transition, Flathead Lake, Montana: American Geophysical Union Abstracts with Programs v.82, p.47.

Hendrix, M.S., Bondurant, A.K., Timmerman, G., Salmon, E.L. III, 2004. Preliminary results from geologic mapping and sedimentologic analysis of late Pleistocene glacial and post-glacial deposits, southern Flathead and northern Mission Valleys, western Montana: Geological Society of America, Abstracts with Programs 36.

Hofmann, M.H. and Hendrix, M.S., 2003a. Quaternary history of the Mission Valley, NW-Montana: Results of geologic mapping: Geological Society of America, Abstracts with Programs, v.35/6.

Hofmann, M.H. and Hendrix, M.S., 2003b. Results of geologic mapping of the Mission fault system and associated Geology, Northwest Montana: Geological Society of America, Abstracts with Programs, v35/5.

Hofmann, M.H. and Hendrix, M.S., 2004. Geologic Map of the East Bay 7.5' Quadrangle, Northwest Montana: Montana Bureau of Mines and Geology, Open-File Report 496.

Hofmann, M.H., Hendrix, M.S., Moore, J.N., Sperazza, M., Shapley, M., Wittkop, C., and Stone, J., 2003. Sedimentary indicators of significant late Pleistocene- early Holocene lake level fluctuation: preliminary results from Flathead Lake, Montana: Eos Tran. AGU, 84/47.

Hofmann, M.H., Hendrix, M.S., Moore, J.N., and Sperazza, M., (in press). Late Pleistocene and Holocene depositional history of sediments in Flathead Lake,

Montana: evidence from high-resolution seismic reflection interpretation. Submitted to Sedimentary Geology in November 2004.

Hofmann, M.H., in prep. Sedimentary record of glacial dynamics, lake level fluctuations, and tectonics: Late Pleistocene – Holocene structural and stratigraphic analysis of the Flathead Lake basin and the Mission Valley, Montana, USA.

Johns, W.M., 1970. Geology and Mineral Deposits of Lincoln and Flathead Counties, Montana: Bulletin-Montana Bureau of Mines and Geology 79, 182pp.

Kirschvink, J.L., 1980. The least-squares line and plane and the analysis of paleomagnetic data. Geophys. J. R. Asron. Soc. 62, p.699-718.

Kogan, J., 1980. A seismic sub-bottom profiling study of recent sedimentation in Flathead Lake, Montana: M.S. Thesis, University of Montana, Missoula, Montana.

Levish, D.R., 1997. Late Pleistocene sedimentation is glacial Lake Missoula and revised glacial history of the Flathead lobe of the Cordilleran ice sheet, Mission Valley, Montana: unpublished PhD dissertation, University of Colorado, Boulder, Colorado, 191pp.

Lowe, D.R., 1982. Sediment gravity flows: II. Depositional models with special reference to deposits of high-density turbidity currents: Journal of Sedimentary Petrology, v.52, p.279-297.

Lund, S.P. and Banerjee, S.K., 1985. Late Quaternary paleomagnetic field secular variation from two Minnesota lakes: Journal of Geophysical Research, v.90, no.B1, p.803-825.

Martinson, D.G., Menke, W., Stoffa, P., 1982. An inverse approach to signal correlation: Journal of Geophysical Research, v.87, no. B6, p.4807-4818.

Martinson, D.G., Nicklas, G.P., Hays, J.D., Imbrie, J., Moore, T.C. Jr., Shckleton, N.J., 1987. Age dating and the orbital theory of ice ages: development of a high-resolution 0 to 300,000-year chronostratigraphy: Quaternary Research, 27, p.1-29.

Miall, A.D., 1996. The Geology of Fluvial Deposits: Sedimentary Facies, Basin Analysis, and Petroleum Geology: Springer, New York, 582pp.

Nobles, L.H., 1952, Glacial geology of the Mission Valley, western Montana [Ph.D. dissertation]: Cambridge, Massachusetts, Harvard University, 125pp.

Nagy, E.A, Valet, J.P., 1993. New advances for paleomagnetic studies of sediment cores using u-channels: Geophysical Research Letters, Vol. 20, No. 8, p. 671-674.

Ostenaa, D.A., Manley, W., Gilbert, J., LaForge, R., Wood, C., and Weisenberg, C.W., 1990. Flathead Reservation Regional Seismotectonic Study: An Evaluation for Dam Safety [Unpublished Report]: Denver, U.S. Bureau of Reclamation, Seismotectonic Report 90-8, 161pp.

Ostenaa, D.A., Levish, D.R., Klinger, R.E., 1995. Mission fault study. U.S. Bureau of Reclamation, Seismotectonic Report 94-8.

Paillard, D., Labeyrie, L., and Yiou, P., 1996. Macintosh program performs time-series analysis: EOS Trans, AGU, 77, p.379.

Pardee, J.T., 1910. The glacial Lake Missoula: Journal of Geology 18, p.376-386.

Pardee, J.T., 1942. Unusual currents in glacial Lake Missoula: Geological Society of America Bulletin 53, p.1569-1600.

Richmond, Fryxell, R., Neff, G.E., Weiss, P.L., 1965a. The Cordilleran ice sheet of the northern Rocky Mountains, and related Quaternary history of the Columbia Plateau,

in Wright, H.E., and Frey, D.G., eds., The Quaternary of the United States: Princeton University Press, p. 231-242.

Richmond, G.M., Mudge, M.R., Lemke, R.W., Fryxell, R., 1965b. Relation of alpine glaciation to the Continental and Cordilleran ice sheets: INQUA VII Congress Guidebook to Field Trip E, p.53-73.

Richmond, G.M., 1986. Tentative correlation of deposits of the Cordilleran ice sheet: Quaternary Science Reviews, v.5, p.129-144.

Ritter, D.F., 1982. Complex river terrace development in the Nenana Valley near Healy, Alaska: Geological Society of America Bulletin, v.93, p.346-356.

Shaw, J., Munro-Stasiuk, M., Sawyer, B., Neaney, C., Lesemann, J.E., Musacchio, A., Rains, B., and Young, R.R., 1999. The Channeled Scabland: Back to Bretz?: Geology, v.27, p.605-608.

Smith, D.G., 1966. Glacial and fluvial landforms adjacent to the Big Arm embayment, Flathead Lake, Western Montana [Master's Thesis]: Missoula, University of Montana, 74pp.

Smith, L.N., 2004. Late Pleistocene stratigraphy and implications for deglaciation and subglacial processes of the Flathead Lobe of the Cordilleran Ice Sheet, Flathead Valley, Montana, USA: Sedimentary Geology, 165, p. 295-332.

Sperazza, M., in prep. An Examination of Proxy Data for Paleoclimate Reconstruction, Chronostratigraphic Determination, and Grain Size Estimation from Sediments in Flathead Lake, Montana.

Stoffel, K.L., 1980. Glacial geology of the Southern Flathead Valley, Montana [Masters Thesis]: Missoula, Montana, University of Montana, 149pp.

Thomas, G.S.P., and Connel, R.J., 1984. Iceberg drop, dump, and grounding structures from Pleistocene glacio-lacustrine sediments, Scotland: Journal of Sedimentary Petrology, v.55, p.243-249.

Verosub, K.L., Mehringer, P.J.Jr., Waterstraat, P., 1986. Holocene secular variation in Western North America: paleomagnetic record from Fish Lake, Harney County, Oregon: Journal of Geophysical Research, v.91, no.B3, p.3609-3623.

Verosub, K.L., 1998. Paleomagnetism: Faster Is Better: Science, 281, p.1297-1298.

Verosub, K.L., Harris, A.H., Karlin, R., 2001. Ultrahigh-resolution paleomagnetic record from ODP Leg 169S, Saanich Inlet, British Columbia: initial results: Marine Geology 174, p.79-93.

Waitt, R.B., Jr., 1985. Case of periodic, colossal jökulhlaups from Pleistocene glacial Lake Missoula: Geological Society of America Bulletin 96, p. 1271-1286.

Waitt, R.B., Atwater, B.F., 1989. Stratigraphic and geomorphic evidence for dozens of last-glacial floods: *in* Hanshaw, P.M. ed., Glacial geology and geomorphology of North America; Vol. 1, Glacial Lake Missoula and the channeled scabland: Field trips for the 28th international geologic congress, American Geophysical Union, p.37-50.

Weeks, R., Laj, C., Endignoux, L., Fuller, M.D., Roberts, A.P., Manganne, R., Blanchard, E., Goree, W., 1993. Improvements in long core measurement techniques: applications in paleomagnetism and paleooceanography: Geophysical Journal International, 114, p. 651-662.

Wegmann, K.W., and Pazzaglia, F.J., 2002. Holocene strath terraces, climate change, and active tectonics: The Clearwater River basin, Olympic Peninsula, Washington State: GSA Bulletin, v.114, no.6, p.731-744.

Wold, R.J., 1982. Seismic reflection study of Flathead Lake, Montana. U.S. Geological Survey, Miscellaneous field studies, map MF-1433, scale 1:117,647.

Zdanowicz, C.M., Zielinski, G.A., Germani, M.S., 1999. Mount Mazama eruption; calendrical age verified and atmospheric impact assessed: Geology, vol.27, no.7, p.621-624.

Appendix A

Inclination and Declination Records

This appendix contains the inclination and declination records for the nine Flathead Lake cores measured for paleomagnetic secular variation correlation with the Fish Lake, OR record. Each figure is divided into two sections, one for the inclination curves and the other for the declination curves. The Flathead Lake depth series records are measured in meters below the core top, and have had no depth adjustments. The Fish Lake records are in age (cal yr BP). The Flathead Lake age series records have been time adjusted by the calculated age-models based on the magnetic correlations, ^{14}C dates, and the volcanic tephras (Appendix B), and are in the same time scale as the Fish Lake records. The pink lines represent points in the magnetic records that have been correlated, with their corresponding data tables presented in Appendix B. The Mt. Mazama tephra (7,630 cal yr BP) is highlighted in orange, and the Glacier Peak tephra (13,180 cal yr BP) is highlighted in blue. Magnetic correlations beyond the age limit of the Fish Lake record (11,300 cal yr BP) have been correlated to core FL-03-16K due to its abundance of ^{14}C dates and continuous record.

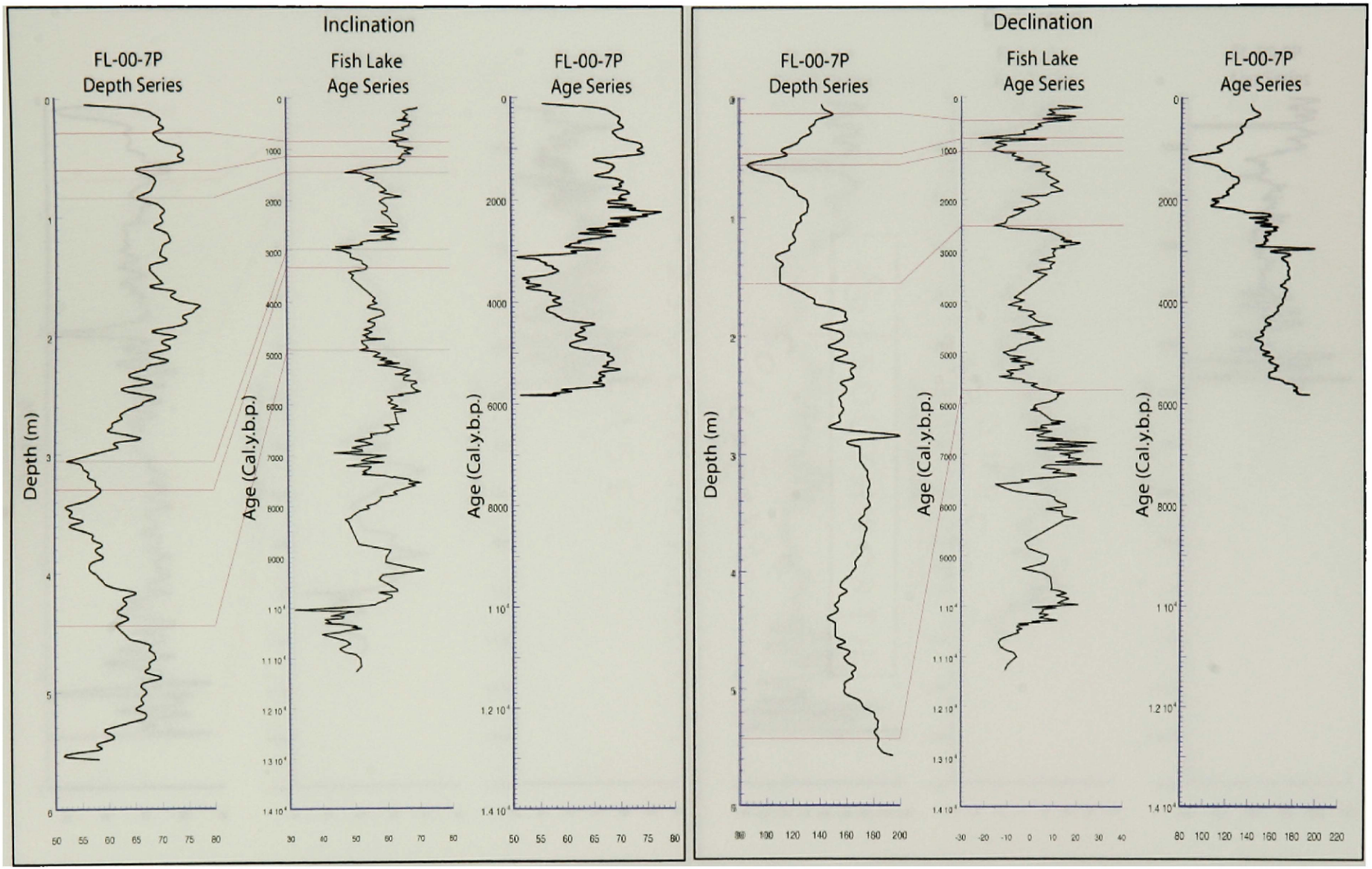

A1. Inclination and declination records for core FL-00-7P.

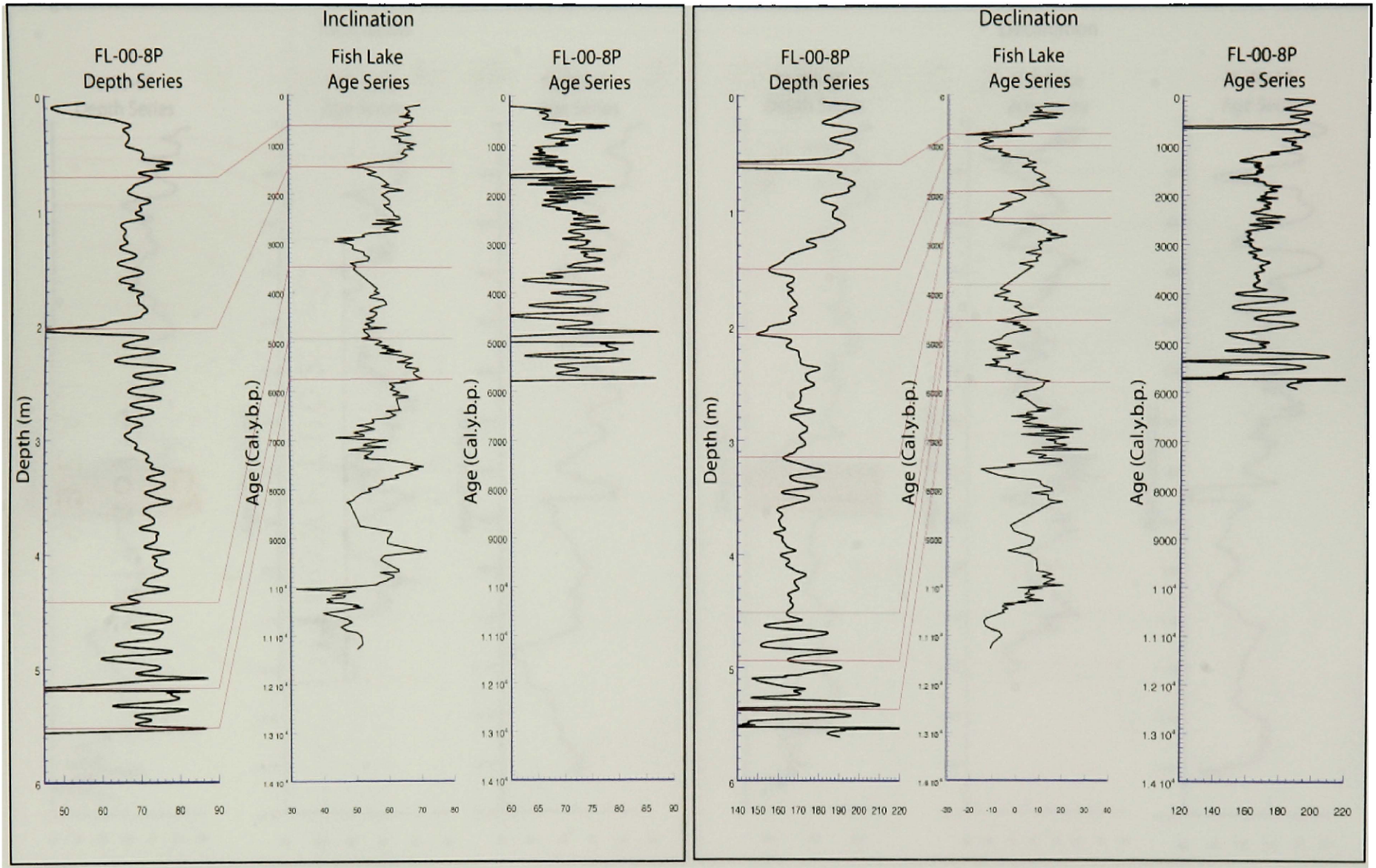

A2. Inclination and declination records for core FL-00-8P.

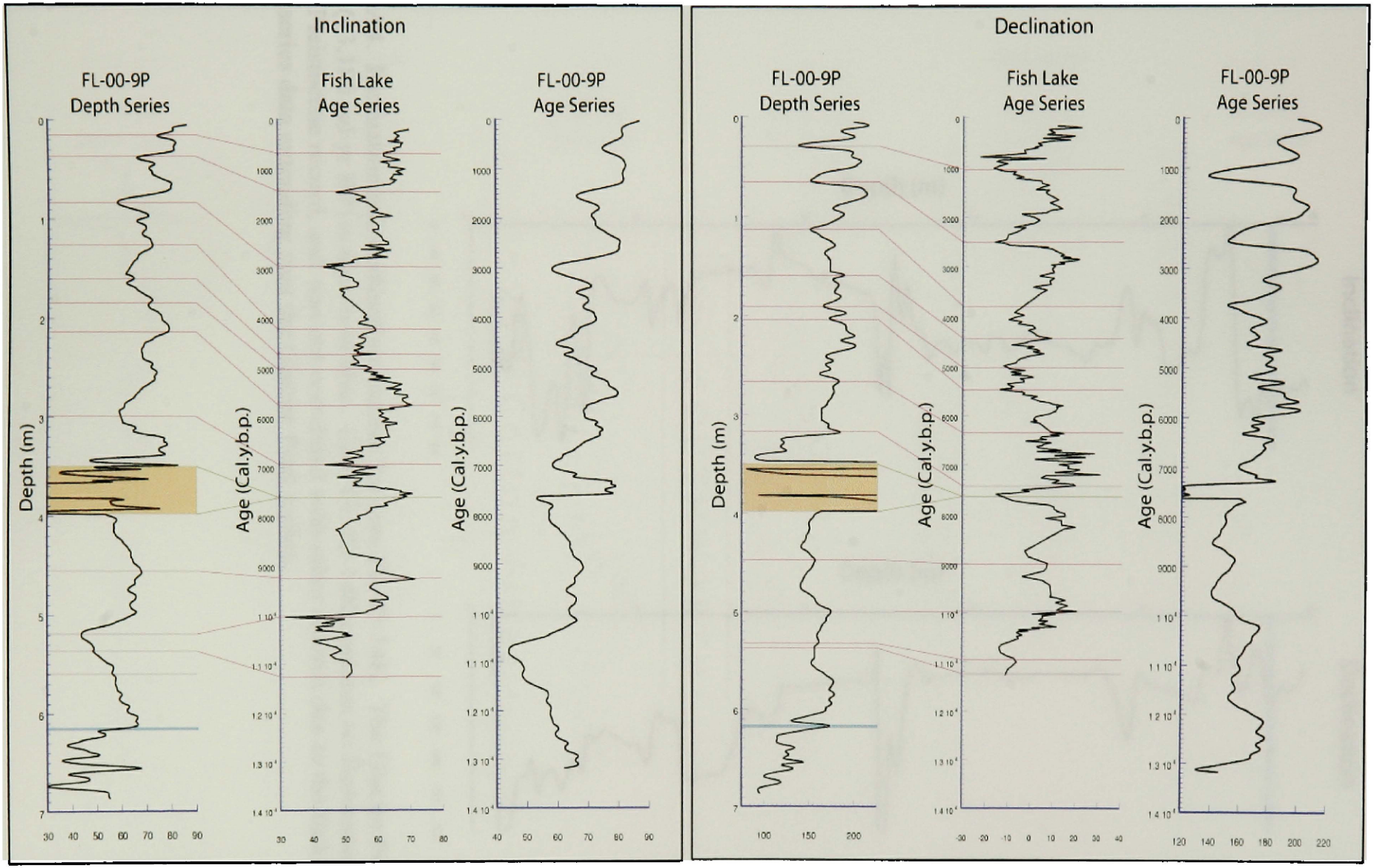

A3. Inclination and declination records for core FL-00-9P.

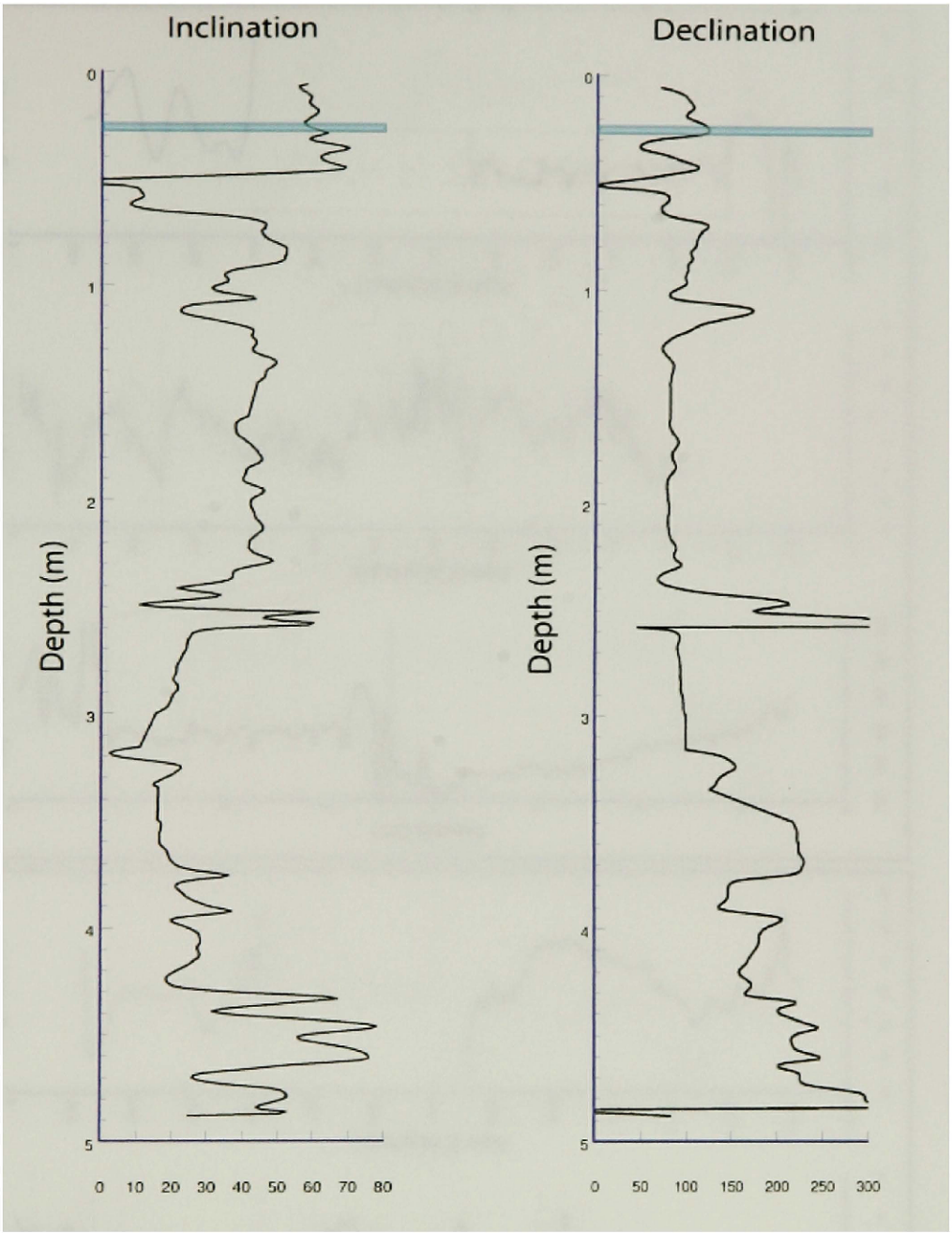

A4. Inclination and declination records for core FL-03-14K. The Glacier Peak tephra (13,180 cal yr BP) is shown in blue. Core FL-03-14K contains no Holocene or latest Pleistocene record, and was not correlated with other records due to the lack of time series data extending past the Glacier Peak tephra.

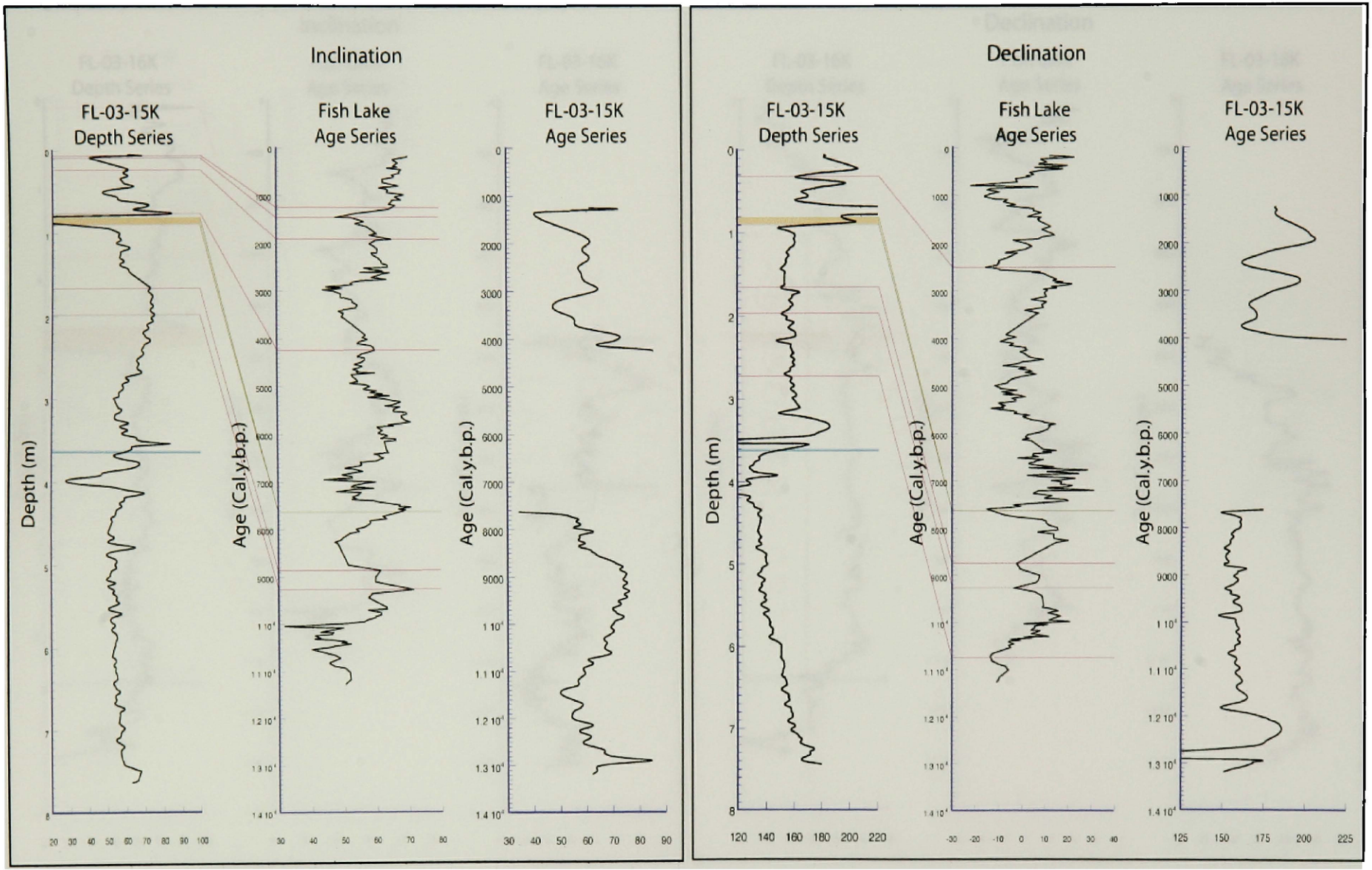

A5. Inclination and declination records for core FL-03-15K.

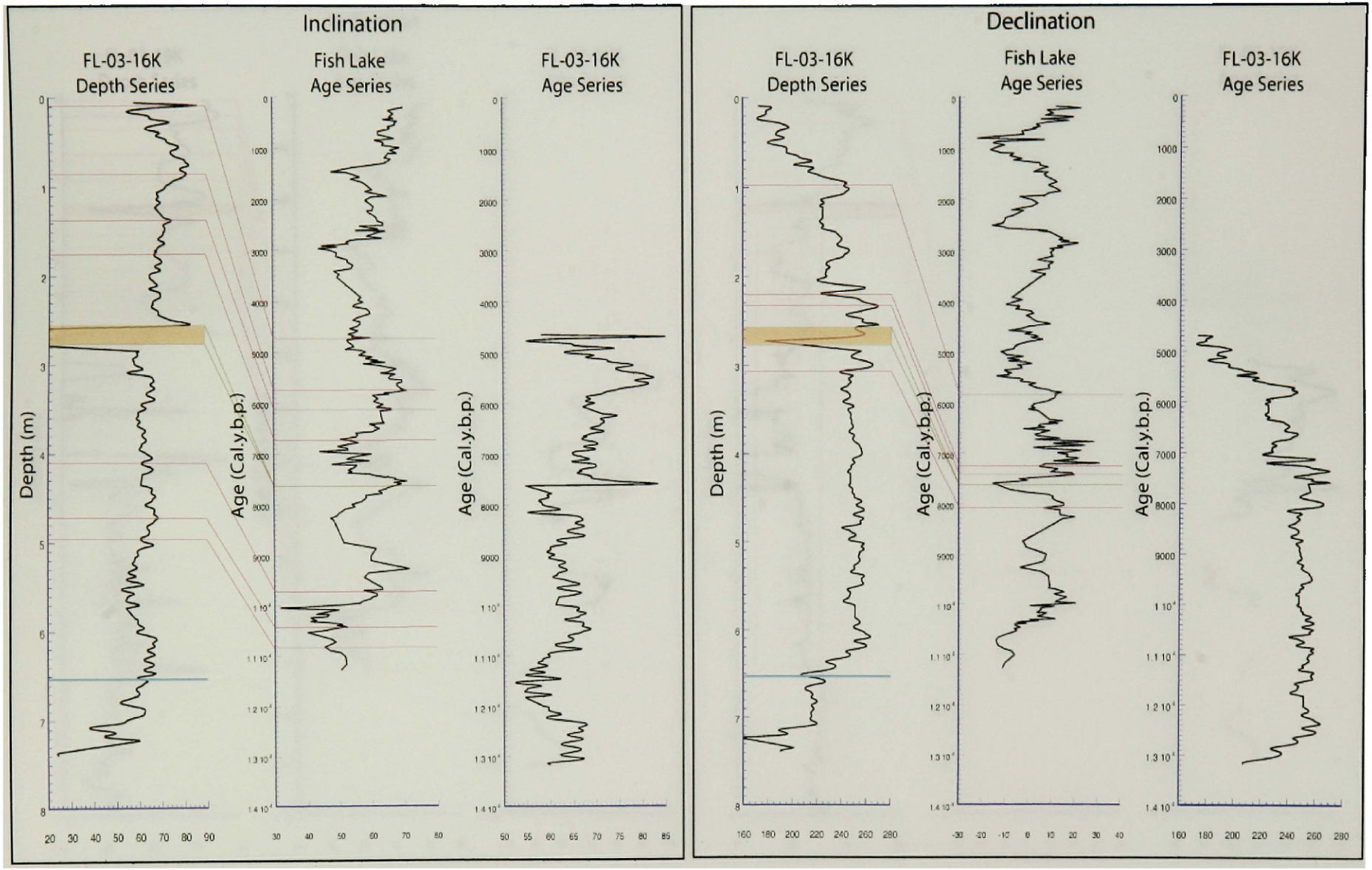

A6. Inclination and declination records for core FL-03-16K.

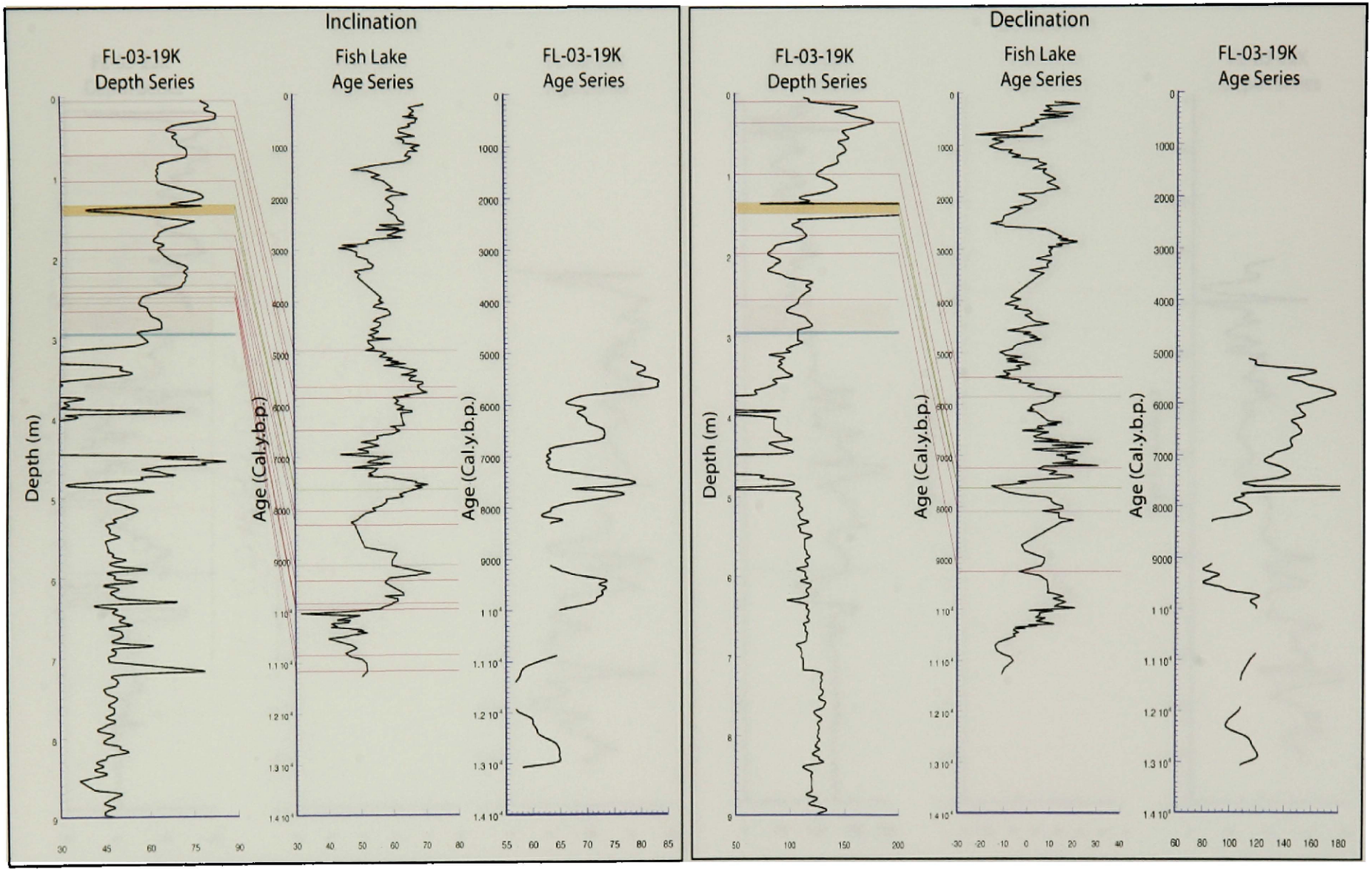

A7. Inclination and declination records for core FL-03-19K.

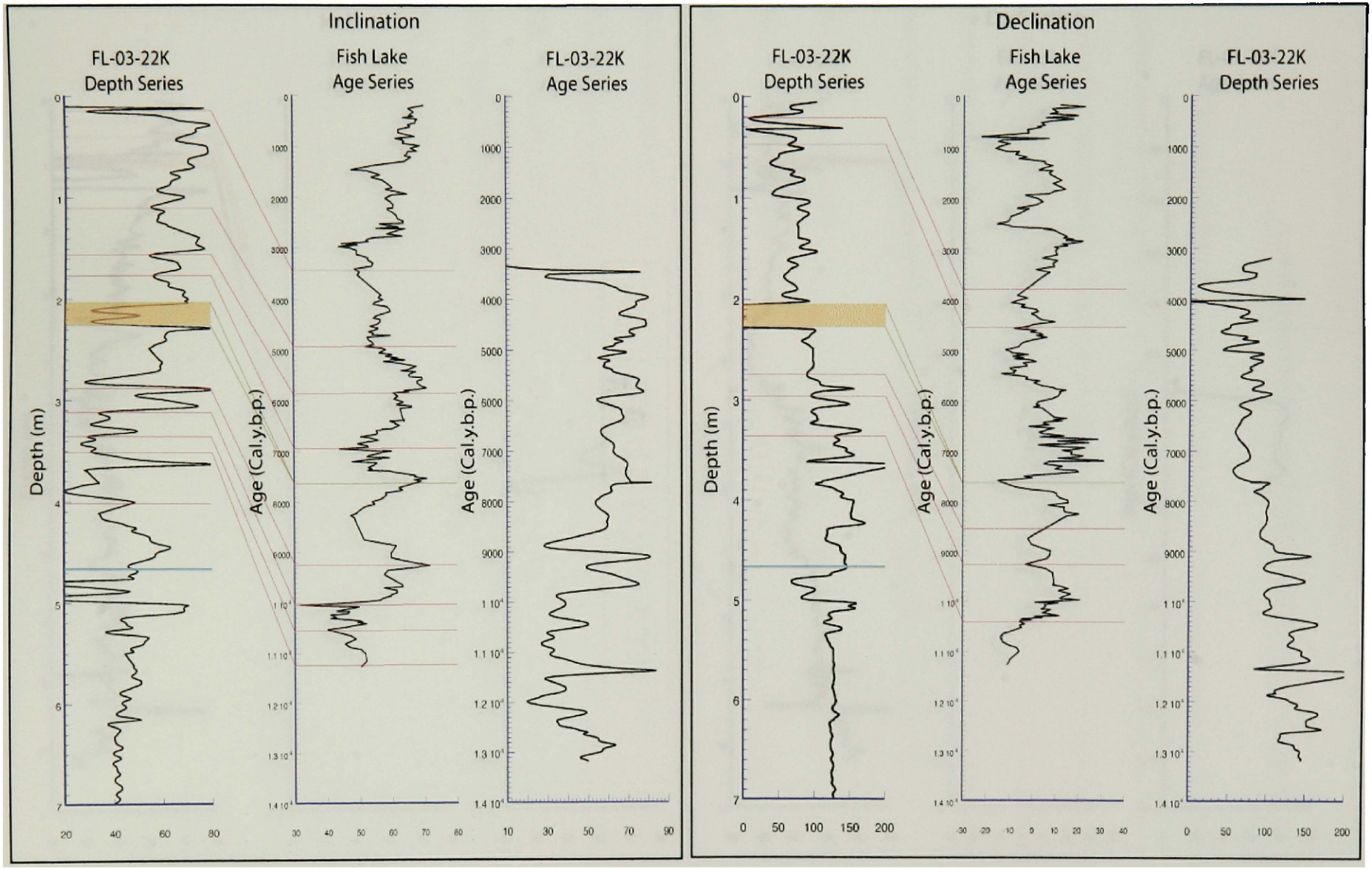

A8. Inclination and declination records for core FL-03-22K.

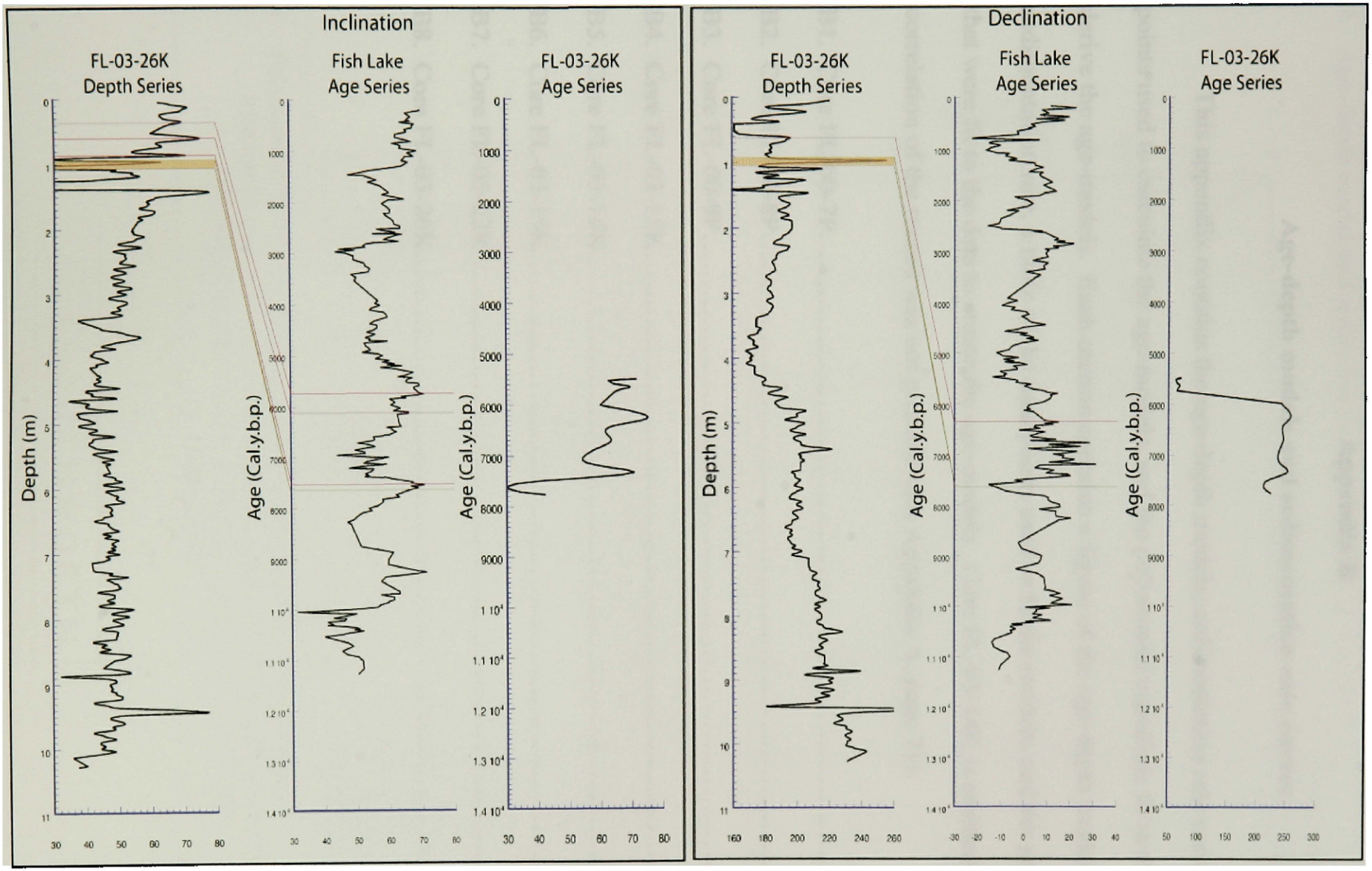

A9. Inclination and declination records for core FL-03-26K.

Appendix B

Age-depth models and sedimentation rate curves

This appendix contains the age-depth models, sedimentation rate curves, the data points used to calculate the age-models, and the polynomial equations fit to the data to derive the age-models. Each section contains a figure of the age-depth model and sedimentation rate, a table of the data points used to fit the models, and the polynomials that were fit to the data to create the age-models. Core FL-03-14K is omitted as magnetic correlation of the record was not possible (see Appendix A, page 71).

A. Age-depth model and sedimentation rate curves for FL-00-7P.

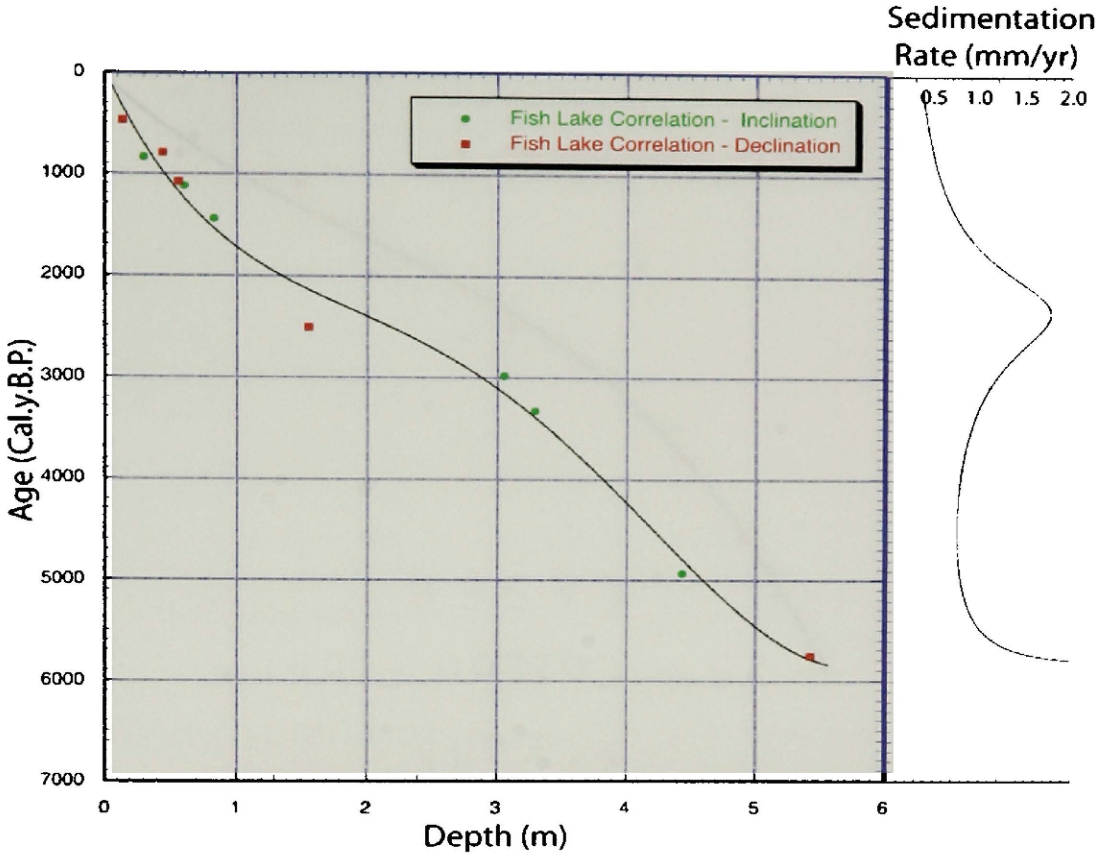

B. Table showing points used for the construction of the age-depth model.

Depth (mbct)	Age (Cal yr BP)	Error (+/-)	Data Type
0.139	476.38	-	declination
0.298	844.34	-	inclination
0.447	801.05	-	declination
0.567	1082.4	-	declination
0.606	1125.7	-	inclination
0.835	1450.4	-	inclination
1.559	2511	-	declination
3.059	2987.1	-	inclination
3.298	3333.5	-	inclination
4.442	4935.2	-	Inclination
5.435	5757.6	-	declination

C. Polynomial fit for use as the age-model and the associated R values.

Interval $0<x\leq 5.435$, where x is depth in meters and y is age in cal yr BP:

$$y=(-26.22)+(2827.4)x+(-1408.5)x^2+(359.46)x^3+(-29.398)x^4$$

$$R=0.99537$$

A. Age-depth and sedimentation rate curves for FL-00-8P.

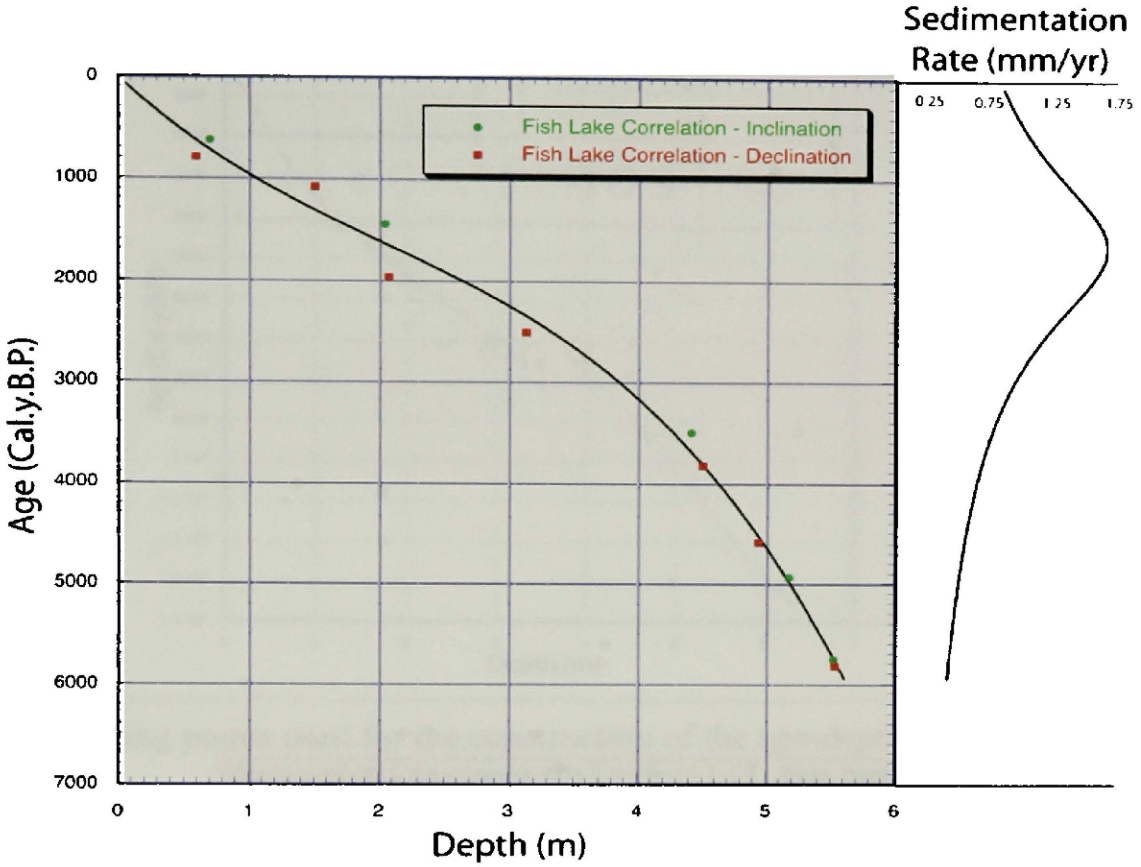

B. Table showing points used or the construction of the age-depth model.

Depth (mbct)	Age (cal yr BP)	Error (+/-)	Data Type
0.60419	801.05	-	declination
0.70726	627.89	-	Inclination
1.5074	1082.4	-	declination
2.0472	1450.4	-	inclination
2.0743	1969.9	-	declination
3.1376	2511	-	declination
4.4178	3506.6	-	inclination
4.5101	3831.3	-	declination
4.9413	4588.8	-	declination
5.18	4935.2	-	inclination
5.5299	5757.6	-	inclination
5.5381	5822.6	-	declination

C. Polynomial fit for use as the age-model and the associated R-value.

Interval $0<x\leq5.5381$, where x is depth in meters and y is age in cal yr BP:

$$y=(4.0952)+(1211.1)x+(-300.27)x^2+(48.679)x^3$$

$$R=0.99638$$

A. Age-depth model and sedimentation rate curves for FL-00-9P.

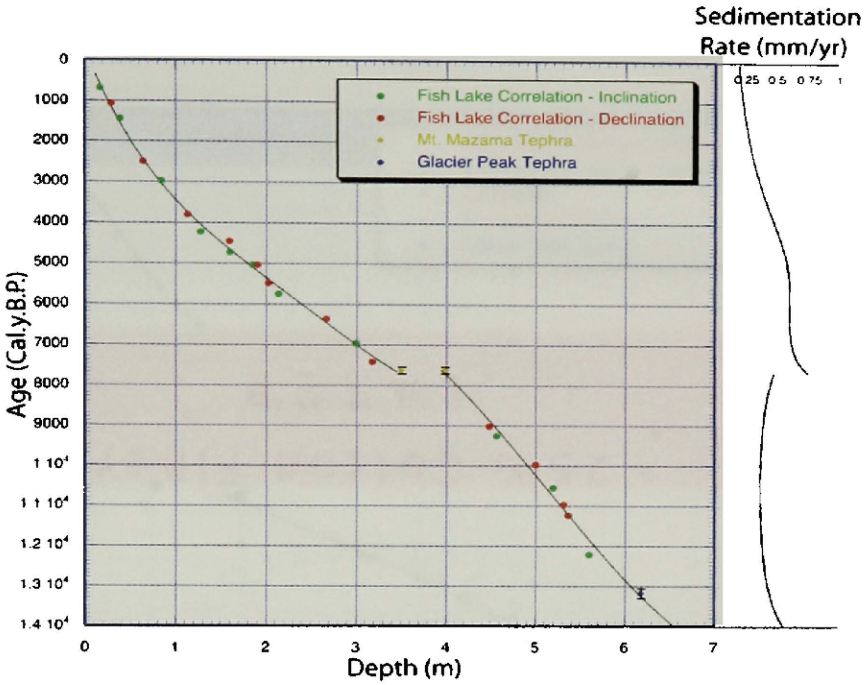

B. Table showing points used for the construction of the age-depth model.

Depth (mbct)	Age (cal yr BP)	Error (+/-)	Data Type
0.16539	692.82	-	inclination
0.29173	1082.4	-	declination
0.38815	1450.4	-	inclination
0.64415	2511	-	declination
0.84031	2987.1	-	inclination
1.1362	3809.6	-	declination
1.2792	4242.5	-	inclination
1.595	4459	-	declination
1.6017	4740.4	-	inclination
1.8543	5043.4	-	inclination
1.9042	5043.4	-	declination
2.0306	5497.9	-	declination
2.1403	5757.6	-	inclination
2.6722	6363.7	-	declination
2.998	6969.7	-	inclination
3.1809	7424.3	-	declination
3.5	7630	80	tephra
3.985	7630	80	tephra
4.4842	9026	-	declination
4.5673	9264.1	-	inclination
5.0028	9978.3	-	declination
5.199	10563	-	inclination
5.312	10974	-	declination
5.3619	11255	-	declination
5.3752	11255	-	inclination
5.6	12220	-	inclination
6.179	13180	120	tephra

C. Polynomials fit for use as the age-model and the associated R values.

Interval $0<x\leq3.5$, where x is depth in meters and y is age in cal yr BP:

$$y=(-290.36)+(5664.8)x+(-2603.2)x^2+(756.9)x^3+(-82.744)x^4$$

$$R=0.99851$$

Interval $3.985<x\leq6.179$, where x is depth in meters and y is age in cal yr BP:

$$y=(17634)+(-9545.3)x+(2388.7)x^2+(-155.12)x^3$$

$$R=0.99296$$

A. Age-depth model and sedimentation rate curves for FL-00-15K.

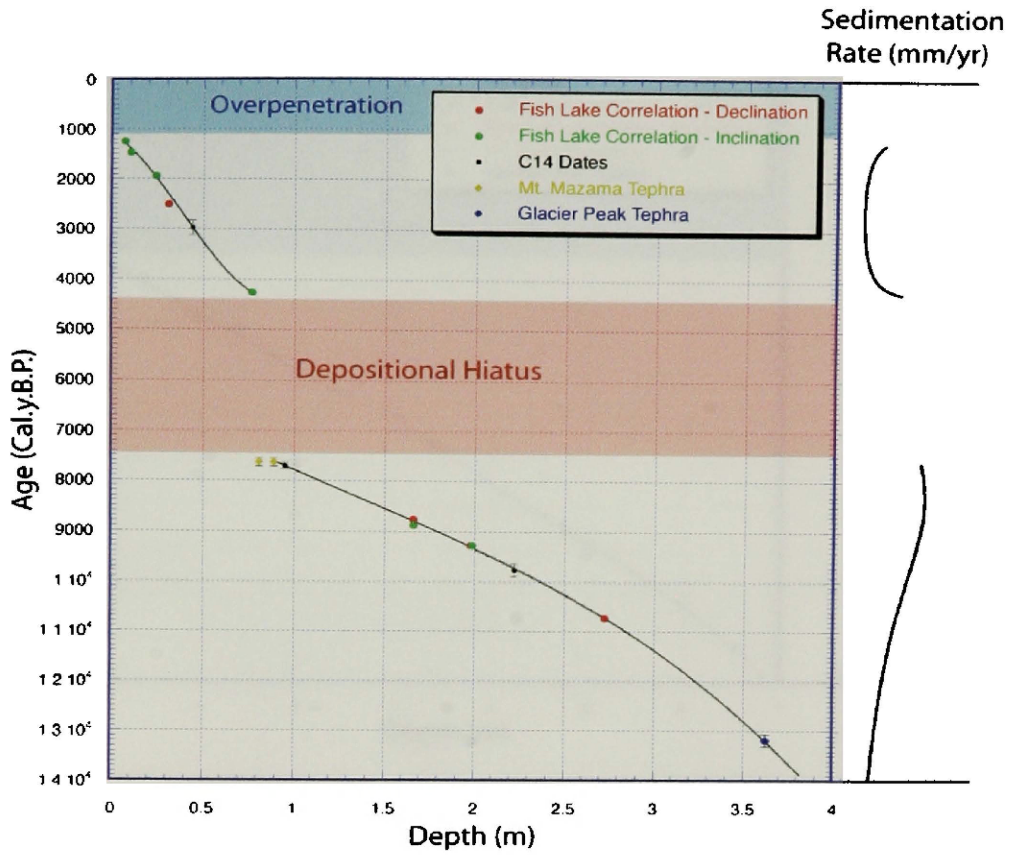

B. Table showing points used for the construction of the age-depth model.

Depth (mbct)	Age (cal yr BP)	Error (+/-)	Data Type
0.069	1241	-	inclination
0.099	1468	-	inclination
0.239	1936	-	inclination
0.31	2510	-	declination
0.44	2980	145	C14
0.766	4254	-	inclination
0.81	7630	80	tephra
0.89	7630	80	tephra
0.95	7700	65	C14
1.659	8757	-	declination
1.659	8871	-	inclination
1.977	9274	-	declination
1.987	9274	-	Inclination
2.22	9760	125	C14
2.724	10725	-	declination
3.62	13180	120	tephra

C. Polynomials fit for use as the age-depth model and the associated R values.

Interval $0<x\leq0.81$, where x is depth in meters and y is age in cal yr BP:

$$y=(1123.7)+(1969.1)x+(8175.2)x^2+(-7061.6)x^3$$

$$R=0.99921$$

Interval $0.89<x\leq3.62$, where x is depth in meters and y is age in cal yr BP:

$$y=(5975)+(2172.3)x+(-484.36)x^2+(119.94)x^3$$

$$R=0.99969$$

A. Age-depth model and sedimentation rate curves for FL-03-16K.

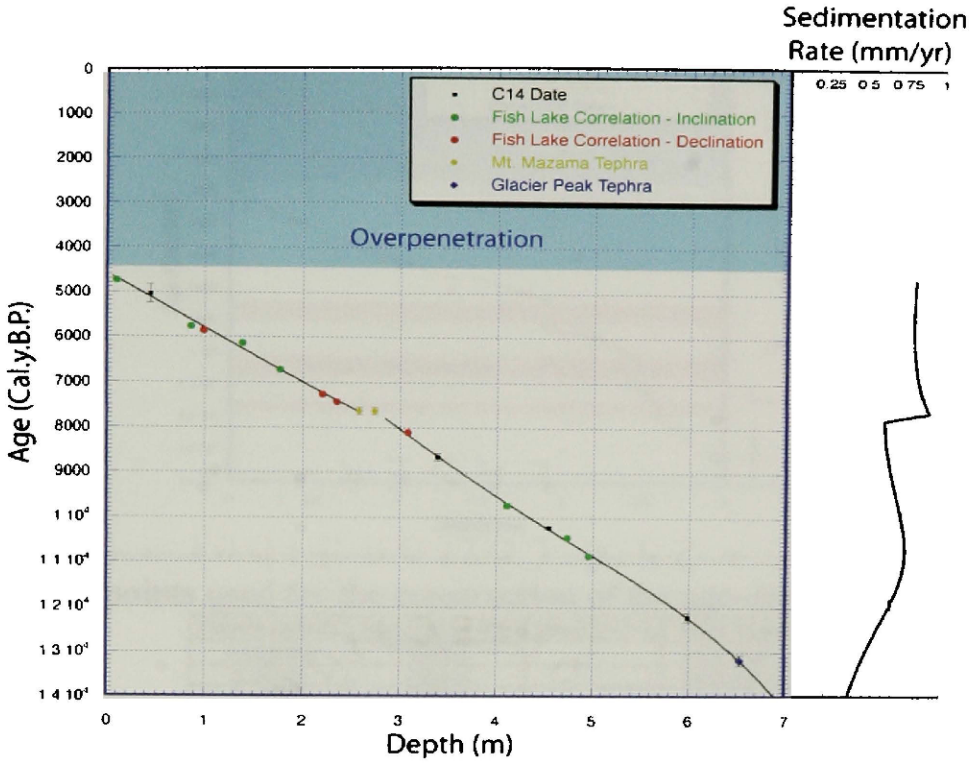

B. Table showing points used for the construction of the age-depth model.

Depth (mbct)	Age (cal yr BP)	Error (+/-)	Data Type
0.093234	4740.4	-	inclination
0.44	5040	205	C14
0.85617	5757.6	-	inclination
0.9845	5844.2	-	declination
1.3795	6125.6	-	inclination
1.7658	6710	-	inclination
2.2021	7251.1	-	declination
2.3464	7424.3	-	declination
2.58	7630	80	tephra
2.74	7630	80	tephra
3.0795	8095.3	-	declination
3.39	8650	80	C14
4.1037	9718.6	-	inclination
4.54	10210	40	C14
4.7288	10433	-	inclination
4.955	10844	-	inclination
5.99	12220	95	C14
6.53	13180	120	tephra

C. Polynomials fit for use as the age-model and the associated R values.

Interval $0<x\leq 2.58$, where x is depth in meters and y is age in cal yr BP:

$$y=(4585)+(1202.2)x+(8.9093)x^2+(2.1626)x^3+(-3.1253)x^4$$

$R=.99771$

Interval $2.74<x\leq 6.53$, where x is depth in meters and y is age in cal yr BP:

$$y=(5229)+(-835.48)x+(1091.5)x^2+(-208.28)x^3+(13.672)x^4$$

$R=.9998$

A. Age-depth model and sedimentation rate curves for FL-03-19K.

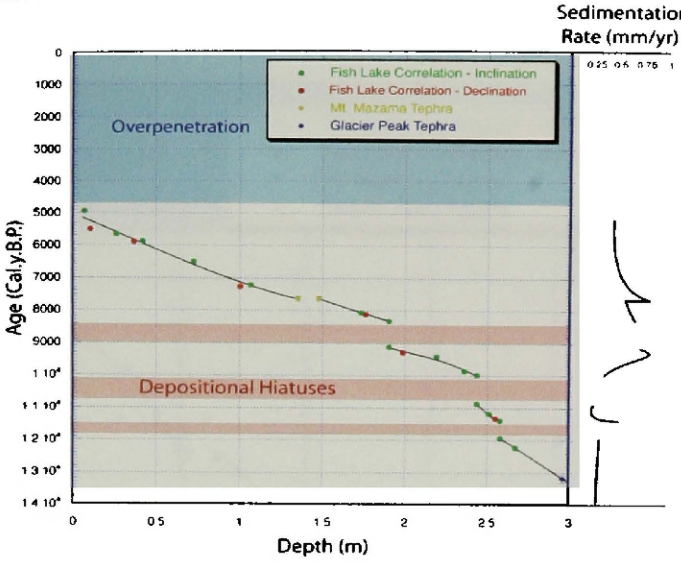

B. Table showing points used for the construction of the age-depth model.

Depth (mbct)	Age (cal yr BP)	Error (+/-)	Data Type
0.066582	4935.2	-	inclination
0.10196	5497.9	-	declination
0.25866	5649.4	-	inclination
0.36481	5887.5	-	declination
0.41536	5865.9	-	inclination
0.72116	6493.6	-	inclination
1.0017	7251.1	-	declination
1.0649	7207.8	-	inclination
1.353	7630	80	tephra
1.476	7630	80	tephra
1.73	8050	-	inclination
1.76	8100	-	declination
1.9	9107	-	inclination
1.9	8310	-	inclination
1.985	9270	-	declination
2.19	9400	-	inclination
2.36	9850	-	inclination
2.435	10856	-	inclination
2.435	9967	-	inclination
2.51	11168	-	inclination
2.55	11312	-	declination
2.578	11379	-	inclination
2.578	11926	-	inclination
2.67	12220	-	inclination
2.96	13180	120	tephra

C. Polynomials fit for use as the age-model and the associated R values.

Interval $0<x\leq1.353$, where x is depth in meters and y is age in cal yr BP:

$$y=(5026.8)+(2192.4)x+(166.69)x^2+(-261.52)x^3$$

$$R=0.98848$$

Interval $1.476<x\leq1.9$, where x is depth in meters and y is age in cal yr BP:

$$y=(4353.8)+(2697.6)x+(-323.83)x^2$$

$$R=0.99999$$

Interval $1.9<x\leq2.43$, where x is depth in meters and y is age in cal yr BP:

$$y=(-20629)+(41803)x+(-19997)x^2+(3282.8)x^3$$

$$R=0.99407$$

Interval $2.43<x\leq2.58$, where x is depth in meters and y is age in cal yr BP:

$$y=(1374900)+(-1658200)x+(670280)x^2+(-90080)x^3$$

$$R=1.0$$

Interval $2.58<x\leq2.96$, where x is depth in meters and y is age in cal yr BP:

$$y=(5754.3)+(1620)x+(300.24)x^2$$

$$R=1.0$$

A. Age-depth model and sedimentation rate curves for FL-03-22K.

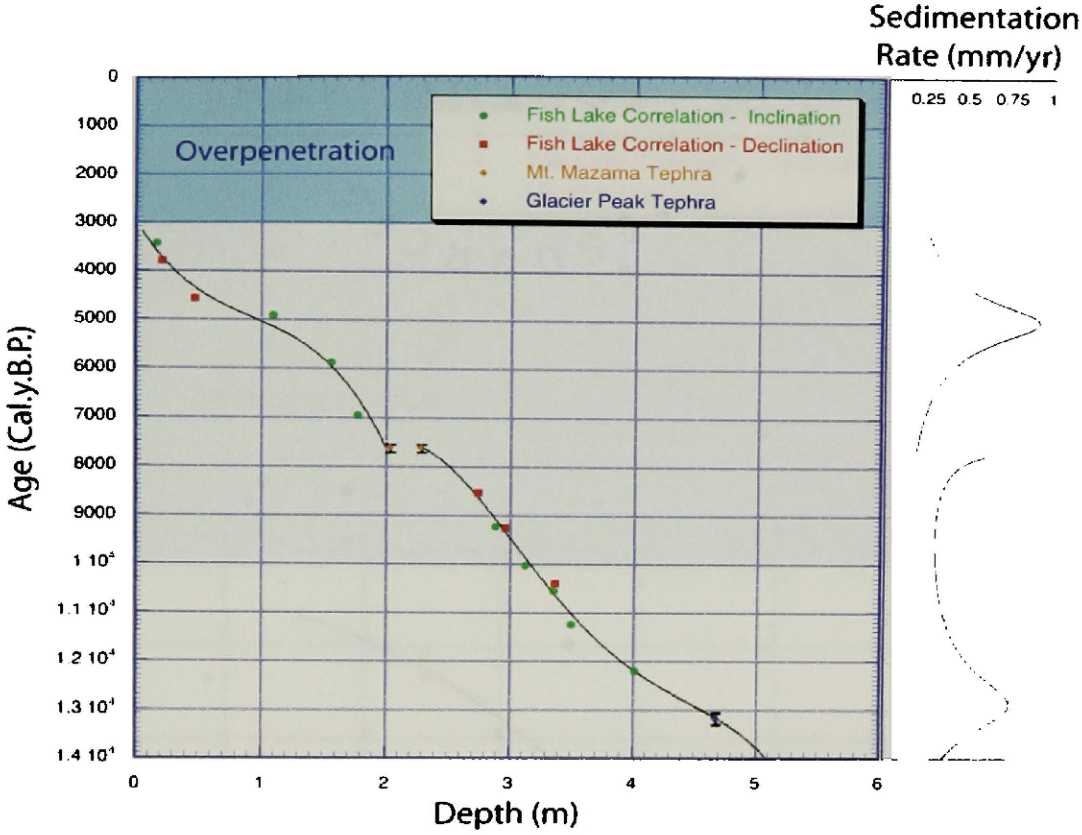

B. Table showing points used for the construction of the age-depth model.

Depth (mbct)	Age (cal yr BP)	Error (+/-)	Data Type
0.169	3441.7	-	inclination
0.218	3809.6	-	declination
0.477	4588.8	-	declination
1.104	4935.2	-	inclination
1.568	5887.5	-	inclination
1.777	6969.7	-	inclination
2.035	7630	80	tephra
2.285	7630	80	tephra
2.748	8549.8	-	declination
2.888	9242.4	-	inclination
2.967	9264.1	-	declination
3.127	10043	-	inclination
3.365	10563	-	inclination
3.375	10411	-	declination
3.505	11255	-	inclination
4.02	12220	-	inclination
4.675	13180	120	tephra

C. Polynomials fit for use as the age-model and the associated R values.

Interval $0<x\leq2.035$, where x is depth in meters and y is age in cal yr BP:

$$y=(2964.9)+(4289.8)x+(-3424.2)x^2+(1219.4)x^3$$

$$R=0.99021$$

Interval $2.285<x\leq4.675$, where x is depth in meters and y is age in cal yr BP:

$$y=(56445)+(-62573)x+(28058)x^2+(-5176.1)x^3+(345.21)x^4$$

$$R=0.99641$$

A. Age-depth model and sedimentation rate curves for FL-03-26K.

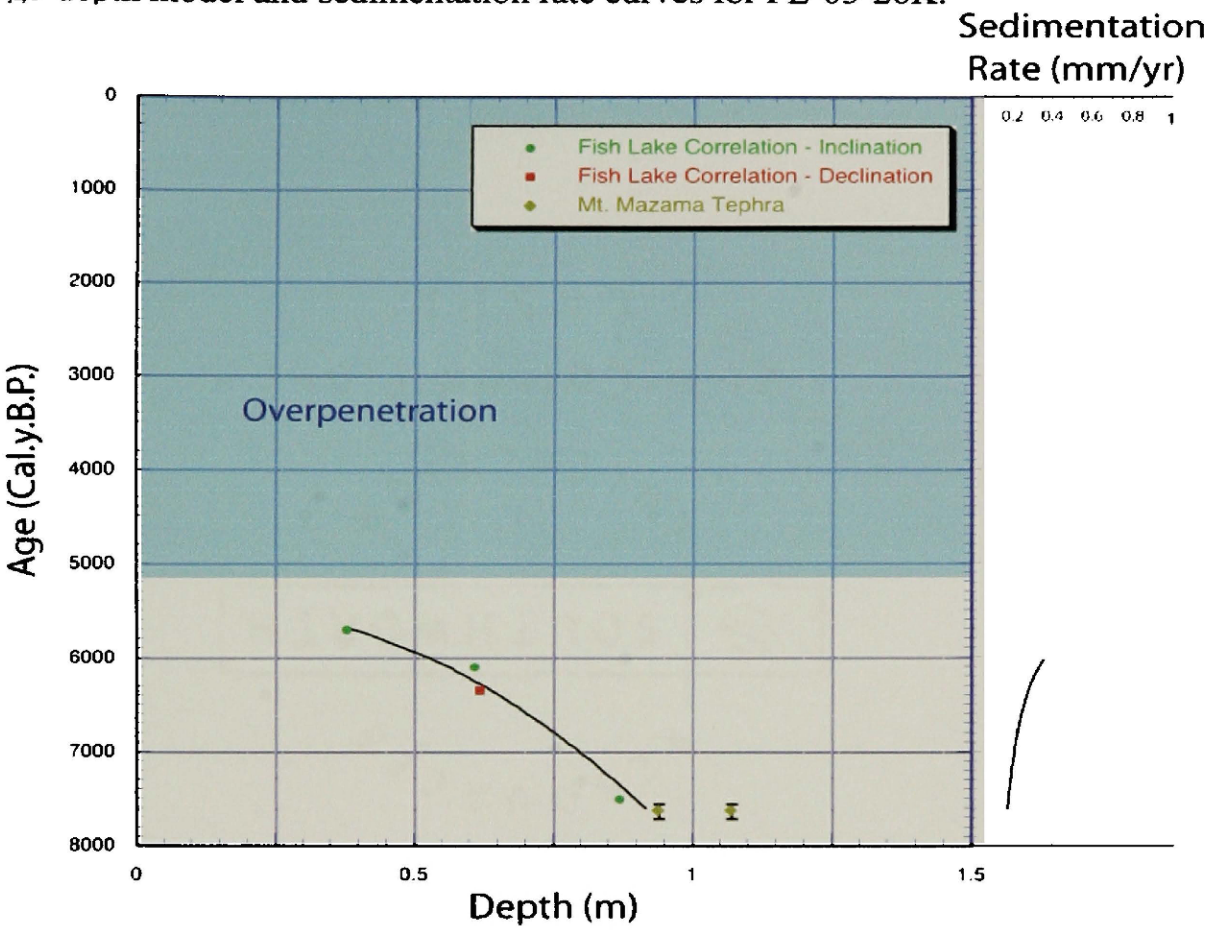

B. Table showing points used for the construction of the age-depth model.

Depth (mbct)	Age (cal yr BP)	Error (+/-)	Data Type
0.38	5170	-	inclination
0.61	6110	-	inclination
0.619	6358	-	declination
0.87	7510	-	inclination
0.94	7630	80	tephra
1.07	7630	80	tephra

C. Polynomial fit for use as the age-model and the associated R value.

Interval $0.38<x\leq0.92$, where x is depth in meters and y is age in cal yr BP:

$y=(5587.5)+(-1113.7)x+(3617.1)x^2$

$R=0.9851$